Advancing Chinese Hamster Ovary Cell Culture Processes in Different Scales

Weiterentwicklung von Chinese Hamster Ovary Zellkulturprozessen in Verschiedenen Skalen

Von der Fakultät für Maschinenwesen der Rheinisch-Westfälischen Technischen Hochschule Aachen zur Erlangung des akademischen Grades einer Doktorin der Naturwissenschaften genehmigte Dissertation

vorgelegt von

Anne Neuß

Berichter/in: Univ.-Prof. Dr.-Ing. Jørgen Magnus

Prof. Dr. rer. nat. Janina Bahnemann

Tag der mündlichen Prüfung: 04. Juli 2025

Diese Dissertation ist auf den Internetseiten der Universitätsbibliothek online verfügbar.

Danksagung

Diese Dissertation wurde während meiner Tätigkeit als wissenschaftliche Mitarbeiterin am Lehrstuhl für Bioverfahrenstechnik der RWTH Aachen angefertigt. Mein besonderer Dank gilt Prof. Jørgen Magnus für die Betreuung meiner Arbeit und die wertvolle Chance, den Bereich der Zellkulturtechnik am Lehrstuhl weiterentwickeln zu dürfen. Ebenso bin ich Herrn Prof. Jochen Büchs für die Möglichkeit zur Promotion am Lehrstuhl, seine Unterstützung und die zahlreichen wissenschaftlichen Diskussionen bis zu seinem Ruhestand und darüber hinaus sehr dankbar. Prof. Janina Bahnemann danke ich herzlich für die Übernahme des Zweitgutachtens. Herrn Prof. Jakob Andert spreche ich meinen Dank für die Übernahme des Vorsitzes der Prüfungskommission aus.

Ein besonderer Dank gilt außerdem den zahlreichen Studierenden, die mich während dieser Zeit begleitet und unterstützt haben. Insbesondere möchte ich hier die Zellkultur-Hilfskräfte Nele, Raoul, Jacinta, Laurin, Julia und Mareike hervorheben. Die gemeinsame Arbeit war für mich stets eine große Freude und hat in vielerlei Hinsicht wesentlich zum Fortschritt dieser Dissertation beigetragen.

Ebenso danke ich meinen Kolleginnen und Kollegen am Lehrstuhl für die hervorragende Zusammenarbeit, die vielen anregenden Gespräche und die sehr angenehme Arbeitsatmosphäre. Besonders schätze ich den starken Zusammenhalt im Team, die selbstverständliche gegenseitige Unterstützung und die Freundschaften, die in dieser Zeit entstanden sind.

Meiner Familie gilt mein tiefster Dank. Sie haben mir jederzeit Rückhalt gegeben, mich ermutigt und mit Geduld und Vertrauen unterstützt. Ohne ihre ständige Zuversicht und ihren Glauben an mich wäre diese Arbeit nicht möglich gewesen.

Zusammenfassung

Chinese Hamster Ovary (CHO) Zellen sind der wichtigste Produktionsorganismus in der biopharmazeutischen Industrie für Antikörper und therapeutische Proteine. Industrielle Prozesse sind heutzutage etabliert. Sie beruhen jedoch häufig auf historischen oder empirischen Erkenntnissen und nicht auf einem umfassenden Prozessverständnis. Daher konzentriert sich die aktuelle Forschung auf Methoden zur kosteneffizienten Prozessentwicklung mit Fokus auf Hochdurchsatzlösungen und Online-Messmethoden.

In dieser Arbeit wurde die Online-Überwachung der Atmungsaktivität über drei Größenordnungen für CHO-Zellen etabliert. Die drei verwendeten Zelllinien wurden durch die Sauerstofftransferrate (OTR) in Schüttelkolben charakterisiert. Spezifische Merkmale des OTR-Verlaufs zeigten, wann Glukose und Glutamin aufgebraucht waren. Die Online-OTR-Messung in Schüttelkolben wurde zur Untersuchung des Einflusses verschiedener hydromechanischer Spannungsniveaus auf das Wachstum, den Stoffwechsel und die Produktion der CHO-Zellen verwendet. Die spezifische Wachstumsrate und der Verbrauch der Metaboliten korrelieren linear mit der logarithmisch aufgetragenen durchschnittlichen Energiedissipationsdichte. Produktkonzentration sank unter turbulenten Bedingungen um 40 %. Zur Erhöhung des Durchsatzes wurde die OTR-Überwachung für 96-well Mikrotiterplatten mit runder und quadratischer Geometrie eingesetzt. Unter Verwendung der maximalen Sauerstofftransferkapazität als Scale-down-Parameter konnten identische OTR-Verläufe erzielt werden. Zwei Beispiele zeigten die breite Anwendbarkeit der OTR-Überwachung in Mikrotiterplatten. Medienscreening erwies sich als vielversprechend. Dies zeigte sich durch Analyse verschiedener Glutaminkonzentrationen. Außerdem wurden Kill-Curve-Experimente vereinfacht. Schließlich wurde auf der Grundlage der Erkenntnisse aus den geschüttelten Gefäßen ein datengesteuerter Scale-up-Ansatz für einen Rührkesselreaktor durchgeführt. Nahezu identische Ergebnisse in Bezug auf OTR-Verlauf, Metaboliten- und Produktkonzentrationen wurden von 400 µL bis erzielt, wobei der durchschnittliche volumetrische 600 mL Arbeitsvolumen Leistungseintrag als Scale-up-Parameter verwendet wurde.

Diese Arbeit ebnet den Weg für eine effiziente Prozessentwicklung mit Säugetierzellkulturen vom kleinen, geschüttelten Maßstab bis hin zu Rührkesselreaktoren unter Nutzung der online Überwachung der OTR.

Abstract

Chinese hamster ovary (CHO) cells are the predominant production organism in the biopharmaceutical industry for antibodies and therapeutical proteins. Industrial processes are established nowadays. However, they often rely on historical or empirical evidence instead of deep process understanding. Therefore, current research focuses on tools for cost-effective process development with particular interest in high-throughput solutions and online measurement methods.

This thesis established the use of respiration activity online monitoring over three orders of magnitude for CHO cells. The three cell lines used were characterized by monitoring the oxygen transfer rate (OTR) in shake flasks. Specific characteristics of the OTR progression indicated glucose and glutamine depletion. Online OTR monitoring in shake flasks was used to investigate the influence of different hydromechanical stress levels on CHO cells' growth, metabolism and production. The specific growth rate and metabolite depletion correlate linearly with logarithmically plotted average energy dissipation rate. The product concentration decreased by 40 % under turbulent conditions. To increase the throughput, OTR monitoring was established for 96-deep-well microtiter plates with round and square geometry. Using the maximal oxygen transfer capacity as scale-down parameter, identical OTR progressions were achieved. Two examples showed the broad applicability of OTR monitoring in microtiter plates. Media screening was shown to be promising by analyzing various glutamine concentrations. Additionally, kill curve experiments were streamlined. Finally, a data-driven scale-up approach to a stirred tank reactor was performed based on the findings from the small shaken vessels. Nearly identical results in OTR progression, metabolite and product concentrations were achieved from 400 µL to 600 mL working volumes utilizing the average volumetric power input as scale-up parameter.

The presented work paves the way for efficient process development with mammalian cell cultures from small shaken scales to stirred tank reactors using online monitoring of the OTR.

Publications and conference contributions

Parts of this thesis have been previously published:

- Neuss, Anne; Vegesack, Nele von; Liepelt, Raoul; Büchs, Jochen; Magnus, Jørgen Barsett (2024). Online monitoring of the respiration activity in 96-deepwell microtiter plate Chinese hamster ovary cultures streamlines kill curve experiments. Biotechnology progress 40 (5), e3468.
- Neuss, Anne; Tomas Borges, Jacinta Sofia; Vegesack, Nele von; Büchs, Jochen; Magnus, Jørgen Barsett (2024). Impact of hydromechanical stress on CHO cells' metabolism and productivity: Insights from shake flask cultivations with online monitoring of the respiration activity. New biotechnology 84, 96–104.
- Neuss, Anne; Steimann, Thomas; Tomas Borges, Jacinta Sofia; Dinger, Robert; Magnus, Jørgen Barsett (2025). Scale-up of CHO cell cultures: from 96-well-microtiter plates to stirred tank reactors across three orders of magnitude. Journal of Biological Engineering 19, 5.

Contributions to further publications during the preparation of this thesis:

- Hertel, Oliver[§]; Neuss, Anne[§]; Busche, Tobias; Brandt, David; Kalinowski, Jörn; Bahnemann, Janina; Noll, Thomas (2022). Enhancing stability of recombinant CHO cells by CRISPR/Cas9-mediated site-specific integration into regions with distinct histone modifications. Frontiers in Bioengineering and Biotechnology 10:1010719.
- Hertel, Oliver[§]; Neuss, Anne[§] (2024). Enhancing cell line stability by CRISPR/Cas9-Mediated site-specific integration based on histone modifications. In: Hacker, David L. (eds) Recombinant Protein Expression in Mammalian Cells. Methods in Molecular Biology 2810.
- Brauneck, Gesa; Engel, Dominik; Grebe, Luca Antonia; Hoffmann, Maximilian; Lichtenberg, Philipp Georg; Neuss, Anne; Mann, Marcel; Magnus, Jørgen Barsett. Pitfalls in early bioprocess development using shake flask cultivations. Accepted for publication in Engineering in Life Science.

§Both authors contributed equally to the publication

Contributions to conferences and seminars as oral presentations during the preparation of this thesis:

- Neuss, Anne; Müller, Nina; Büchs, Jochen; Magnus, Jørgen Barsett (2023).
 Establishing a true small-scale model for CHO cell culture through non-invasive online monitoring of the respiration activity. Bioprocess International Europe, Amsterdam, Netherlands.
- Neuss, Anne; Müller, Nina; Büchs, Jochen; Magnus, Jørgen Barsett (2023).
 Applications of TOM and µTOM for mammalian cell cultures. Seminar on scientific and practical aspects of orbital shaking in biology. iAMB RWTH Aachen University, Aachen, Germany.
- Neuss, Anne; Steimann, Thomas; Dinger, Robert; Magnus, Jørgen Barsett (2024). Utilizing oxygen transfer rate monitoring to transfer cell cultures from microtiter plates to stirred tank reactors. 28th ESACT (European Society for Animal Cell Technology) Meeting, Edinburgh, United Kingdom.

Research projects in the area of biochemical engineering require close cooperation with other specialists and experts. The cell lines CHO-K1 and CHO DP12 were kindly provided by the cell culture technology group at Bielefeld University (Thomas Noll, Bielefeld, Germany).

Contents

1	Intro	duction	1
	1.1 Re	combinant biopharmaceuticals	1
	1.2 Ch	nese hamster ovary (CHO) cells	1
	1.3 Ke	y aspects of CHO cell metabolism	2
	1.4 Ov	erview of CHO cell culture processes	3
	1.5 Ob	jectives and overview	4
2	Mate	rial and Methods	6
	2.1 Ce	l lines and culture media	6
	2.2 Ce	l passaging and pre-cultures	6
	2.3 Ma	in-culture experiments	7
	2.3.1	Microtiter plate (MTP) cultivations	7
	2.3.2	Shake flask cultivations	8
	2.3.3	STR cultivations	8
	2.4 Mo	nitoring of the OTR	9
	2.5 De	termination of offline parameters	9
	2.5.1	Sample preparation	9
	2.5.2	VCD and viability	. 10
	2.5.3	Glucose and lactate concentrations	. 10
	2.5.4	Glutamine concentration	. 10
	2.5.5	Antibody concentration	. 10
	2.6 Kill	curve experiments	. 11
	2.7 Tes	st of antifoam agents	. 12
	2.8 Ca	culations and correlations	. 13
	2.8.1	Determination of P/V, ε , Re, and $\lambda_{\rm K}$ in shake flasks	. 13
	2.8.2	Determination of μ_{max}	. 14

	2	.8.3	Determination of cell-specific production and uptake rates	. 14
	2	.8.4	Correlations of metabolites, μ , and the antibody concentration with $\pmb{\varepsilon}_{\varnothing}$.	. 14
	2	.8.5	Calculation of OTR _{max} in shake flasks and 96-deep-well MTPs	. 15
	2	.8.6	Calculation of OTR, OTR _{max} , k _L a, and Ne in STRs	. 15
3	С	НО	cell characterization by online monitoring of the OTR	. 17
	3.1	Bac	kground	. 17
	3.2	Cor	mparison of different media	. 18
	3.3	Cha	aracterization of different CHO cell lines	. 19
	3.4	Sun	nmary	. 24
4	A	naly	sis of hydromechanical stress on CHO cells in shake flasks	. 25
	4.1	Bac	kground	. 25
	4.2	Influ	uence of varying $arepsilon_{\varnothing}$ on the OTR of CHO DP12 shake flask cultivations	. 28
	4.3	Influ	uence of varying $oldsymbol{arepsilon}$ on the metabolism	. 31
	4.4	Influ	uence of varying $oldsymbol{arepsilon}_{arnothing}$ on the antibody production	. 35
	4.5	Sun	nmary	. 37
5	S	cale	-down of CHO cell cultures to 96-deep-well MTPs	. 38
	5.1	Bac	kground	. 38
	5.2	Tra	nsfer of online monitoring to 96-deep-well MTPs	. 41
	5.3	Min	imal filling volume for CHO cell cultivations in 96-deep-well MTPs	. 44
	5.4	App	olication example: different amounts of the media component glutamine .	. 47
	5.5	App	lication example: kill curve experiments	. 51
	5	.5.1	Online monitoring of kill curve experiments in shake flasks	. 51
	5	.5.2	Online monitored kill curve experiments in 96-deep-well MTPs	. 54
	5	.5.3	Transfer of the MTP kill curve method to a second antibiotic	. 57
	5.6	Sun	nmary	. 60
c		مامد	up of CHO calle from MTD to a STD	G

9	Α	Appendix	99
8	В	Bibliography	80
7	С	Conclusion and outlook	76
	6.5	Summary	74
	6.4	Scale-up of CHO cell cultivations to a STR with constant P/Vø	70
	6.3	Scale-up from small shaken vessels to a STR based on OTR _{max}	67
	6.2	Influence of antifoam on the OTR of CHO cell cultures	65
	6.1	Background	62

Abbreviations

μΤΟΜ Micro(μ)-scale Transfer-rate Online Measurement device

BHK21 Baby hamster kidney cells
CFD Computational fluid dynamics
CHO Chinese hamster ovary cells
DHFR Dihydrofolate reductase

DMSO Dimethylsulfoxide GOI Gene of Interest

GS Glutamine synthetase

HEK Human embryonic kidney cells

MTP Microtiter plate MTX Methotrexate

NS0 Murine myeloma cells
OTR Oxygen transfer rate
OUR Oxygen uptake rate

PBS Phosphate-buffered saline

PGG Polypropylenglycol

PTM Post-translational modification

R Coefficient of determination

Shaking frequency

RAMOS Respiration activity monitoring system

rpm Revolutions per minute
STR Stirred tank reactor
TCA Citric acid cycle

TOM Transfer-rate Online Measurement device

Symbols and units

μ	Specific growth rate	s ⁻¹
$\mu_{\sf max}$	Maximal specific growth rate	s ⁻¹
d	Maximum inner flask diameter	m
d sт	Stirrer diameter	m
d_0	Shaking diameter	cm
d _R	Reactor diameter	m
€ max	Maximal energy dissipation rate	W kg ⁻¹
ε Ø	Average energy dissipation rate	W kg ⁻¹
g	Gravitational acceleration	m s ⁻²
k∟a	Volumetric mass transfer coefficient	h ⁻¹
L_{O2}	Oxygen solubility	mol L ⁻¹ bar ⁻¹
η	Dynamic viscosity of a fluid	Pa s

rpm or s⁻¹

n _{ST}	Stirrer speed	s ⁻¹
Ne'	Modified Newton number for shake flasks	-
Ne	Newton number (power number)	-
Ne _{gassed}	Gassed Newton number (power number)	-
Ne _{ungassed}	Ungassed Newton number (power number)	-
Osmol	Osmolality	Osmol kg ⁻¹
OTR	Oxygen transfer rate	mmol L ⁻¹ h ⁻¹
OTR _{max}	Maximal oxygen transfer rate	mmol L ⁻¹ h ⁻¹
P/V	Volmetric power input	kW m ⁻³
P/Vø	Average volumetric power input	kW m ⁻³
P/V_{max}	Maximal local volumetric power input	kW m ⁻³
р	Pressure	bar
p _R	Reactor pressure	bar
q	Cell-specific production or uptake rates	pmol cells ⁻¹ d ⁻
q _{in}	Volumetric gas flow rate at standard conditions	vvm
_	at reactor inlet	
q out	Volumetric gas flow rate at standard conditions at reactor outlet	vvm
Re	Reynolds number	_
RQ	Respiratory quotient	_
Ug	Superficial gas velocity	m s ⁻¹
VCD	Viable cell density	cells mL ⁻¹
V_L	Filling volume	m^3
V_{m}	Molar gas volume at standard conditions	L mol ⁻¹
y* 02	Oxygen mole fraction in the gas phase	mol mol ⁻¹
y∟	Oxygen mole fraction equivalent to the dissolved oxygen in the liquid	mol mol ⁻¹
y O2,out	Oxygen mole fraction at the reactor outlet	mol mol ⁻¹
y O2,in	Oxygen mole fraction in the gas supply	mol mol ⁻¹
λк	Kolmogorov's length of microscale	μm
V	Kinematic viscosity	m ² s ⁻¹
ρ	Liquid density	kg m ⁻³

List of figures

Figure 1:	Experimental strategy for kill curve experiments.	12
Figure 2:	Oxygen transfer rate (OTR) of CHO cells in two different media	18
Figure 3:	Characterization of sciCHO and CHO-K1 cells	20
Figure 4:	Cultivation of CHO DP12 cells in shake flasks under standard conditions.	22
Figure 5:	Cultivation of CHO DP12 cells in shake flasks with varying average energy dissipation rates (ϵ_{\varnothing})	30
Figure 6:	Correlation of the maximal specific growth rate (μ_{max}) and the time of glucose and glutamine depletion to varying average energy dissipation rates (ϵ_{\varnothing}).	32
Figure 7:	Analysis of the lactate concentration at varying average energy dissipation rates (ϵ_\varnothing)	34
Figure 8:	Correlation of the final antibody concentration to the logarithm of varying average energy dissipation rates (ϵ_{\varnothing})	36
Figure 9:	Parallel cultivation of CHO-K1 cells in round 96-deep-well microtiter plates and shake flasks	41
Figure 10:	Oxygen transfer rate (OTR) of CHO DP12 cell cultures in shake flasks and microtiter plates.	43
Figure 11:	Cultivation of CHO DP12 cells in round and square 96-deepwell microtiter plates with varying filling volumes	45
Figure 12:	Oxygen transfer rate (OTR) of CHO DP12 cells with varying initial glutamine concentrations	48
Figure 13:	Final antibody concentrations for CHO DP12 cultivations with different initial amounts of glutamine.	50
Figure 14:	Kill curves of CHO-K1 cells in shake flasks with varying concentrations of the antibiotic puromycin	52
Figure 15:	Kill curves of CHO-K1 cells and sciCHO cells in round 96-deep-well microtiter plates with varying concentrations of the antibiotic puromycin.	55
Figure 16:	Kill curves of CHO-K1 and sciCHO cells in a round 96-deep- well microtiter plate with varying concentrations of the antibiotic hygromycin B	58

Figure 17:	Influence of different antifoam agents on the oxygen transfer rate (OTR) of CHO DP12 cells	5
Figure 18:	OTR _{max} -based scale-up of CHO DP12 cell cultivations 68	8
Figure 19:	Scale-up of CHO DP12 cell cultivations with constant P/Vø 7	1
Figure 20:	Offline measured metabolite and product concentrations of the cultivations shown in Figure 19	3
App. Figure 1:	Cultivation of CHO DP12 cells in shake flasks under standard conditions (independent repetition of the experiment in Fig 1) 99	9
App. Figure 2:	Viable cell density and viability of CHO DP12 cells in shake flasks with varying average energy dissipation rates ($\epsilon \varnothing$) 100	0
App. Figure 3:	Mean oxygen transfer rate of CHO DP12 cells in shake flasks with varying average energy dissipation rates (ϵ_{\varnothing})	1
App. Figure 4:	Cultivation of CHO DP12 cells in shake flasks with variation of shaking frequencies	2
App. Figure 5:	Glutamine and glucose concentrations of CHO DP12 cell cultivations in shake flasks with varying average energy dissipation rates (ϵ_{\varnothing}).	3
App. Figure 6:	Cell-specific production and uptake rates of CHO DP12 cell cultivations in shake flasks with varying average energy dissipation rates ($\epsilon \varnothing$)	4
App. Figure 7:	Antibody concentrations of CHO DP12 cell cultivations in shake flasks with varying average energy dissipation rates ($\epsilon \varnothing$) 105	5
App. Figure 8:	Reproducibility of oxygen transfer rate (OTR) determination of CHO-K1 cell cultures	6
App. Figure 9:	Oxygen transfer rate (OTR) of CHO DP12 cell cultures. Figure 10 with the corresponding standard deviations indicated as shaded areas	7
App. Figure 10:	Oxygen transfer rate (OTR) of CHO DP12 cell cultures monitored by the µTOM device with different filling volumes 108	8
App. Figure 11:	Original oxygen transfer rate (OTR) data of kill curves including the outliers due to temperature adaptations after medium exchange	9
App. Figure 12:	Experimental strategy used with the antibiotic hygromycin B 110	0

App. Figure 13:	cultivations	111
App. Figure 14:	Offline measured metabolite and product concentrations of the cultivations shown in Figure 18	112
List of tables	S	
Table 1:	Characteristic parameters of shake flask cultivations	. 29
Table 2:	Summarized antibiotic concentrations, at which all untransfected cells were killed in the experiments performed in this study.	. 59
App. Table 1:	OTR _{max} values for different filling volumes in round 96-deep-well microtiter plates	113
App. Table 2:	Variables for calculation of the scale-up parameters	114

1 Introduction

1.1 Recombinant biopharmaceuticals

The market share of biopharmaceuticals in the overall pharmaceutical market in Germany in 2022 was 32.9 % (17.8 billion €). 59 % of all newly approved pharmaceuticals were biopharmaceuticals (Lücke and Bädeker, 2023). This reflects the global trend of the increasing importance of biopharmaceuticals in recent years (Walsh and Walsh, 2022). Since the production of insulin as the first recombinant protein in 1982, it has expanded to many product classes. Products include proteins, monoclonal antibodies, growth factors, antisense oligonucleotides for gene and stem cell therapies, and bi- and tri-specific monoclonal antibodies (Crommelin et al., 2020; Wurm, 2004). Most of these products are produced in mammalian cell cultures. Commonly used cell lines are Chinese hamster ovary (CHO) cells, Baby hamster kidney (BHK21) cells, and Murine myeloma (NS0) cells. CHO cell lines are among the most used mammalian expression systems today (Kim et al., 2012; Li et al., 2010). At first glance, the choice of mammalian systems for large-scale production does not seem to be sensible, as they are much more difficult to cultivate than bacteria or yeasts, for example. They have a comparatively large doubling time and require expensive cultivation media (Sindelar et al., 2013). However, they have a decisive advantage, which is due to the formation of human-like post-translational modifications (PTMs) (Lalonde and Durocher, 2017). Disulfide bridges between cysteine residues and glycosylation are particularly important to avoid immune responses in patients (Walsh and Walsh, 2022).

1.2 Chinese hamster ovary (CHO) cells

CHO cell lines are of particular importance for biopharmaceuticals, as they account for around 70-80 % of all proteins produced (Lemire et al., 2021; Li et al., 2010). The origin of CHO cells dates to 1957 when Puck first isolated cells from the ovary of an adult Chinese hamster (Tjio and Puck, 1958). Since then, numerous sub-cell lines have been developed and were adapted to growth in suspension. Three of the major cell lines are CHO-K1, CHO DG44, and CHO-S cells (Lewis et al., 2013). Nowadays, CHO cells are

mainly used for the production of recombinant proteins and antibodies (Kunert and Reinhart, 2016). They have additional advantages compared to other mammalian expression systems such as BHK21 or NS0 cells. They grow in suspension and are therefore more easily scalable than adherent cell systems. For CHO cells, there are chemically defined, serum-free media for cultivation that ensure biologically safe and reproducible production and enable high productivity (Dumont et al., 2016). In addition, CHO cells are relatively tolerant to fluctuations in process parameters such as pH, temperature, pressure, or oxygen level shifts. Thanks to many years of experience in production processes with contamination profiles and the low susceptibility of CHO cells to viral infections, there is also a certain degree of safety in the production processes (Kim et al., 2012; Lai et al., 2013).

1.3 Key aspects of CHO cell metabolism

CHO cells are immortalized cells and therefore exhibit typical characteristics of fastgrowing / tumor cells. The main carbon source is glucose. In normal mammalian cells, glucose is metabolized to pyruvate and supplied to the citric acid cycle (TCA) to produce energy in oxidative phosphorylation. Immortalized cells take up much more glucose than normal cells and exhibit increased rates of glycolysis (Ferguson and Rathmell, 2008). This is known as aerobic glycolysis or Warburg effect (Warburg, 1956). At the molecular level, pyruvate kinase is present in its dimeric form in immortalized cells. This means that it has a low affinity for its substrate phosphoenolpyruvate. Phenotypically, this leads to the intermediate products from glycolysis being used for the production of macromolecules (amino acids, phospholipids, nucleotides, etc.) (Jang et al., 2013; Mazurek et al., 2005). Pyruvate is converted into lactate and not supplied to the TCA cycle. As a result, only 2 ATP instead of 36 ATP are obtained from one molecule of glucose (Park et al., 2022). This is a fast but inefficient method of energy production. Nevertheless, this is advantageous for fast-growing cells, as they have to make a compromise between energy production and molecule supply (Ferguson and Rathmell, 2008). To compensate for the loss of energy from aerobic glycolysis, immortalized cells have a second way of generating energy and a second crucial carbon source: glutamine. Depending on the cell line, the culture conditions and the physiological state of the cells about 35 % of energy comes from glutamine (Park et al., 2022). Glutamine is metabolized into glutamate and ammonium. Glutamate is then converted to α -ketoglutarate and supplied to the TCA cycle. It is subsequently used for energy generation (Mazurek, 2011). Ammonium is built as a byproduct and has different negative effects on CHO cell cultures like a decrease in specific cell growth or antibody production (Pereira et al., 2018). Many CHO cells additionally undergo another phenomenon, which is called lactate switch. After a phase of lactate production, it is consumed again. The mechanism behind is not fully understood but different studies dealt with the cause of lactate switch. Hartley et al. (2018) summarized those studies. Some of them suggest that lactate consumption begins when glucose is low or depleted, others suggest that it starts when glutamine is depleted or that it is triggered by the extracellular lactate concentration. However, the lactate switch has a good positive correlation with the phenotype of high glycoprotein productivity (Park et al., 2022).

1.4 Overview of CHO cell culture processes

Nowadays, the cultivation of CHO cells in suspension cultures is well-established for the production of biopharmaceuticals (Sharker and Rahman, 2021). Industrial cell culture processes are conducted in sizes of up to 10 000 L and achieve cell-specific productivities up to about 20 pg cell⁻¹ day⁻¹ (Kim et al., 2012; Li et al., 2010). In order to achieve these dimensions, research was carried out in various areas of cell culture processes over the past decades. A fundamental understanding of processes is crucial to enhancing robustness and product quality. The main areas of cell culture process understanding comprise: 1. cell line engineering and clone selection, 2. media formulations and improvements, 3. bioreactor culture conditions in small and larger scales, 4. online and offline sensors providing valuable information about the process, 5. good process understanding to enable scale-up, 6. downstream applications (Li et al., 2010). Over decades, extensive efforts in CHO cell line engineering have aimed to increase productivity and product quality by enhancing cell growth, viability, and stress resistance. Early strategies focused on overexpressing beneficial genes and inhibiting or deleting disadvantageous genes. Recent approaches include methods to improve responses to stress and enhance protein production. Additionally, targeted gene

knockouts or gene integration enables efficient cell line generation. An elaborate step is clone selection after cell line engineering as this requires high-throughput instruments (Tihanyi and Nyitray, 2020; Zhang et al., 2022). The use of serum-free, chemically defined media is standard for CHO cell cultivations nowadays. Platform media are usually utilized for initial screenings. Afterward, well-polished media compositions are developed for each process. As there are many components in the medium and interactions are crucial, medium optimization is still a time- and laborintensive work (Ling, 2020; Ritacco et al., 2018). Bioreactor conditions are decisive for a robust and reproducible process. The main parameters to monitor and control are temperature, oxygen availability, agitation and aeration, hydromechanical stress, CO₂ concentration, pH value, osmolality, viable cell density (VCD), viability, and metabolites (Li et al., 2010; O'Brien and Hu, 2020). There are well-established methods to monitor all of them. However, many of those parameters are routinely monitored offline by sampling. To streamline processes, there are numerous efforts to invent online or atline monitoring solutions – for example, Raman probes, capacitance sensors, or nearinfrared spectroscopy (Kambayashi et al., 2020; Metze et al., 2020; Tanemura et al., 2023). Understanding the process is not only important to keep productivity and product quality constant, but also for scaling up processes. It is mandatory to achieve comparable conditions at all scales - from small shaken systems for screening approaches to large production scale reactors - to keep growth, productivity, and product quality constant over scales. A common tool to study the conditions is scaledown models (Lemire et al., 2021; Li et al., 2010).

All in all, CHO cell culture processes are well-established and robust. However, there are still numerous possibilities to improve processes and reduce production costs. Currently, research focuses on developing high-throughput systems, inventing new online process monitoring and control systems, and, the usage of disposable systems (Li et al., 2010).

1.5 Objectives and overview

As was shown in previous chapters, CHO cell culture processes are well established but there are still opportunities to improve processes. This is where this thesis comes in. The aim is to apply online monitoring of the oxygen transfer rate (OTR) to mammalian systems at different scales – enabling high-throughput measurements and data-driven scale-up processes.

The first step was to characterize the CHO cell cultures used in this thesis by online monitoring of the respiration activity in shake flasks (Chapter 3). Two different commercially available media were tested, and three different CHO cell lines were compared (CHO-K1, sciCHO, and CHO DP12).

One decisive parameter that influences mammalian cell culture processes is hydromechanical stress. Therefore, the CHO DP12 cell's behavior to varying hydromechanical stress levels in shake flasks was investigated (Chapter 4). Energy dissipation rates were varied and the impact on the cells' activity and metabolism was studied by online monitoring of the OTR. Antibody production was further analyzed.

For monitoring the OTR, a device is available that enables measurement in 96-deep-well microtiter plates called the micro(μ)-scale Transfer-rate Online Measurement (μ TOM) device (Dinger et al., 2022). As this represents a high-throughput variant of OTR monitoring, the application of the device was transferred to CHO cell cultures, and a scale-down of the processes from the shake flask was carried out (Chapter 5). The possibilities of μ TOM applications in media development issues were shown by analyzing different glutamine concentrations. Furthermore, kill curve experiments were scaled down from shake flasks to 96-deep-well microtiter plates showing its application in screening processes and the field of cell line development.

Finally, the topic of scale-up was addressed (Chapter 6). With the knowledge of the studies on hydromechanical stress (Chapter 4) and the OTR monitoring of cell cultures (Chapters 3 and 5), a data-driven scale-up to a stirred tank reactor (STR) was performed showing comparability between three orders of magnitude.

2 Material and Methods

2.1 Cell lines and culture media

In this study, two non-producing CHO cell lines were used. Cell line one is a CHO-K1 cell line (strain ATCC 61-CCL), which was adapted to suspension. Cell line two was obtained from Cell Lines Services GmbH (Eppelheim, Germany) as a suspension cell line and is named sciCHO. According to the manufacturer, the sciCHO cell line was derived from a non-engineered CHO-K1 subclone and was tested and optimized for stable and transient transfection. Moreover, the suspension-adapted cell line CHO DP12 (clone#1934, ATCC CRL-12445) was utilized as a model production cell line. It produces an anti-IL-8 antibody.

All cell lines were cultured in the chemically defined TCX6D medium (Sartorius, Goettingen, Germany). It was supplemented with 8 mM glutamine (Sigma Aldrich/Merck, Darmstadt, Germany) for all cell lines unless otherwise specified. For the CHO DP12 cell line, 200 nM methotrexate (MTX, Sigma Aldrich/Merck) was added to the pre-cultures to prevent the transgene's loss. MTX was not supplemented to main-culture experiments. Pre- and main-cultures of the CHO-K1 and sciCHO cells were cultivated in the medium SciNX (Cell Lines Service GmbH) supplemented with 8 mM of glutamine for one experiment (Chapter 3.2).

2.2 Cell passaging and pre-cultures

Vials of all cell lines were stored in the vapor phase of liquid nitrogen. For that, $1x10^7$ cells were resuspended in 1.5 mL of freezing medium including 90 % (v/v) TCX6D medium and 10 % (v/v) dimethylsulfoxide (DMSO) (Sigma Aldrich/Merck). The cell suspension was transferred to cryovials. The vials were frozen with a cooling rate of -1°C min⁻¹ in a Nalgene Mr FrostyTM freezing container (Thermo Fisher Scientific, Waltham, USA) in a -80°C freezer. After 24-48 h the vials were transferred to the liquid nitrogen vessel.

Before cultivations, one vial was rapidly thawed and immediately transferred to 10 mL of phosphate-buffered saline (PBS) (Carl Roth, Karlsruhe, Germany) to remove toxic

DMSO by washing the cells. The suspension was centrifuged at 200 g for 7 min (Rotina 35 R with a swing-out rotor, Hettich, Tuttlingen, Germany). The supernatant was discarded under sterile conditions and the cells were resuspended in 15 mL fresh culture medium. All cell lines were cultured in 250 mL Corning polycarbonate Erlenmeyer flasks (Corning, Glendale, USA) with a vent-cap. The cultivations were carried out in an incubator (ISF1-X Kühner AG, Birsfelden, Switzerland) under controlled conditions (36.5°C, 70 % humidity and 5 % CO₂). The shaking frequency on the orbital shaker was set to 140 rpm with a 50 mm shaking diameter. Some precultures used for the experiments in Chapter 4 were performed on a Kuhner LSBshaker (Kühner AG). Cells were cultivated in 250 mL glass TOM flasks (Kühner AG). Every glass flask was flushed with a gas mixture of 5 % CO₂ in synthetic air (ca. 19.95 % O₂ and 74.1 % N₂) by an in-house built construction. The temperature was set to 36.5°C. The CHO-K1 cell line was split every 2-3 days to a seeding cell density of 1.5x10⁵ cells mL⁻¹, and the sciCHO and CHO DP12 cell lines were split every 3-4 days to a seeding cell density of 3.0x10⁵ cells mL⁻¹. The filling volumes of the 250 mL flasks were between 20-50 mL.

2.3 Main-culture experiments

All main-culture experiments were started from the shake flask pre-cultures (Chapter 2.2). The seeding cell density was set to 5x10⁵ cells mL⁻¹. All experiments were performed at 36.5°C.

2.3.1 Microtiter plate (MTP) cultivations

The MTP cultivations were all conducted in the μ TOM device (Dinger et al., 2022) which was mounted in a Kuhner ISF1-X incubator (Kühner AG). Shaking conditions were set to 850 rpm at 3 mm shaking diameter. The μ TOM device was flushed with gas from a gas cylinder (5 % CO₂ in synthetic air with ca. 19.95 % O₂ and 74.1 % N₂). To prevent evaporation, the gas was humidified through a washing bottle. For cultivations, 96-deep-well MTPs were used and sealed with a sterile cover (AreaSeal film, Excel Scientific, Victorville, USA). In this study, round well plates (Round-Deep

well plate, 96 U-bottom well, rimless, height 42.4 mm; VWR, Darmstadt, Germany) and square-well plates (Riplate® SW 96, PP, 2 mL; Ritter, Schwabmünchen, Germany) were used. Both MTPs were equipped with U-bottoms. Different filling volumes from 200 μ L to 1000 μ L were used. If offline analyses (Chapter 2.5) were performed, 3 wells per condition were sampled from the MTP in the μ TOM device. The MTP was then placed back into the device and cultivated further.

2.3.2 Shake flask cultivations

The main-cultures were all carried out in the Kuhner incubator ISF1-X and were online monitored by the Transfer-rate Online Measurement (TOM) device (Kühner AG). All cultivations were performed at 36.5°C, 70 % humidity, and 5 % CO₂. According to the experiment, 100, 250, or 500 mL glass flasks were used. The 100 and 500 mL standard Erlenmeyer flasks (DWK LifeScience, Wertheim, Germany) were closed with flex caps (Kühner AG). The 250 mL flasks were TOM flasks (Kühner AG). The filling volume for all flasks was 20 % of the nominal flask volume. Standard shaking conditions were 140 rpm at 50 mm shaking diameter. According to the experiment, the shaking frequency was varied from 140 to 450 rpm, and the shaking diameter was set to 50 or 25 mm respectively. For each experiment, six shake flasks were connected to the Kuhner TOM device (Kühner AG). Three of these were used solely for online monitoring. The other three were sampled daily (1.5 mL) for offline analyses (Chapter 2.5).

2.3.3 STR cultivations

The STR cultivations were performed in a 1.5 L Applikon ez2-Control reactor (Getinge, Gothenburg, Sweden). The filling volume was 600 mL. The aeration rate was set to 0.2 vvm using a ring sparger and a gas mixture of 5 % CO₂ in synthetic air (ca. 19.95 % O₂ and 74.1 % N₂). The reactor was equipped with a single six-blade Rushton turbine. The stirrer speed was set to 360 rpm for the first cultivation (Chapter 6.3) and between 100 and 250 rpm for the second one (Chapter 6.4). The calculation of the stirrer speed is described in Chapter 2.8.6. The dissolved oxygen tension (DOT) was measured with an Applikon LumiSens sensor (Getinge). Antifoam SE15 (Sigma

Aldrich/Merck) was diluted at 1:10 and added on demand. Samples were taken daily for offline analyses (Chapter 2.5).

2.4 Monitoring of the OTR

The OTR was monitored in all main-culture experiments in MTPs and shake flasks. For shake flask cultivations, the Kuhner TOM device (Kühner AG) was used which is a slightly modified commercial version of the RAMOS (Respiration activity monitoring system) system (Anderlei et al., 2004; Anderlei and Büchs, 2001). The OTR monitoring in the 96 deep-well MTPs was conducted in the µTOM device (Dinger et al., 2022). The measuring principles of both devices are similar and described elsewhere (Anderlei and Büchs, 2001; Dinger et al., 2022). The stop or measuring phase was set to 18 min in the TOM device and to 20 min in the µTOM device. The entire measuring cycle (stop and flow phases) was 60 min in both devices. These settings were proposed by Ihling et al. (2021) who showed the adaptation of the OTR monitoring technique from microbial cultivations to mammalian cells. They also demonstrated that slightly different measuring phases (like 18 and 20 min) resulted in very comparable OTR results. The calculation of the OTR is temperature-dependent. Consequently, outliers in the OTR occur after opening the incubator hood for sampling. Those outliers were removed from the data and excluded from graphs and further analyses. For the STR cultivations, the off-gas analysis BlueVary (BlueSense, Herten, Germany) was utilized to measure the oxygen and carbon dioxide concentrations which were then used to calculate the OTR.

2.5 Determination of offline parameters

2.5.1 Sample preparation

The culture broth of the main-cultures (Chapter 2.3) was used directly after sampling for determination of VCD and viability (Chapter 2.5.2). The leftover culture broth was centrifuged at 2000 g for 3 min (mini centrifuge Rotilabo, Carl Roth). For further analyses, the supernatant was stored at -20°C.

2.5.2 VCD and viability

VCD and viability were either determined by the Neubauer Chamber method or with a CEDEX AS20 device (Roche, Basel, Switzerland), both using the trypan blue exclusion method. For the Neubauer Chamber method, samples were stained with erythrosin B, which works equal to trypan blue but is not toxic. The average of four quadrants manually counted with a Neubauer Chamber (C-Chip, Neubauer improved, Carl Roth) was utilized to calculate VCD and viability. The samples measured by the CEDEX were automatically stained with 1:2 diluted Trypan Blue Solution (Gibco/Thermo Fisher Scientific).

2.5.3 Glucose and lactate concentrations

Glucose and lactate concentrations in the supernatant were determined by an HPLC method. An organic acid resin column (Rezex ROAOrganic Acid H+ (8 %), 300 × 7.8 mm, Phenomenex Inc., Torrance, USA) was used for separation. The flow rate was set to 0.8 mL min⁻¹ and temperature to 40°C. 5 mM H₂SO₄ was used as the mobile phase and the isocratic mode for separation. For detection, a refractive index detector (RefractoMax 520, Shodex, Munich, Germany) was utilized. The HPLC system was the Dionex Ultimate 3.000 system (Thermo Scientific).

2.5.4 Glutamine concentration

To determine glutamine concentrations in the supernatant, the kit L-Glutamine / Ammonia (*Rapid*) (Megazyme Ltd., Bray, Ireland) was used according to the manufacturer's instructions.

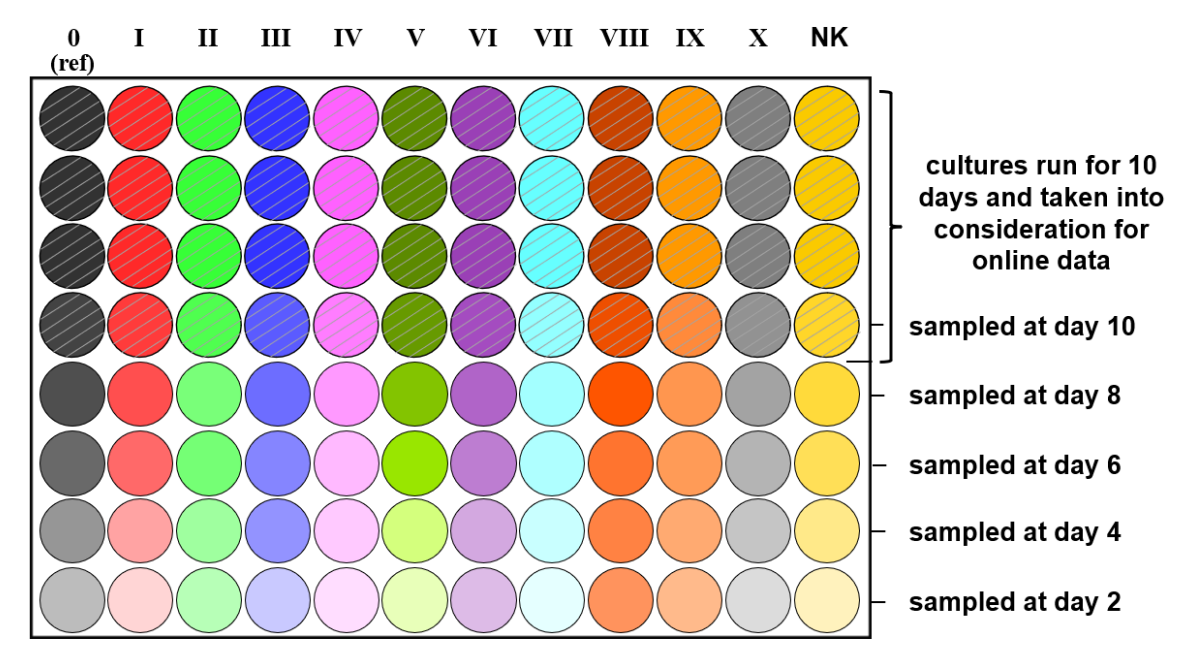
2.5.5 Antibody concentration

For determination of the IgG antibody concentration in the supernatant, a Chromolith® Protein A column (4.6 x 25 mm, Sigma Aldrich/Merck) with a pore size of 300 Å was used with an in-house protocol.

2.6 Kill curve experiments

Kill curve experiments are an intermediate step in mammalian cell line generation. If antibiotics are used for selection, the minimal concentration to kill the untransfected parental cell line is to be determined (see also Chapter 5.1). In this study, kill curve experiments were either conducted in 100 mL shake flasks or 96-deep-well MTPs. The general cultivation conditions and the OTR online monitoring are described above (Chapters 2.3 and 2.4). Only the antibiotics puromycin (InvivoGen, San Diego, USA) or hygromycin B (Carl Roth) were added to the medium in various concentrations at the beginning of the cultivation. In the following, the medium exchange is described. For shake flask experiments, the cell suspension was transferred to a 50 mL tube and centrifuged (Rotina 35 R, Hettich) for 7 min at 200 g every second day. The supernatant was discarded under sterile conditions and the pellet was resuspended in fresh medium supplemented with 8 mM glutamine and varying concentrations of antibiotics. Samples for offline analysis were taken from 100 mL glass offline shake flasks, which were cultured in parallel in the same incubator and under the same conditions as the online monitored shake flasks.

For MTP experiments, 11 antibiotic concentrations were added in 8 replicates. Another 8 wells were filled only with TCX6D medium as a negative control (Figure 1). Every second day, the plate was centrifuged at 1150 g for 5 min. The supernatant was discarded under sterile conditions and the cell pellets were resuspended in fresh medium supplemented with 8 mM glutamine and varying concentrations of antibiotics (Figure 1). With every medium exchange, one well per condition was sampled for analysis of VCD and viability (Chapter 2.5.2).



Culture wells with 11 different antibiotic concentrations (0-X) and a negative control (NK) in 8 replicates

Figure 1: Experimental strategy for kill curve experiments. One kill curve experiment in a 96-deep-well microtiter plate was conducted with 11 different antibiotic concentrations (0-X), including one reference (ref.) with no antibiotic in eight replicates. Another eight wells were used as negative control (NK, yellow) with non-inoculated medium. Every two days, one well per antibiotic concentration was sampled for offline analysis. Afterward, the medium was exchanged for the remaining wells. A total of four wells per concentration (diagonal-hatched) ran over the entire cultivation time of 10 days. Those four wells were taken into consideration for the online monitored oxygen transfer rate (OTR) in the μTOM device.

2.7 Test of antifoam agents

In this study, different types of antifoams were tested, namely: Pluronic F68 (Gibco), Antifoam SE15 (Sigma Aldrich/Merck), Triton X405 (Sigma Aldrich/Merck, Plurafac LF1300 (BASF, Ludwigshafen, Germany) and Polypropylenglycol (PGG, Carl Roth). Pluronic F68 was bought as pre-sterilized 10 % solution. All other antifoam agents were diluted at 1:10 and sterilized. The antifoam was added to cell suspensions with a cell density of 5x10⁵ cells mL⁻¹ in round 96-deep-well MTPs in dilutions from 1:50 to 1:10 000. The MTP was cultivated and online monitored in the μTOM device.

2.8 Calculations and correlations

2.8.1 Determination of P/V, ε , Re, and λ_K in shake flasks

The volumetric power input (P/V) in shake flasks (Equation (1)) was calculated according to Büchs et al. (2000) including the modified Newton number for shake flasks (Ne'), the liquid density (ρ) [kg m⁻³], the shaking frequency (n) [s⁻¹], the maximum inner flask diameter (d) [m], the filling volume (V_L) [m³] and the power (P) [W].

$$\left(\frac{P}{V}\right)_{\emptyset} = Ne' \times \rho \times \frac{n^3 \times d^4}{V_L^{2/3}} \text{ with } Ne' = \frac{P}{\rho \times n^3 \times d^4 \times V_L^{1/3}}$$
 (1)

The corresponding average energy dissipation rate ($\varepsilon \varnothing$) is defined by Equation (2) according to Klöckner and Büchs (2012).

$$\varepsilon_{\emptyset} = \left(\frac{P}{V}\right)_{\emptyset} \times \frac{1}{\rho} = \text{Ne'} \times \frac{n^3 \times d^4}{V_L^{2/3}}$$
 (2)

The Reynolds number (Re) was calculated by using Equation (3) with the dynamic viscosity of a fluid (η) [Pa s].

$$Re = \rho \times \frac{n \times d^2}{\eta} \tag{3}$$

For Re > 60 000, the maximal energy dissipation rate (ε_{max}) is calculated by Equation (4) if the Froud number is > 0.4 and with the shaking diameter (d₀) (Klöckner and Büchs, 2012).

$$\varepsilon_{\text{max}} = 0.1 \left(\pi \times n \times d \right)^3 / h_1 \tag{4}$$

with
$$h_1 = 1.11 \times d_0^{0.18} \times d^{-0.11} \times n^{0.44} \times V_L^{0.34}$$
 (5)

Kolmogorov's length of microscale (λ_K) is calculated by Equation (6) with the kinematic viscosity (v) [m² s⁻¹] (Kolmogorov, 1941, 1962).

$$\lambda_{\rm K} = \sqrt[4]{\frac{v^3}{\varepsilon_{max}}} \tag{6}$$

2.8.2 Determination of μ_{max}

The calculation of the specific growth rate (μ) from the OTR is generally calculated by Stöckmann et al. (2003) as shown in Equation (7) when unlimited growth is present in the exponential growth phase and the cultivation volume does not change.

$$\mu = \frac{\ln(OTR_t) - \ln(OTR_{t_n})}{t - t_n} \tag{7}$$

All calculations in this study were performed in MATLAB[®] (Mathworks, Inc.). For calculation, the data of any individual experiment up to the OTR peak were used. The period for calculation was set to five measuring points (corresponding to 5 hours). From all calculated values the maximal specific growth rate (μ_{max}) was defined. Only data with an R² (coefficient of determination) greater than 0.9 were considered. Afterward, the mean value of the replicates was calculated (Forsten et al., 2024).

2.8.3 Determination of cell-specific production and uptake rates

The cell-specific production or uptake rates (q) [pg cells⁻¹ day⁻¹] of the metabolites (lactate, glucose, glutamine) and antibody concentrations [pg mL⁻¹] were calculated according to Equation (8) with the VCD [cells mL⁻¹].

$$q = \frac{1}{VCD} \times \frac{d \text{metabolite or antibody}}{dt}$$
 (8)

2.8.4 Correlations of metabolites, μ , and the antibody concentration with ε_{\emptyset}

The time of glutamine and glucose depletion were identified from the changes in the OTR progressions. Glutamine depletion leads to a short halt in the increase in the OTR while glucose depletion leads to a rapid fall in OTR. The times of depletion were read out by drawing a vertical straight line from the characteristic changes in the OTR to the x-axis. This method of using the OTR signal to identify depletions and limitations of nutrients has been demonstrated in several other applications for microbial cells before (Hansen et al., 2012; Kottmeier et al., 2010; Sparviero et al., 2023). In this work, the

same principle was used for CHO cells. The time of lactate depletion was determined accordingly by using offline lactate data. The time differences of depletions to the depletions in standard reference cultivations were calculated for all time points. μ_{max} was calculated as described in Chapter 2.8.2. The time differences of glucose and glutamine depletion and the lactate switch as well as μ_{max} were plotted against the logarithm of ϵ_{\varnothing} . A linear fit was applied. The antibody concentrations of the last three measurement points (three days) were averaged and plotted against the logarithm of ϵ_{\varnothing} .

2.8.5 Calculation of OTR_{max} in shake flasks and 96-deep-well MTPs

The maximum oxygen transfer capacity (OTR_{max}) in shake flasks was calculated by the empirical correlation of Meier et al. (2016) (Equation (9)).

$$OTR_{max,shake \ flask} = 3.27 \cdot 10^{-7} \cdot Osmol^{0.05} \cdot n^{(1.18 - \frac{Osmol}{10.1})} \cdot V_L^{-0.74} \cdot d_0^{0.33} \cdot d^{1.88} \cdot p_R \cdot y_{02}^*$$
(9)

Equation (9) comprises osmolality (Osmol) [Osmol kg⁻¹], shaking frequency (n) [rpm], filling volume (V_L) [mL], shaking diameter (d_0) [cm], maximum inner flask diameter (d) [mm], reactor pressure (p_R) [bar], and the oxygen mole fraction in the gas phase (y^*_{O2}) [mol mol⁻¹].

To calculate OTR_{max} in round 96-deep-well MTPs, Equation (10) by Dinger et al. (2022) can be applied.

$$OTR_{\text{max,MTP}} = 0.008 \cdot V_{L}^{-1.00} \cdot d_{0}^{0.40} \cdot n^{1.00}$$
(10)

Equation (10) comprises the filling volume (V_L) [mL], the shaking diameter (d_0) [mm], and the shaking frequency (n) [rpm].

2.8.6 Calculation of OTR, OTR_{max}, k_La, and Ne in STRs

The OTR for STRs can be calculated by a balance around the gas bubbles (Equation (11)) and by a balance around the whole reactor (Equation (12)) using the following variables: volumetric mass transfer coefficient (k_La) [h^{-1}], oxygen solubility (L_{O2}) [moL L^{-1} bar⁻¹], reactor pressure (p_R) [bar], oxygen mole fraction at the

reactor outlet $(y_{O2,out})$ [mol mol⁻¹], oxygen mole fraction equivalent to the dissolved oxygen in the liquid (y_L) [mol mol⁻¹], molar gas volume at standard conditions (V_m) [L mol⁻¹], volumetric gas flow rate at standard conditions at reactor inlet (q_{in}) [vvm], oxygen mole fraction in the gas supply $(y_{O2,in})$ [mol mol⁻¹], volumetric gas flow rate at standard conditions at reactor outlet (q_{out}) [vvm]. Using $y_{O2,out}$ in Equation(11) is correct when perfect mixing in the bioreactor can be assumed. That is a valid assumption for small bioreactors (but not necessarily for large ones).

$$OTR_{STR} = k_L a \times L_{O2} \times p_R \times (y_{O2,out} - y_L)$$
(11)

$$OTR_{STR} = \frac{1}{V_{m}} (q_{in} \times y_{O_{2},in} - q_{out} \times y_{O_{2},out})$$
 (12)

For Equation (11), the assumption of $y_L = 0$ is made as this is true when the OTR is maximal. Furthermore, RQ (respiratory quotient) is assumed to be ~1 and therefore $q = q_{in} = q_{out}$. Equation (12) is then inserted into Equation (11) to calculate OTR_{max} according to Equation (13).

$$OTR_{max,STR} = \frac{k_L a \times L_{O2} \times p_R \times q \times y_{O2,in}}{k_L a \times L_{O2} \times p_R \times V_m + q}$$
(13)

The k_L a value for STRs can be calculated according to Maier (2002) by Equation (14) with the constants C = 0.32, $\alpha = 0.74$ and $\beta = 0.42$. The superficial gas velocity u_g [m s⁻¹] is calculated by using Equation (15) (pressure (p) = 1 bar, reactor diameter (d_R) [m]).

$$k_{L}a = C \times \left(\frac{P}{V}\right)^{\alpha} \times u_{g}^{\beta} \tag{14}$$

$$u_g = \frac{q \times V_L \times p}{A \times p_R}$$
 with $A = \frac{\pi}{4} \times d_R^2$ (15)

The ungassed Newton number (Ne_{ungassed}) is almost equal to the gassed Newton number (Ne_{gassed}) for low superficial gas velocity (Möckel et al., 1990) and can be calculated by Equation (16) with the liquid density (ρ) [kg m⁻³], the stirrer speed (n_{ST}) [s⁻¹], the stirrer diameter (d_{ST}) [m⁻¹] and the filling volume (V_L) [m³].

$$Ne_{ungassed} = \frac{P_{gassed}}{\rho \times n_{ST}^3 \times d^5} = \frac{\left(\frac{P}{V}\right)_{gassed} \times V_L}{\rho \times n_{ST}^3 \times d_{ST}^5}$$
(16)

3 CHO cell characterization by online monitoring of the OTR

3.1 Background

One current field of research in CHO cell culture processes is the implementation of online monitoring methods (see Chapter 1.4). Online monitoring of some parameters is often already implemented on the STR scale to get insights into culture's behavior. For mammalian cells, online monitoring on smaller scales is not widely used. However, there are various options for small-scale cultures. For shake flasks, Maschke et al. (2022a) recently reviewed the possibilities. In general, three measurement principles can be distinguished: (i) sensor spots that are glued to the inner shake flask wall (Anderlei et al., 2020; Hanson et al., 2007; Wen-Lin Tsai et al., 2012), determining pH values as well as oxygen and carbon dioxide concentrations, (ii) backscattered light, estimating biomass concentrations (Schmidt-Hager et al., 2014; Ude et al., 2014) and (iii) off-gas analysis, measuring oxygen and carbon dioxide concentrations (Aehle et al., 2011; Anderlei et al., 2004; Anderlei and Büchs, 2001). The latter allows to determine the oxygen uptake rate (OUR). The OUR is one of the most important cultivation parameters because it provides valuable information about cell density, cell activity, and the metabolic state of the culture. The OUR can also be used for the development of bioprocesses (Martínez-Monge et al., 2019). In contrast to sensor spots, off-gas analysis is non-invasive and does not alter the culture broth. The OUR equals the OTR, as long as the oxygen concentration in the liquid does not change during measurement. This assumption was assessed to be valid for CHO cell cultures (Ihling et al., 2021). An appropriate way of monitoring the OTR in shake flasks for mammalian cells is by using the RAMOS / TOM systems (see also Chapter 2.4) (Ihling et al., 2021; Ihling et al., 2022a; Ihling et al., 2022b). The systems were intensively used for characterization of different microorganisms (Gamboa-Suasnavart et al., 2018; Ihling et al., 2018; Stöckmann et al., 2003) and recently also for CHO cells. Ihling et al. (2022a) showed that the OTR is directly correlated to the VCD. Furthermore, glucose and lactate concentrations could be calculated from the online data (Ihling et al., 2022a). The online data are, for example, useful to compare different cell lines or media leading to valuable information for further studies. Hence, the first step of this thesis was to characterize the cell lines used by online monitoring of the OTR.

3.2 Comparison of different media

The sciCHO cell line is a derivative of CHO-K1 cells. The supplier of the sciCHO cell line recommends cultivation in sciNX medium. In this medium, cell densities of only roughly $4x10^6$ cells mL⁻¹ and an OTR of approximately 0.6 mmol L⁻¹ h⁻¹ have been achieved in the past (Ihling et al., 2022a). The cell density is very low compared to other CHO cells stated in literature (Reinhart et al., 2015; Velugula-Yellela et al., 2018). To find out whether it is possible to achieve higher growth rates and VCDs for this specific cell line, the cells were cultivated in the medium sciNX and in parallel in the medium TCX6D. With this, fast growth and high maximal VCDs can be attained (Schmitz et al., 2021). As it was shown that the cell density could be directly correlated with the OTR for this cell line, the OTR was chosen as a suitable parameter to compare the two media (Ihling et al., 2022a). The OTR curves are depicted in Figure 2 A.

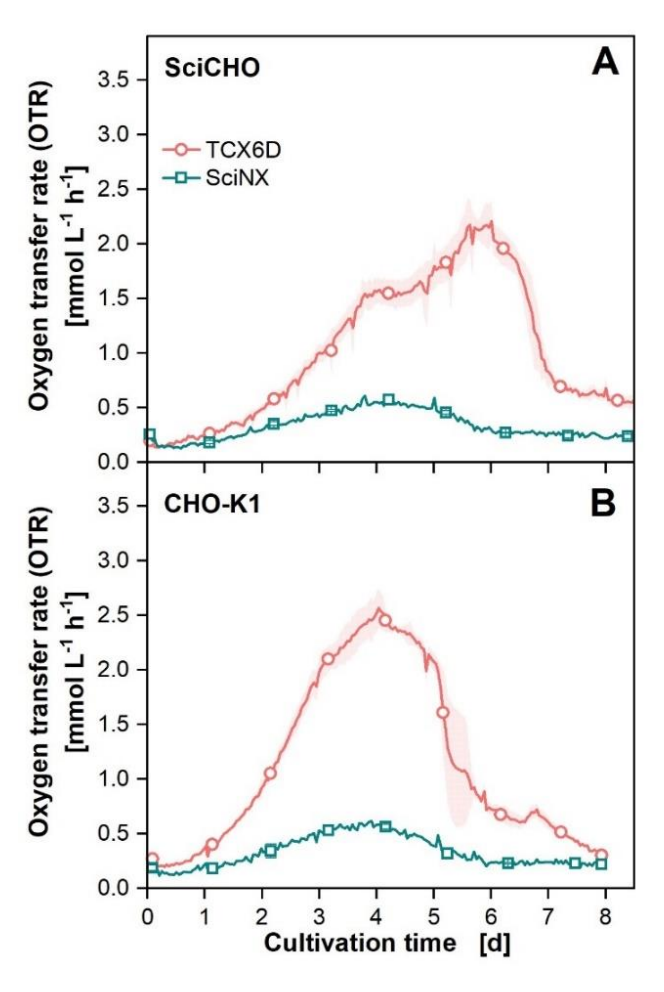


Figure 2: Oxygen transfer rate (OTR) of CHO cells in two different media. A) sciCHO cells and B) CHO-K1 cells cultivated in shake flasks in sciNX (blue line and open squares) and

TCX6D (light red line and open circles). The low standard deviations are shown as shaded areas and indicate good reproducibility. For clarity, only every 24^{th} measuring point over time is marked as a symbol. The lines are drawn through all measured values. The outliers in the OTR data due to temperature adaptations after opening the incubation hood were excluded from the data. Culture conditions TOM device: 100 mL glass flasks, temperature (T) = 36.5° C, shaking frequency (n) = 140 rpm, shaking diameter (d₀) = 50 mm, filling volume (V_L) = 20 mL, 5% CO₂, 70% rel. hum., medium: sciNX or TCX6D + 8 mM glutamine; starting cell density: $5x10^{5}$ cells mL- 1 .

The OTR curves in Figure 2 A show clearly different progressions. The cells cultivated in the medium sciNX reach a maximal OTR of about 0.6 mmol L⁻¹ h⁻¹ as reported before (Ihling et al., 2022a). The OTR increases for about 4 cultivation days and drops again for 2 days before it stays on a constant level (ca. 0.3 mmol L⁻¹ h⁻¹). In contrast, the cells in the medium TCX6D reach an OTR of about 2.1 mmol L⁻¹ h⁻¹ showing two increasing phases (from day 0 to 3.5 and from day 3.5 to 6) with different slopes visible until the maximum is reached. Afterward, there is a sharp drop of the OTR within one day. This experiment clearly showed that the cell line can reach OTRs > 0.6 mmol L⁻¹ h⁻¹ and, therefore, higher cell densities in an appropriate medium. To confirm the influence of the media, the cell line CHO-K1 was cultivated in parallel in both media. The results are illustrated in Figure 2 B and show similar results. The OTR does not exceed 0.6 mmol L⁻¹ h⁻¹ in the medium sciNX whereas an OTR of roughly 2.5 mmol L⁻¹ h⁻¹ was reached in TCX6D. The medium sciNX thus presumably lacks crucial components for higher growth. However, further investigation of media components was not part of this study. As TCX6D was shown to be an appropriate medium for both cell lines, a more detailed characterization of both cell lines is described in Chapter 3.3.

3.3 Characterization of different CHO cell lines

The growth behavior and key metabolites of the two non-producing cell lines sciCHO and CHO-K1 are illustrated in Figure 3.

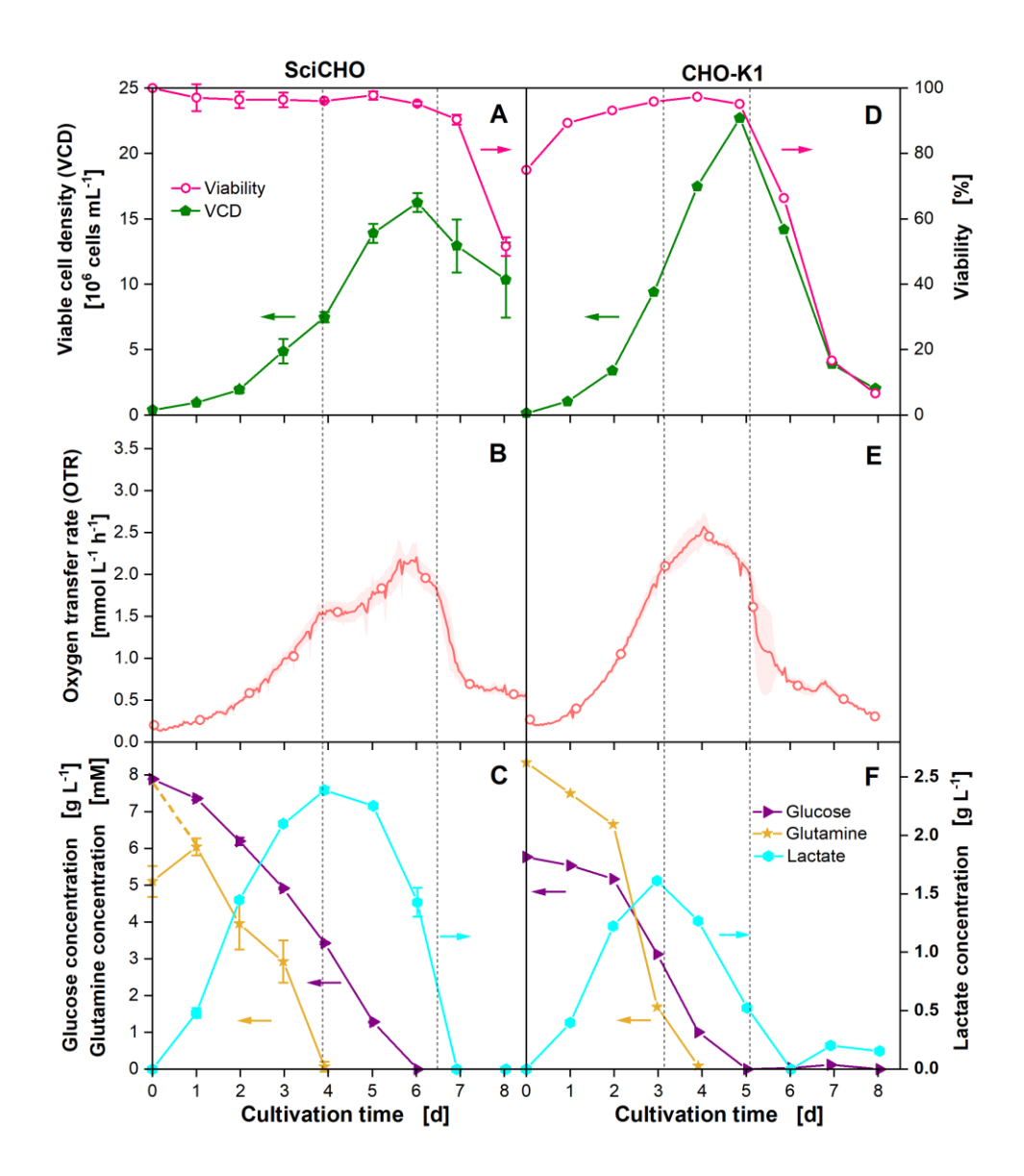


Figure 3: Characterization of sciCHO and CHO-K1 cells. Cultivation of sciCHO (A-C) and CHO-K1 (D-F) cells in shake flasks. The experiments were performed in six (sciCHO) or four (CHO-K1) replicates. Three replicates (sciCHO) / two replicates (CHO-K1) were sampled daily for offline analysis and the remaining were used for online monitoring only. Data are shown as mean values (indicated as error bars or shades for N=3). A) Depicted are the viable cell density (VCD) and the viability determined by the Neubauer Chamber method. B) Shown is the mean oxygen transfer rate (OTR) already depicted in Figure 2. C) Corresponding glucose, glutamine, and lactate concentrations are plotted over time. Depletion of glucose and glutamine is marked by dotted vertical lines over all three parts of the figure. Cultivations were performed in a TOM device. Culture conditions: 100 mL TOM glass flasks, temperature (T) = 36.5°C, shaking frequency (n) = 140 rpm, shaking diameter (d₀) = 50 mm, filling volume (V_L) = 20 mL, 5 % CO₂, 70 % rel. hum., medium: TCX6D + 8 mM glutamine; starting cell density: $5x10^5$ cells mL⁻¹.

Figure 3 A and D show the VCD and the viability of the sciCHO and CHO-K1 cultures. For sciCHO cells, the VCD increases steadily over roughly 6 cultivation days to about 1.5x10⁷ cells mL⁻¹ (green line and closed pentagons) before it drops gradually. The

viability (pink line and open pentagons) remains on a constant level above 96 % for 7 cultivation days before it decreases constantly. The VCD of the CHO-K1 cell line (Figure 3 D) increases for 5 cultivation days – almost linearly between days 2 and 5. The maximal VCD is about 2.3x10⁷ cells mL⁻¹. Afterward, the VCD drops abruptly. The viability is between 80 and 100% for the first 5 days before it drops sharply. The preculture for the CHO-K1 cells was performed in sciNX in contrast to the sciCHO cell preculture which was already done in TCX6D. Therefore, the CHO-K1 cells had to adapt to the new, better performing medium resulting in a reduced initial viability. Comparing both cell lines, the CHO-K1 cell line grows faster and to a higher maximal VCD. The OTR curves (Figure 3 B and E) are already described in Figure 2. The OTR increase for the sciCHO cell line is slower compared to the one of the CHO-K1 cell line which was also already seen for the VCDs. The maximal OTR reached is lower for sciCHO cells than for CHO-K1 cells, according to the findings for maximal VCDs. The correlation of OTR and VCD was already shown by Ihling et al. with other media and cell lines (2022a). The OTR is monitored with a 24-fold higher resolution of measuring points than the VCD (once per hour compared to once a day). This results in shoulders and kinks in the course of the OTR curve over time which are not visible in VCD and can be related to nutrient depletion. Figure 3 C and F demonstrate the relationship of the kinks and shoulders to offline parameters. The glucose concentrations (purple line and triangles) decrease over the first 6 respectively 5 cultivation days. As soon as this carbon source is exhausted, the OTR curve drops sharply. The depletion of glutamine (ochre curve and stars) after about 4 respectively 3 days of cultivation is correlated to the shoulder in the OTR curves. It should be noted that the sciCHO cell line shows a short plateau phase before the second increasing phase starts. The sciCHO cell line needs about a half day to adapt to the altered availability of nutrients before it starts growing again. This is not seen for CHO-K1 cells. Both cell lines show a typical lactate switch. Lactate increases in the first phase (until day 4 for sciCHO cells and day 3 for CHO-K1 cells). The maximal amount of lactate is about 2.4 g L⁻¹ for sciCHO and about 1.7 g L⁻¹ for CHO-K1 cells which are both in a concentration range that should not affect growth (Fu et al., 2016).

A third cell line was used in this thesis as a model organism for antibody-producing CHO cells. The CHO DP12 cell line produces an IgG antibody. The results of a

standard cultivation are depicted in Figure 4. The cultivation conditions are 250 mL shake flasks with a filling volume of 50 mL, shaken at a frequency of 140 rpm, and a shaking diameter of 50 mm. The cells were cultivated in TOM glass shake flasks and connected to the TOM device. Three replicates were cultivated for online monitoring of the OTR only and another three replicates were additionally sampled daily for offline analysis.

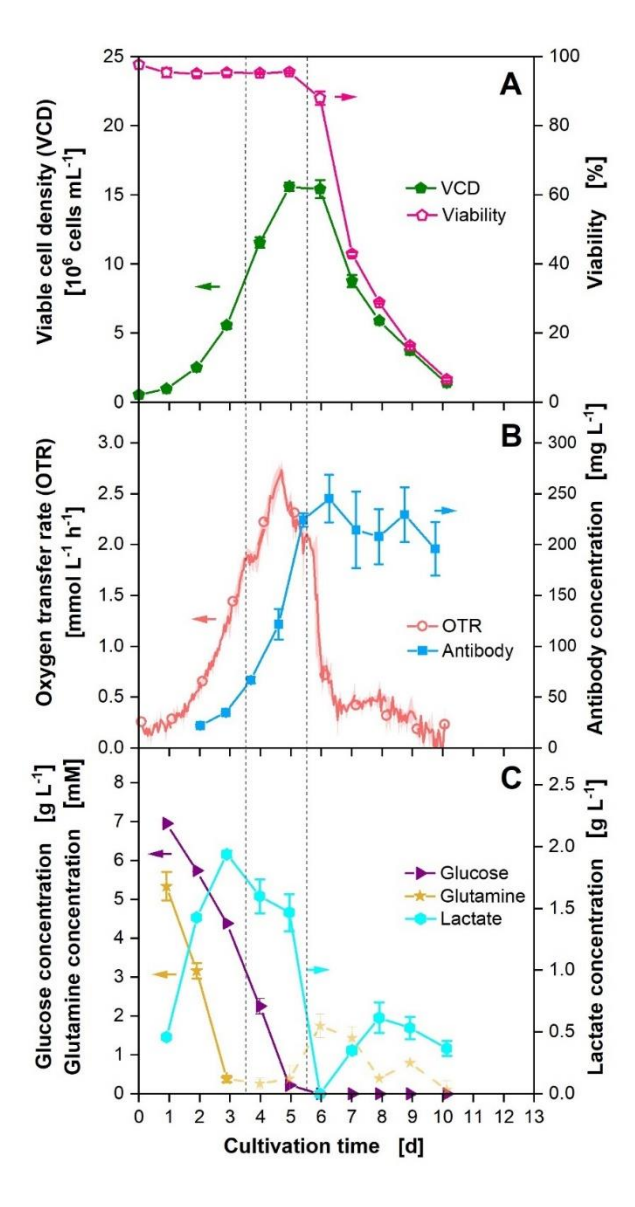


Figure 4: Cultivation of CHO DP12 cells in shake flasks under standard conditions. The experiments were performed in six replicates. Three replicates were sampled daily for offline analysis and three were used for online monitoring only. All data are shown as the mean value of three biological replicates (indicated as error bars or shades). A) Depicted are the viable cell density (VCD) and the viability determined by a CEDEX. B) Shown is the mean oxygen transfer rate (OTR). For clarity, only every 24th measuring point over time is marked as a symbol. The lines are drawn through all measured values. The outliers in the OTR data due to temperature

adaptations after sampling were excluded from the data. In addition, the antibody concentration is shown. C) Corresponding glucose, glutamine, and lactate concentrations are depicted over time. Depletion of glucose and glutamine is marked by dotted vertical lines over all three parts of the figure. Cultivations were performed in a TOM device. Culture conditions: 250 mL TOM glass flasks, temperature (T) = 36.5° C, shaking frequency (n) = 140 rpm, shaking diameter (d₀) = 50 mm, filling volume (V_L) = 50 mL, 5% CO₂, 70% rel. hum., medium: TCX6D + 8 mM glutamine; starting cell density: $5x10^{5}$ cells mL⁻¹.

Figure 4 A displays the VCD and viability of the CHO DP12 cultures. The VCD increases steadily over about 6 cultivation days to ca. 1.5x10⁷ cells mL⁻¹ (green line and closed pentagons) before it drops gradually until the end of cultivation on day 10. The viability (pink line and open pentagons) remains on a constant level above 96 % for 5 cultivation days before it decreases constantly which is comparable to the cell lines in Figure 3. Additionally, Figure 4 B shows the antibody concentration (blue line and closed squares). It rises until cultivation day 6 up to about 250 mg L⁻¹ and stays on a nearly constant level until the end of the cultivation. Hereby, literature-known values for the antibody titer are reached (Klausing et al., 2013; Strasser et al., 2021). The OTR curve (red line and open circles) monitored in this experiment by the TOM device rises to a maximum of about 2.8 mmol L⁻¹ h ⁻¹. The shape of the OTR curve resembles the shape of the VCD curve similar to what was already described for sciCHO and CHO-K1 cells. In Figure 4 C the relationship of the kinks and shoulders to offline parameters is visible again. The glucose concentration (purple line and triangles) decreases over the first 5 cultivation days. As soon as it is depleted, the OTR curve drops sharply. The exhaustion of glutamine (ochre curve and stars) after about 3.5 days of cultivation is correlated to the shoulder in the OTR curve. The measurement method of glutamine by using a spectrophotometric kit is error-prone and subject to uncertainties. It is especially inaccurate at very low glutamine concentrations and when no glutamine is present anymore. This is the case for every measuring point after glutamine depletion. The CHO DP12 cell line exhibits a typical lactate switch as the two other previously described cell lines. Lactate increases until day 3 to about 2 g L⁻¹ before it is consumed again. The experiment was independently repeated (see App. Figure 1) resulting in the same findings.

3.4 Summary

The experiments presented show that OTR determination in shake flasks is a simple online monitoring method to characterize different CHO cell lines. The growth performance in different media can be seen at first glance without the need for any sampling. The medium TCX6D was shown to be a high-performance medium, where the depletion of key metabolites can be immediately read out from the OTR. All in all, it could be demonstrated that OTR monitoring of different CHO cell lines is feasible as an alternative to VCD determination providing a lot more information per time. The characterization of the cell lines provides a good basis for further investigations by online monitoring of the OTR.

4 Analysis of hydromechanical stress on CHO cells in shake flasks

4.1 Background

As described in the introduction (Chapter 1.4), it is crucial to measure and control process parameters and stay in a defined operating range in order to achieve robust and reproducible processes (Nagashima et al., 2013). Because process development and evaluation are often performed in small scales, the process parameters have to be kept constant over scales. Thus, scale-independent parameters like O₂ transfer, CO₂ removal, temperature, or the maximum hydromechanical stress are particularly suitable for the characterization of a process (Neunstoecklin et al., 2015). Nevertheless, many current processes are based rather on historical and empirical observations than on a fundamental understanding of those important parameters (Chalmers, 2015; Nienow et al., 2013). Already at the beginning of adapting mammalian cells to suspension in the 1980s, it was evident that forces by stirring or shaking are a decisive parameter (Hu et al., 2011). Due to the lack of a cell wall and the comparably big size of mammalian cells, they were considered extremely sensitive to stirring or shaking (Chalmers, 2015; Chalmers and Ma, 2015). Consequently, some early studies on the influence of stirring on animal cells were conducted, analyzing under which conditions cell damage occurs (Al-Rubeai et al., 1995; Kunas and Papoutsakis, 1990; Oh et al., 1989). Nowadays, large-scale systems are still stirred with low agitation rates resulting in insufficient mixing and gradients of nutrients and byproducts (Paul and Herwig, 2020). Chalmers (2015), therefore, even stated that not the hydromechanical forces in the bioreactor are responsible for certain effects but the insufficient mixing resulting from the low stirring intensities. Thus, the issue arises as to whether cells would be able to withstand higher hydromechanical forces. In order to approach this question, it will first be considered how hydromechanical stress can be quantified, which variables describe it correctly, and how it can be measured.

Hydromechanical stress arises due to the movement or flow of fluids and comprises different types of stresses (Daub et al., 2014; Hu et al., 2011). This is present in stirred or shaken bioreactors, but also in hoses or downstream devices (Hu et al., 2011). The hydromechanical stress is affected by mixing, aeration (especially bubble forming and

bursting), and laminar or turbulent flows within a liquid (Sieck et al., 2013; Sieck et al., 2014). As hydromechanical stress cannot be measured directly, parameters must be found to quantify it. In the literature, the following parameters have become established: (1) volumetric power input (P/V) (2) energy dissipation rate (ε), and (3) Kolmogorov's length of microscale (λ_K) (Maschke et al., 2022b). The latter describes the cascade process of forming smaller eddies out of large-scale turbulent eddies (Hunt and Vassilicos, 1991). According to the theory, cell damage occurs if the size of the eddies is smaller or similar to the size of the cells (Nienow, 2009). After this theory, animal cells should not be sensitive to hydromechanical stress when keeping the eddy sizes above roughly 18-20 µm (upper size of CHO cells) (Nienow, 2006). A more quantitative concept is the consideration of ε [W kg⁻¹] or the corresponding P/V [W m⁻³]. P/V describes the power input per liquid volume into the reactor. ε describes the irreversible conversion of kinetic energy to heat and is calculated by dividing P/V by ρ (Sieck et al., 2013). It is well known that ε values strongly depend on their spatial distribution in bioreactors (Nienow et al., 2013). Therefore, ε_{max} or the quotient of ε_{max} to εø is considered to be a suitable term for quantifying hydromechanical stress (Daub et al., 2014; Henzler and Biedermann, 1996). Up to date, several different methods to determine ε_{max} have been established: indirect measurements using shear-sensitive systems like the maximum stable drop size (Daub et al., 2014; Peter et al., 2006), flocculation systems (Henzler and Biedermann, 1996; Panckow et al., 2023), or shearsensitive layer aggregates (Villiger et al., 2015) and direct methods like Laser-Doppler anemometry, particle image velocimetry or constant temperature anemometry (Villiger et al., 2015). For studying the effect of different ε on mammalian cells, different methods and devices concerning different phases (from upstream to downstream) of cultivation were developed and reviewed in detail elsewhere (Chalmers, 2015; Hu et al., 2011). Chalmers and coworkers for example developed a microfluidic device where they pumped cells through capillaries mimicking different ε (Ma et al., 2002). In the first studies, where the cells were exposed to hydromechanical stress only once, cell damage occurred only at an ε of 100 W kg⁻¹ (Ma et al., 2002; Mollet et al., 2004). Later on, the authors analyzed exposure to repeated hydromechanical stress to CHO cells and reported lethal effects from 6.4x10³ W kg⁻¹ and sub-lethal effects from 60 W kg⁻¹ (Godoy-Silva et al., 2009a; Godoy-Silva et al., 2009b). However, they used hydromechanical stress only in a laminar regime in capillaries and achieved very high tolerable values (Nienow, 2006). Nienow and colleagues (2006) found that cells in an aerated STR with $\varepsilon_{\varnothing}$ = 25 W kg⁻¹ can grow to the same cell density as in their standard operation conditions of $\varepsilon \varnothing = 0.01-0.02 \text{ W kg}^{-1}$. Sieck et al. (2013) used a 2 L bioreactor as a scale-down model that mimicked the hydromechanical stress of large-scale bioreactors. The study included aeration, agitation, and laminar and turbulent flows. They observed different sub-lethal effects: In comparison to their standard ε_{\emptyset} of 0.01 W kg⁻¹, the productivity decreased by 25 % at an ε_{\emptyset} of 0.4 W kg⁻¹. The decrease was even stronger when the cells were exposed to an ε_{\emptyset} that was periodically oscillating between these two values. The authors did not detect any differences in metabolite consumption, byproduct formation, or product quality (Sieck et al., 2013). In a second study, they investigated the effect of sparging, aeration, and the combination of both individually and identified an influence on viability but not on metabolism, productivity, or product quality (Sieck et al., 2014). Neunstoecklin et al. (2015) analyzed the influence of hydromechanical stress on CHO and Sp2/0 cells (B lymphocyte cells) with a scale-down model consisting of an external loop at a bioreactor with nozzles of different diameters. Laminar and turbulent flows were tested in oscillatory manners. They observed thresholds of hydromechanical stress where below this value the cells do not show any response. Above this threshold, CHO cells reacted with better growth but reduced productivity (Neunstoecklin et al., 2015). The authors showed that the results obtained from their model were transferable to large-scale fermenters. The thresholds observed in 300-L scale were comparable to the ones seen in their previous study with 3-L reactors (Neunstoecklin et al., 2016). Up to now, most of the process engineering considerations concerning the hydromechanical stress of mammalian cells were conducted in STRs or scale-down devices mimicking them. Furthermore, only a few of these approaches dealt with the investigation of sub-lethal effects. However, the development of CHO production processes normally starts in smaller scales like shake flasks or MTPs. The first vessels in seed trains are normally also shake flasks (Hernández Rodríguez et al., 2013). Furthermore, efforts are being made to bring shaken systems to production scale (Zhang et al., 2009).

The fundamentals of ε and the hydromechanical stress in shake flasks were in detail investigated by Büchs and Zoels (2001) and Peter et al. (2006). They established a correlation for determining $\varepsilon_{\varnothing}$ and ε_{\max} in shake flasks and revealed that the shaking diameter and the filling volume have no impact on the hydromechanical stress,

whereas it is influenced by the flask size and the shaking frequency. They also found that the P/V needed for generating the same hydromechanical stress as in STRs is tenfold larger in shake flasks (Peter et al., 2006). To the best of my knowledge, only two approaches considered the hydromechanical stress on CHO cells in shake flasks in a detailed process engineering way up to now. Maschke et al. (2022b) defined design spaces using the concept of Kolmogorov's scale of turbulence where the probability of failure for a CHO cultivation is defined. They asserted that a P/V up to 900 W m⁻³ is suitable. However, they did not analyze sub-lethal effects (Maschke et al., 2022b). Pérez-Rodrigues in contrast studied sub-lethal effects at two different shaking frequencies and shaking diameters. However, they used parameters leading to out-of-phase conditions and calculated ε_{max} even though the criteria for using the corresponding equation of a Re > 60 000 was not given (Pérez-Rodriguez et al., 2022). Therefore, the results must be considered with caution and are not comparable to this and other studies. Hence, a fundamental investigation of the hydromechanical stress in shake flasks is of interest.

The most common parameters in former hydromechanical stress research for CHO cells were the VCD or μ (Gaugler et al., 2024; Maschke et al., 2022b; Neunstoecklin et al., 2015; Nienow et al., 2013; Sieck et al., 2013). As described earlier (Chapter 3.1), both of these parameters are directly correlated to the OUR (Ihling et al., 2021; Ihling et al., 2022a; Stöckmann et al., 2003) whereas this was chosen as a suitable parameter to analyze hydromechanical stress.

The purpose of this chapter is to examine the impact of hydromechanical stress on CHO cells in shake flasks by varying the energy dissipation in a systematic process engineering manner. The impact on the cells' activity and metabolism is studied by monitoring the OTR. Furthermore, the impact on productivity will be analyzed.

4.2 Influence of varying ϵ_{\emptyset} on the OTR of CHO DP12 shake flask cultivations

To study hydromechanical stress in shake flasks, the variation of P/V_{\varnothing} or the corresponding $\varepsilon_{\varnothing}$ was investigated as a suitable choice (Büchs et al., 2000; Peter et al., 2006). As can be seen from Equations (1) and (2), P/V_{\varnothing} and $\varepsilon_{\varnothing}$ should be able to

be varied by the nominal shake flask size (inner flask diameter), the shaking frequency, and the filling volume. However, Peter et al. (2006) showed the filling volume does not influence ε_{max} and, thus, the hydromechanical stress. Therefore, the relative filling volume was kept constant in the following experiments. The parameters used in this study and the corresponding calculated ε_{\emptyset} and ε_{max} are summarized in Table 1. The shaking diameter does not affect either parameter. However, it needed to be varied for the highest shaking frequencies because otherwise, the liquid volume would overflow at the corresponding filling volume. In Table 1, ε_{\emptyset} and ε_{max} are listed. For shake flask experiments, ε_{max} (P/V_{max}) is equal to ε_{\emptyset} (P/V_{\emptyset}) if Re is < 60,000 (Peter et al., 2006). Furthermore, λ_{K} was calculated. As can be seen from Table 1, λ_{K} is larger than the maximal cell size of CHO cells (18-20 µm) for $\varepsilon_{\emptyset} \le 1.45$ W kg⁻¹. According to the theory of Kolmogorov, the cells should not be damaged by those cultivation conditions. For $\varepsilon_{\emptyset} = 3.84$ W kg⁻¹, λ_{K} is 15 µm and therefore in the range of the cell's size. Cell damage could occur in this range of energy dissipation (Maschke et al., 2022b; Nienow, 2006; Nienow et al., 2013).

Table 1: Characteristic parameters of shake flask cultivations. ε_{\emptyset} , ε_{max} , Re, and λ_{K} were calculated by using Equations (2)-(6).

Flask size [mL]	V _L [mL]	n [rpm]	d₀ [mm]	ε _ø [W kg ⁻¹]	ε _{max} [W kg ⁻¹]	Re [-]	λ _K [μm]
100	20	140	50	0.08	0.08	8400	59
250	50	140	50	0.12	0.12	15423	54
250	50	200	50	0.32	0.32	22032	42
250	50	350	50	1.45	1.45	38557	29
500	100	450	25	3.84	17.0	76508	15

Shake flask experiments for all ε_{\emptyset} listed in Table 1 were conducted. Hence, a much wider range of different ε_{\emptyset} was tested than in Maschke's work who tested up to roughly

0.9 W kg⁻¹ (Maschke et al., 2022a). The results of the OTR monitoring in this study are depicted in Figure 5.

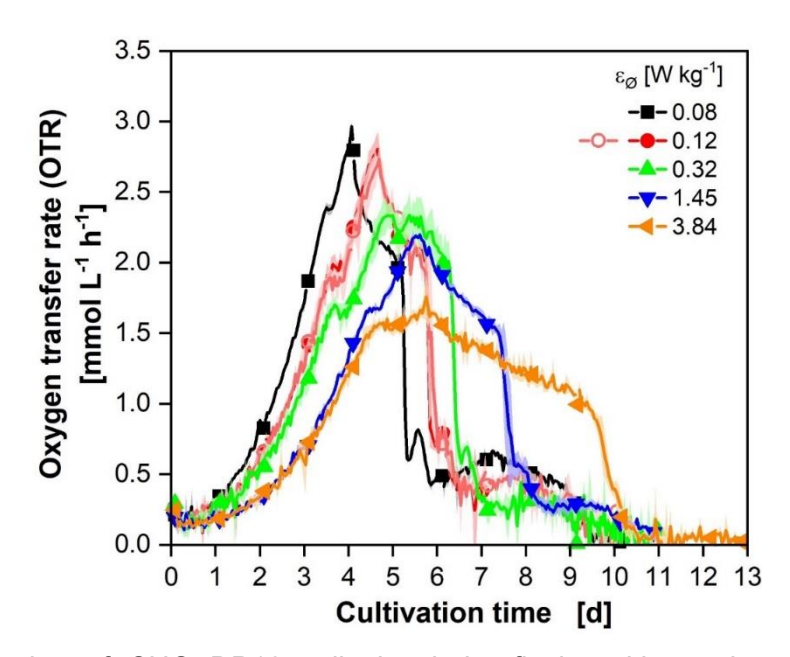


Figure 5: Cultivation of CHO DP12 cells in shake flasks with varying average energy dissipation rates (ϵ_{\varnothing}). The mean oxygen transfer rate (OTR) of three replicates is shown with standard deviations illustrated as shaded areas. For clarity, only every 24th measuring point over time is marked as a symbol. The lines are drawn through all measured data points. The outliers in the OTR data due to temperature adaptations after opening the incubation hood were excluded from the data. The curves in dark and light red are from the independent experiments depicted in Figure 4 and App. Figure 1. Culture conditions: flask size, shaking frequency, shaking diameter, and filling volume see Table 1, temperature (T) = 36.5°C, 5 % CO₂, 70 % rel. hum., medium: TCX6D + 8 mM glutamine; starting cell density: $5x10^5$ cells mL-1.

As becomes evident from Figure 5, the shape of the OTR curves differentiate for varying ε_\emptyset which corresponds to an altered respiratory activity. Thus, the sub-lethal effects of hydromechanical stress on CHO DP12 cells can be seen at first glance. For example, the maximum reached OTR value decreases with increasing ε_\emptyset while the process duration is lengthened. It becomes also apparent that the increase of the OTR is slower with higher ε_\emptyset . A detailed analysis of the metabolic differences is described in Chapter 4.3. The results are underpinned by VCD and viability analysis (App. Figure 2). Here, prolonged cultivation phases and lower maximal reached VCDs are visible with increasing ε_\emptyset . Prolonged phases of high viability can also be observed. However, due to the higher data density of the online monitored OTR, the impact of the ε_\emptyset on the cell's behavior is much clearer from online monitoring and the online

measured values are less error-prone and more independent from the operator than the offline analyses. Despite the altered shape of the OTR curves at varying ε_{\emptyset} , all cultivations reached the same final oxygen transfer (integral of the OTR, see App. Figure 3). It can be concluded that the cells consumed the nutrients completely in all cultivations independently of the hydromechanical forces present. This shows that – in contrast to what Maschke et al. (2022b) found in their setup - the CHO DP12 cells did not stop growing when reaching an ε_{\emptyset} of about 0.9 W kg⁻¹. On the other hand, the results presented in this work are in accordance with the literature where lethal effects only occur at very high εØ (Godoy-Silva et al., 2009b; Hu et al., 2011; Tanzeglock et al., 2009). In general, it must be mentioned that the different studies are hardly comparable with each other, as different cell lines, media, and setups were used. In this study, additional experiments were performed where the shaking frequency was only increased after two days of cultivation to vary ε_{\emptyset} (App. Figure 4). From these experiments, it can be concluded that the effect of different ε_{\emptyset} is not due to lengthened lag phases, but to different levels of hydromechanical stress. Here, the OTR curves of $\varepsilon \varnothing$ up to 1.45 W kg⁻¹ are very close together. The OTR curves of $\varepsilon \varnothing = 2.88$ W kg⁻¹ and $\varepsilon \varnothing = 3.84 \text{ W kg}^{-1}$ are noticeably different and show a lengthened cultivation time and a reduced maximal OTR similar to the experiments in Figure 5.

4.3 Influence of varying ε_{\emptyset} on the metabolism

The impact of varying hydromechanical stress levels on the CHO DP12 cell line's metabolism will be further examined. For this, the OTR curves from Figure 5 were analyzed concerning μ_{max} and the two key metabolites glucose and glutamine whose consumption is directly visible from the OTR curve as described in Chapter 3.3. The results are displayed in Figure 6.

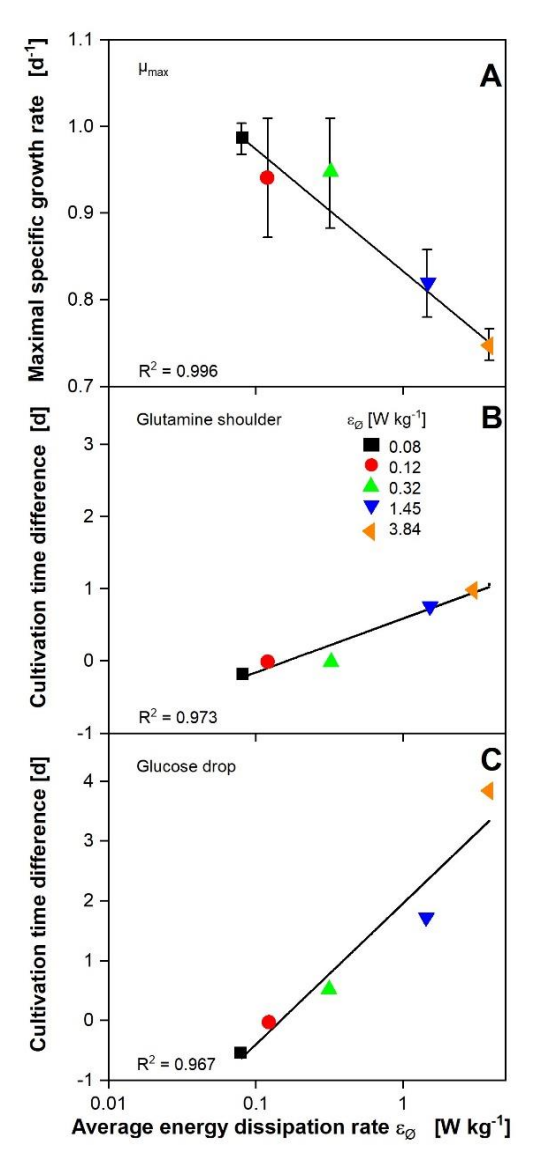


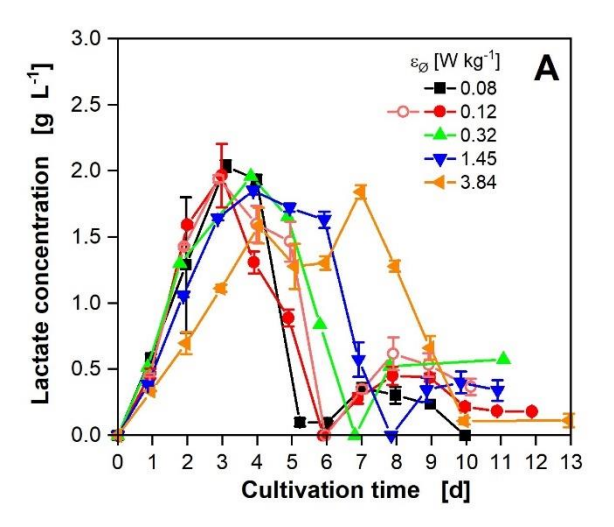
Figure 6: Correlation of the maximal specific growth rate (μ_{max}) and the time of glucose and glutamine depletion to varying average energy dissipation rates (ϵ_{\varnothing}). Analysis of the CHO DP12 cultivations from Figure 5. ϵ_{\varnothing} is plotted logarithmically. A) μ_{max} calculated from the individual replicates of the OTR data in Figure 5. B) Cultivation time difference to the standard cultivation with $\epsilon_{\varnothing} = 0.12$ W kg⁻¹ of glutamine depletion read out from the glutamine shoulder in the OTR data in Figure 5. C) Cultivation time difference to the standard cultivation with $\epsilon_{\varnothing} = 0.12$ W kg⁻¹ of glucose depletion read out from the glucose drop in the OTR data in Figure 5. A linear fit was performed for all figures (shown as a black line).

Figure 6 A shows the respective μ_{max} for the different tested $\varepsilon_{\varnothing}$. μ_{max} was calculated as described in Chapter 2.8.2. As it becomes evident, μ_{max} decreases with an increasing $\varepsilon_{\varnothing}$ from roughly 1 d⁻¹ (black square) for the lowest $\varepsilon_{\varnothing}$ to approximately 0.75 d⁻¹ (orange left side triangle) for the highest $\varepsilon_{\varnothing}$. From the visualization of the data, it is evident that μ_{max} is in a good semi-logarithmic correlation (R² = 0.996) with $\varepsilon_{\varnothing}$ implying that higher hydromechanical stress makes the CHO DP12 cells as a whole grow slower. This can

be due to two reasons: 1. every single cell is growing slower or 2. some cells do not survive because of hydromechanical stress. In literature, effects on μ_{max} were also associated with different impacts of hydromechanical stress. In contrast to this study, Neunstoecklin et al. (2015) observed better growth with increasing hydromechanical stress but overall only slight differences between different stresses. In the setup of Maschke et al. (2022b), who used 500 mL shake flasks, a reduced growth rate was observed at an ϵ_{\varnothing} of approximately 0.9 W kg⁻¹. However, they did not test ϵ_{\varnothing} above this value.

The time of glutamine and glucose depletion were set in relation to this time of the standard cultivation with $\varepsilon_{\varnothing}=0.12~\mathrm{W~kg^{-1}}$ and plotted against the logarithm of $\varepsilon_{\varnothing}$ (Figure 6 B). There is a logarithmic correlation of the time difference values for both metabolites with $\varepsilon_{\varnothing}$. With an increasing $\varepsilon_{\varnothing}$, glutamine and glucose are depleted later in the cultivation process which is a logical consequence of the reduced growth rate. Without the online OTR data, the effect would not have been obvious. The offline data (see App. Figure 5) confirm the observations but because of the lower data density, the trend is less well visible. Additionally, the cell-specific glucose and glutamine uptake rates were calculated and shown in App. Figure 6 A and B. For both metabolites, there are no significant differences in the specific uptake rates. Thus, every single cell has the same metabolic rate for glucose and glutamine. In literature, some studies did not see any effect on key metabolites at different levels of hydromechanical stress (Godoy-Silva et al., 2009b; Sieck et al., 2013; Sieck et al., 2014) whereas Keane et al. (2003) even observed an increasing glucose uptake with higher hydromechanical stress.

Summing up, the data provide a detailed insight into the culture behavior and key metabolites of CHO DP12 cells at different ε_{\emptyset} leading to new findings concerning sublethal effects caused by hydromechanical stress. However, the lactate concentration was not considered yet. The lactate switch will be analyzed by the offline data shown in Figure 7.



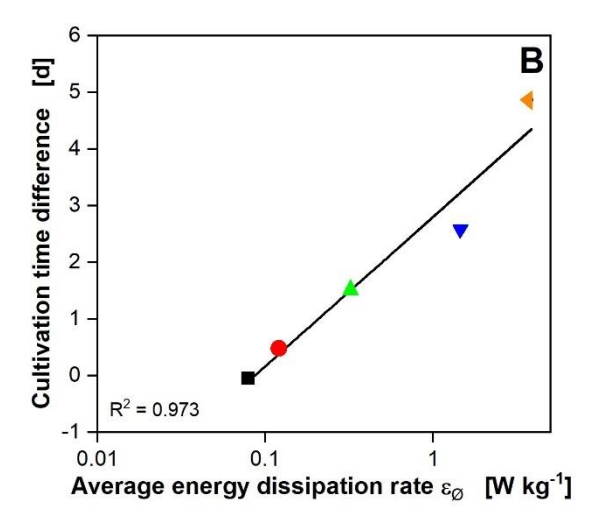


Figure 7: Analysis of the lactate concentration at varying average energy dissipation rates $(\varepsilon_{\varnothing})$. Analysis of the CHO DP12 cultivations from Figure 5. A) Illustrated are the mean lactate concentrations of three biological replicates over time for the cultivations depicted in Figure 5. B) The cultivation time difference to the standard cultivation with $\varepsilon_{\varnothing} = 0.12$ W kg⁻¹ of the lactate depletion read out from the offline data in A. $\varepsilon_{\varnothing}$ is plotted in logarithmic scale. Culture conditions: flask size, shaking frequency, shaking diameter, and filling volume see Table 1, temperature (T) = 36.5°C, 5 % CO₂, 70 % rel. hum., medium: TCX6D + 8 mM glutamine; starting cell density: 5×10^5 cells mL⁻¹.

The offline lactate concentrations are shown in Figure 7 A. They point out that the time at which lactate is depleted completely – before it starts rising again – is shifted with increasing $\varepsilon_{\varnothing}$. The shift is distinct enough to be noticeable in the offline data even though they were sampled only once a day. For all $\varepsilon_{\varnothing}$, lactate concentrations rise for the first 3-4 cultivation days. For the three lowest $\varepsilon_{\varnothing}$ the lactate concentrations decrease rapidly afterward while the concentrations for the two highest $\varepsilon_{\varnothing}$ stay high for about three days before they drop again. In Figure 7 B, the time points at which lactate dropped to zero were set in relation to the standard cultivation with $\varepsilon_{\varnothing} = 0.12 \text{ W kg}^{-1}$ and plotted against $\varepsilon_{\varnothing}$ in a semi-logarithmic plot. The plot quantifies the lactate switch. As becomes evident, the time of lactate switch is correlated to the logarithm of $\varepsilon_{\varnothing}$ similarly to glucose and glutamine depletion. In addition, the cell-specific lactate production rate was calculated and plotted in App. Figure 6 C. In accordance with the results of specific glucose and glutamine uptake, there are overall no significant differences in the cell-specific lactate uptake rates.

When looking at the results as a whole, it can be said that the whole cells grow more slowly with increased ε_{\emptyset} and thus show delayed consumption of key metabolites. As mentioned before, this can be due to two reasons: 1. each individual cell doubles more

slowly, or 2. not all cells survive under increased hydromechanical stress. The first theory is in contrast to the calculated cell-specific uptake and production rates, as these do not differ significantly for varying ϵ_{\emptyset} . However, the second theory is in contrast to Kolmogorov's length of microscale. According to this theory, the cells should only be destroyed by the eddies at the highest ϵ_{\emptyset} . However, both approaches have weaknesses. The determination of the cell-specific uptake and production rates is very imprecise, as on the one hand, the individual measurement results are subject to errors and on the other hand, the data density is low. Considerably higher sample densities would be necessary to make more accurate statements. Kolmogorov's length of microscale is an old, empirical theory that provides guide values for the size of the eddies. Therefore, the reason for slowed respiratory activity cannot be answered completely.

Summarizing the effects of varying hydromechanical stress on CHO DP12's metabolism, an increasing $\varepsilon_{\varnothing}$ leads to a delayed depletion of nutrients: the time for glucose and glutamine depletion and the lactate switch increase with logarithmically increasing $\varepsilon_{\varnothing}$ while μ_{max} decreases. The cell-specific uptake and production rates do not differ significantly. The key metabolites are important parameters for a successful CHO cultivation process, but productivity is the most essential parameter. Therefore, the analysis of the antibody production follows.

4.4 Influence of varying ε_{\emptyset} on the antibody production

The CHO DP12 cell line produces an IgG antibody. Its concentration was measured by Protein A chromatography over the whole cultivation process for all experiments (see App. Figure 7). To compare the final antibody titers, the last three measured values were averaged and plotted against the logarithm of ε_{\emptyset} . The results are depicted in Figure 8.

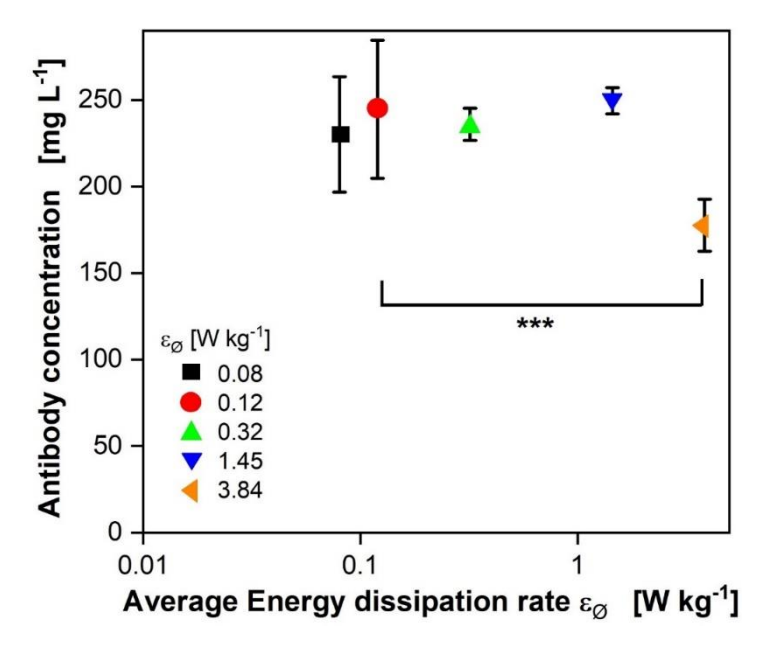


Figure 8: Correlation of the final antibody concentration to the logarithm of varying average energy dissipation rates ($\varepsilon_{\varnothing}$). Analysis of the CHO DP12 cultivations from Figure 5. The mean value of the last three cultivation days was calculated. Statistically significant differences against the reference cultivation ($\varepsilon_{\varnothing} = 0.12 \text{ W kg}^{-1}$) are indicated by stars (*** p < 0.001).

As becomes obvious from Figure 8, the antibody concentration is similar within the standard deviations for all experiments up to ε_{\emptyset} = 1.45 W kg⁻¹ and reaches the reported maximal product titer for this cell line of roughly 250 mg L⁻¹. In contrast, the final antibody concentration for the cultivation with the highest ε_{\emptyset} (3.84 W kg⁻¹) was only approximately 180 mg L⁻¹ (orange left side triangle) and is statistically different from the other concentrations (p < 0.001). To explain this difference, it is important to consider ε_{max} . The consideration is irrelevant in shake flasks if the Re number is < 60,000. Under these conditions, there is a laminar flow in the shake flask and ε_{max} is equal to ε_{\emptyset} (Klöckner and Büchs, 2012). This applies to all cultivations except for the one with the highest ε_{\emptyset} (see Table 1). For the latter, a Re of 76 508 was calculated according to Equation (3). That means under these conditions the flow should be turbulent. ε_{max} was calculated according to Equation (4) and is approximately 17 W kg⁻¹. Thus, it is about four times greater than $\varepsilon_{\varnothing}$. Therefore, the hydromechanical forces in this cultivation were much higher than in all the other ones and the flow regime was different. Nienow et al. (2013) already stated that the flow regime is an important factor in the influence of hydromechanical stress on mammalian cells and Neunstoecklin et al. (2015) found that CHO cells were more sensitive at turbulent flow conditions than at laminar flows. According to Kolmogorov's theory, the cells should

be influenced by the eddies which could also have an influence on antibody production. In general, low growth rates of CHO cells are associated with higher productivity independently from different ε (Kim et al., 2013). Different growth rates caused by increasing ε did not lead to higher final antibody concentrations in this study. Additionally, the cell-specific antibody productivity (see App. Figure 6 D) is not statistically different for any of the cultivations.

To sum up, the final antibody titer is not influenced by varying energy dissipation in the laminar flow regime, but if a turbulent regime is present, the final titer declined about 40 %.

4.5 Summary

This chapter examined the influence of varying levels of hydromechanical stress on CHO DP12 shake flask cultivations. The energy dissipation was used as a quantifiable variable that describes the hydromechanical stress. By varying ε_{\emptyset} , it could be demonstrated that an increase in hydromechanical stress leads to a slowdown in the respiration activity and prolongs the cultivation process. The ε_Ø range tested represents the largest feasible range for shake flask cultures which are limited due to the technical specifications of standard shakers. Under these conditions, they cannot be operated at higher shaking speeds than 450 rpm. No lethal effects were noticed in the entire range. A halt in cell growth was also not observed. The viable maximal cell density decreased with increasing $\varepsilon_{\varnothing}$. A detailed examination of the respiratory activity showed that μ_{max} , the time for glucose and glutamine depletion, and the lactate switch correlate linear with logarithmically plotted ϵ_{\emptyset} . Cell-specific uptake and production rates did not statistically differ between the cultivations. The antibody titer reaches the highest reported value for this cell line (250 mg L⁻¹) for all cultivations within a laminar flow. In the only cultivation within a turbulent flow ($\varepsilon_{\varnothing} = 3.84 \text{ W kg}^{-1}$), the final titer was reduced by about 40 %.

5 Scale-down of CHO cell cultures to 96-deep-well MTPs

5.1 Background

The smallest cultivation vessels in common use are MTPs. With MTPs, the cultivation volume can be minimized, while increasing the throughput at the same time (Klöckner and Büchs, 2012). MTPs are easy to handle, highly parallelized, and cost-effective (Hemmerich et al., 2018). Therefore, they are a common tool in early-stage bioprocess development and in experiments where high throughput is necessary (Hemmerich et al., 2018; Klöckner and Büchs, 2012). At present, several online monitored MTP devices are available and reviewed elsewhere (Bareither and Pollard, 2011; Hemmerich et al., 2018). For mammalian cells, different fully automated MTP-based systems are published, meaning that pipetting and sampling are automatically performed. Those devices are mostly used for early clone screening (Markert et al., 2019; Markert and Joeris, 2017; Mora et al., 2018; Wang et al., 2018; Wutz et al., 2018). However, among the existing online monitoring MTP devices, there are only a few in use with mammalian cells. Chen et al. (2009) established the microbioreactor system M24 with a working volume of 5 mL for CHO cells. With this, dissolved oxygen, pH, and temperature could be non-invasively online monitored at the individual well level. For adherent cells, pH, cell activity, and protein production could be online monitored with a silicone optical technology-based spatial filter (Nakashima et al., 2019). This is an optical absorption measurement method. The spatial filter, created with silicone optical technology, reduces noise by selectively transmitting only forward light, resulting in an improved signal-to-noise ratio compared to conventional optical systems. The filter, a light-emitting diode, and color sensors are components of a 24channel plate reader, which enables the continuous monitoring of a 24-well MTP (Nakashima et al., 2019). More recently, the OTR of CHO cells has been determined by the μRAMOS device (Ihling et al., 2023). The μRAMOS consists of a 48-well MTP with a round geometry and an oxygen-sensitive fluorescent dye embedded in a matrix that measures the oxygen partial pressure in the gas phase (Flitsch et al., 2016). With the µRAMOS, cytotoxicity tests for CHO cells could be performed (Ihling et al., 2023). In 2022, the so-called µTOM device, which monitors the OTR for every individual well of a 96-deep-well MTP, was published by Dinger et al. (2022). It was shown for microbial cultivations that the measurements in the μ TOM device (96 wells) were highly comparable to those in the RAMOS device (shake flasks) (Dinger et al., 2022). Furthermore, the μ TOM device was used to examine batch-to-batch variations of media components, to identify suitable substrates and for toxicity tests (Forsten et al., 2023; Niehoff et al., 2023; Wahjudi et al., 2023). Up to now, the μ TOM device has not been used with mammalian cells. Nevertheless, it could be an effective device for high-throughput experiments with mammalian cells. The scope of possible applications is wide. It can be, for example, used to screen media components and clones or in early process development steps. Two examples with different backgrounds will be examined in this study.

One step of process development is the optimization of culture media. Nowadays, the use of commercially available media is common for suspension cells in academic research. Key components of cell culture media and the development from early formulations to modern chemically defined media are reviewed in detail (Ling, 2020; Ritacco et al., 2018). Media development and optimization is elaborate as it consists of around 60-80 components (Parampalli et al., 2007). Therefore, high-throughput screening devices like the μ TOM would be a valuable tool for the development and optimization of those media.

Another crucial step in the development of a CHO production process is cell line generation. For mammalian cells, this is still a laborious and time-consuming process. The challenges and recent progress are well-reviewed by Ho et al. (2013). Currently, the research focus is on cell line stability during long-term cultivations, the site-specific integration of product genes, and the development of faster and more effective selection- and screening systems (Tihanyi and Nyitray, 2020). The selection of clones after transfection is a crucial step in cell line generation. By introducing a selection marker with the Gene of Interest (GOI), the transfected cells have a selection advantage, compared to the untransfected cells (Lanza et al., 2013). In the biopharmaceutical industry, metabolic selection systems, such as the dihydrofolate reductase (DHFR) or the glutamine synthetase (GS) selection system, are frequently used for CHO cells (Bebbington et al., 1992; Kaufman and Sharp, 1982). An easier and more universal way of selection is the use of antibiotics as there is no requirement for modified cell lines (Ho et al., 2013). However, if antibiotics are applied for selection, it is necessary to perform kill curve experiments. With these experiments, the minimal

concentration to kill the untransfected parental cell line is to be determined (Delrue et al., 2018; Mortensen and Kingston, 2009). Kill curve experiments are rarely mentioned in literature because they are an intermediate step in cell line generation. Nevertheless, they are important and are usually still performed in current cell line generation research with antibiotic selection. The choice of the antibiotic and its appropriate concentration is crucial for cell line generation. One reason is that the selection effectiveness directly influences the quality of selected pools of transfected cells and the resulting single-cell clones (Lanza et al., 2013). If some untransfected cells survive selection, low-producing cell pools will result (Yeo et al., 2017). There are several antibiotics with quite different modes of action available for selection. Typical antibiotics for mammalian cells are geneticin, blasticidin, zeocin, hygromycin B, and puromycin (Lanza et al., 2013; Schiøtz et al., 2011). While geneticin and blasticidin interfere with protein synthesis, zeocin intercalates into DNA and cleaves it. Hygromycin B is an aminoglycoside antibiotic that inhibits protein synthesis by disrupting translocation and promoting mistranslation (Mortensen and Kingston, 2009). The mode of action of puromycin was recently investigated by Aviner (2020). It is an aminonucleoside antibiotic that inhibits protein synthesis by ribosome-catalyzed incorporation into the C-terminus of elongating nascent chains, blocking further extension and resulting in premature termination of translation (Aviner, 2020). Because of those differences, antibiotics have different efficiencies in selection. In the literature, some comparative studies for selection with antibiotics are available: Lanza et al. (2013) took four antibiotics analyzing the resulting populations with high productivity. They identified zeocin as the best selection agent for the chosen setup and cell lines. For cell lines from Atlantic salmon kidneys, kill curve experiments with six different antibiotics were performed to find the most potent antibiotic. In this setup, blasticidin and puromycin were the best-performing agents (Schiøtz et al., 2011). More recently, exemplary kill curves for CHO-DG44 and CHO-S cells with hygromycin B were published (Naddafi et al., 2019). Kill curve experiments for suspension cells are often conducted in TubeSpin® reactors or shake flasks because a defined minimal volume is necessary to allow daily sampling. This results in a high medium consumption and, therefore, in significant costs. Furthermore, it is a laborious and time-consuming experiment due to the necessity of daily sampling. A solution to simplify the protocols, save time, and decrease medium costs could be online monitoring through the µTOM device. Thus, sampling would no longer be necessary and smaller cultivation vessels could be used.

The following section first describes how the transfer from shake flasks to the MTP cultivations in the μ TOM device proceeded (Chapters 5.2 and 5.3). Afterward, two application examples will show the wide applicability of the μ TOM device (Chapters 5.4 and 5.5).

5.2 Transfer of online monitoring to 96-deep-well MTPs

The first step of using the μ TOM device is to show whether cultivations of CHO cells are possible and if they are comparable to shake flask cultivations. In Figure 9, the results of parallel cultivations in the TOM device in glass flasks (black line and filled squares) and the μ TOM device in round 96-deep-well MTPs (red line and open circles) are visualized. All cultivation vessels were started from one master mix with a cell density of $5x10^5$ cells mL⁻¹.

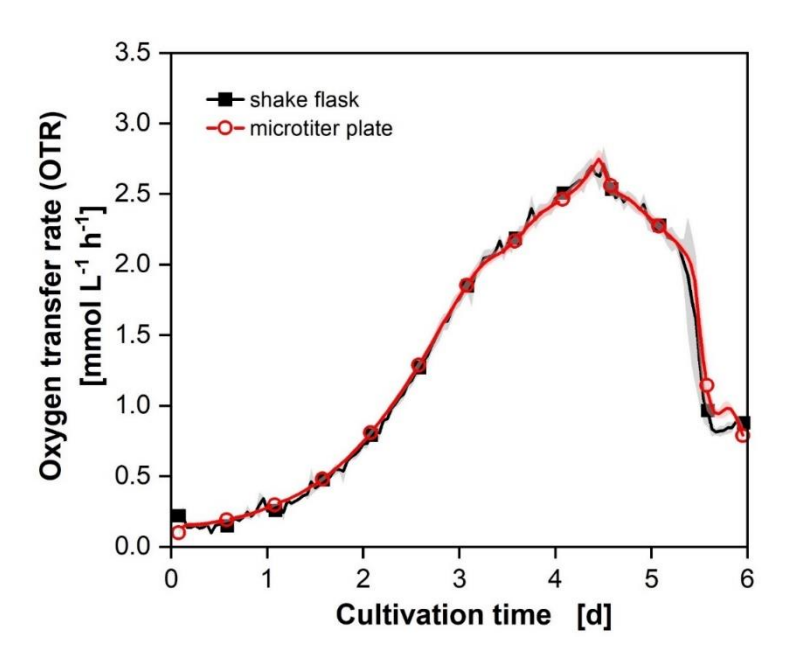


Figure 9: Parallel cultivation of CHO-K1 cells in round 96-deep-well microtiter plates and shake flasks. The oxygen transfer rate (OTR) was determined by the Kuhner TOM device in shake flasks (N = 3; black lines and squares) and in the μ TOM device in a round 96-deep-well microtiter plate (N = 53; red lines and circles). The low standard deviations are shown as shaded areas and indicate good reproducibility. For clarity, only every twelfth measuring point over time is marked as a symbol. Culture conditions TOM device: 100 mL glass flasks, temperature (T) = 36.5°C, shaking frequency (n) = 140 rpm, shaking diameter (d₀) = 50 mm, filling volume (V_L) = 20 mL, 5 % CO₂, 70 % rel. hum., medium: TCX6D + 8 mM glutamine;

starting cell density: $5x10^5$ cells mL⁻¹. Culture conditions μ TOM device: round 96-deep-well microtiter plate, temperature (T) = 36.5° C, shaking frequency (n) = 850 rpm, shaking diameter (d₀) = 3 mm, filling volume (V_L) = 1 mL, 5 % CO₂, humidified, medium: TCX6D + 8 mM glutamine; starting cell density: $5x10^5$ cells mL⁻¹. All experiments (shake flasks and microtiter plate) were started from one master mix.

The shake flask cultivations were performed with a shaking frequency of 140 rpm at a shaking diameter of 50 mm. The MTP cultivation was carried out at 850 rpm at a shaking diameter of 3 mm. These operating conditions were chosen to reach a similar OTR_{max} in both types of bioreactors. As a consequence, oxygen limitation, which would lead to undesirable side effects and altered cultivation conditions, is prevented. The OTR_{max} for shake flasks was calculated with Equation (9) (Osmol = 0.3 Osmol kg⁻¹, n = 140 rpm, $V_L = 20 \text{ mL}$, $d_0 = 5 \text{ cm}$, d = 65 mm, $p_R = 1 \text{ bar and } y^*_{O2} = 0.21 \text{ mol mol}^{-1}$) to about 10.2 mmol L⁻¹ h⁻¹. For the 96-deep-well MTP, Equation (10) was used $(V_L = 1 \text{ mL}, d_0 = 3 \text{ mm} \text{ and } n = 850 \text{ rpm})$. In this case, OTR_{max} is 10.5 mmol L⁻¹ h⁻¹. Thus, the OTR_{max} in both cultivation devices is very close and should lead to similar cultivation conditions. Looking at Figure 9, the OTR curves of the shake flask and MTP cultivations are essentially equal, meaning that the cells obviously experience the same environmental conditions in both scales. With this experiment, it could be shown that for a quite fast-growing CHO cell line, the oxygen supply is sufficient in round 96deep-well MTPs and the hydromechanical stress is not too high if choosing the right cultivation conditions. This is in contrast to the statements by Meyer et al. (2012). They claimed that the maximum oxygen transfer capacity in MTPs for mammalian cells is not high enough due to the surface tension when simultaneously keeping the hydromechanical stress low (Meyer et al., 2012). Additionally, Figure 9 shows that the reproducibility of the cultivations is extremely high for both cultivation vessels. This is indicated by the almost not visible shades, which represent the standard deviations of 3 replicates (shake flasks) and 53 replicates (MTP). For 48 well MTPs, this high reproducibility was also shown by Ihling et al. (2023). The reproducibility is not only verified for the single experiment started from one master mix (meaning cells, medium, and glutamine were pre-mixed and then divided into the cultivation vessels), but also for experiments performed over three months (App. Figure 8). The shape of the OTR curves is the same for experiments performed from different pre-cultures and different passages in shake flasks and MTPs. Only the lag phase slightly differs between experiments, leading to time-shifted curves (App. Figure 8 A). If the graphs are shifted along the x-axis to compensate for those differences, the curves are again almost perfectly aligned (App. Figure 8 B).

Thus, it could be shown that the μ TOM device is in general suitable for OTR monitoring of CHO cells and that the MTP cultivations are highly comparable to shake flask cultivations for the CHO-K1 cell line.

In order to verify the scale-down approach between shake flasks and MTPs also for CHO DP12 cell cultures, two independent experiments were conducted. In both experiments, a round 96-deep-well MTP and shake flasks were inoculated with CHO DP12 cells and the OTR was monitored online in both scales. For scale transfer, the same parameters were used as described above for the CHO-K1 cell line. The experiments are shown in Figure 10.

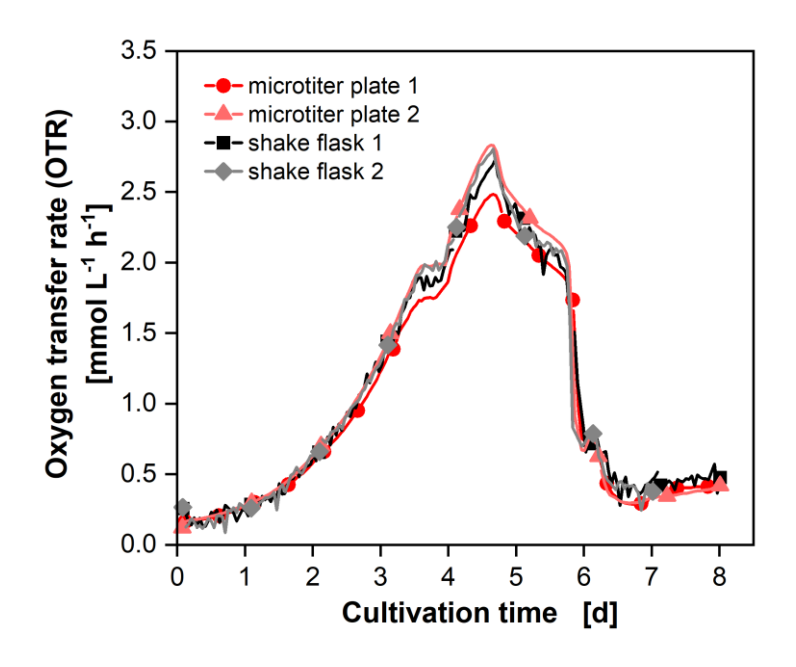


Figure 10: Oxygen transfer rate (OTR) of CHO DP12 cell cultures in shake flasks and microtiter plates. Two independent experiments (1 and 2) were performed. For both experiments, a round 96-deep-well microtiter plate and shake flasks were inoculated. The µTOM device was used for online monitoring of the microtiter plates (dark red line and circles; light red line and triangles) and the TOM device for the shake flasks (black line and squares; grey line and diamonds). For clarity, only every 24th measuring point over time is marked as a symbol. The microtiter plate experiments were performed in 72 (Experiment 1) and 66 (Experiment 2) replicates and the shake flask experiments in 3 replicates each. For clarity, the low standard deviations are not shown in this figure but can be found in App. Figure 9. Culture TOM device: 250 mL glass flasks, temperature (T) = 36.5°C, shaking diameter $(d_0) = 50 \text{ mm}$, frequency (n) = 140 rpm, shaking filling volume $(V_L) = 50 \text{ mL}$, 5 % CO₂, 70 % rel. hum., medium: TCX6D + 8 mM glutamine; starting cell density:

 5×10^5 cells mL⁻¹. Culture conditions μ TOM device: round 96-deep-well microtiter plate, temperature (T) = 36.5°C, shaking frequency (n) = 850 rpm, shaking diameter (d₀) = 3 mm, filling volume (V_L) = 1 mL, 5 % CO₂, humidified, medium: TCX6D + 8 mM glutamine; starting cell density: 5×10^5 cells mL⁻¹.

As can be seen from Figure 10, the OTR curves of all four cultivations match very well. Results are reproducible between different experiments over different scales. The low standard deviations of the OTR curves for the single experiments are shown in App. Figure 9. The OTR progression is the same as described previously for CHO DP12 cells (see Chapter 3.3). The cells experience equal conditions in all cultivations indicated by the similarity of the measured OTR progressions in shake flasks and MTPs. The OTR is directly correlated to the VCD (Ihling et al., 2022a). The VCDs of the data presented here are illustrated in Figure 18 and show no statistically significant difference (ANOVA, p-value < 0.05). It could thus be shown that an OTR_{max} based scale-up is also suitable for CHO DP12 cells. In the following, it will be investigated whether similar results are reachable with working volumes smaller than 1 mL.

5.3 Minimal filling volume for CHO cell cultivations in 96-deep-well MTPs

The μ TOM device was used to online monitor CHO DP12 cell cultures in 96-deep-well MTPs with round and square geometry with different filling volumes. The results are shown in Figure 11.

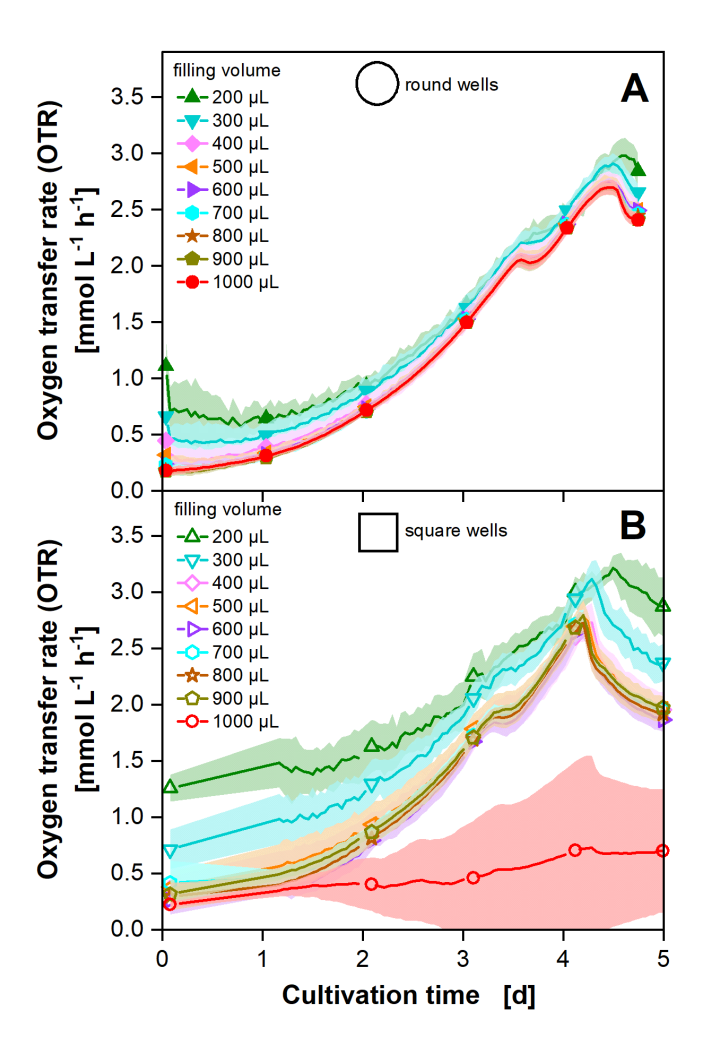


Figure 11: Cultivation of CHO DP12 cells in round and square 96-deep-well microtiter plates with varying filling volumes. A) Oxygen transfer rate (OTR) curves of cultivations in a round 96-deep-well plate with different filling volumes (N = 8 for each filling volume) monitored by the μ TOM device. B) OTR curves of cultivations in a square 96-deep-well plate with different filling volumes (N = 3 or 6 for each filling volume). For clarity, only every 24th measuring point over time is marked as a symbol. The standard deviations are shown as shaded areas. Culture conditions: temperature (T) = 36.5°C, shaking frequency (n) = 850 rpm, shaking diameter (d₀) = 3 mm, varying filling volume (V_L), 5 % CO₂, humidified, medium: TCX6D + 8 mM glutamine; starting cell density: 5×10^5 cells mL⁻¹.

Figure 11 A shows that the OTR curves of the cultivations with 400 to 1000 μ L filling volume in round well MTPs are essentially equal. The standard deviation of the OTR measurement increases with decreasing filling volume. This effect was described by Dinger et al. (2022). Regarding two main engineering parameters – OTR_{max} and P/V – the equal results can be explained as follows: The OTR_{max} increases with decreasing filling volume (App. Table 1). This means that oxygen limitation does not occur in any case. The decisive factor when regarding the OTR_{max} is that no oxygen limitation

occurs. It is not necessary to achieve exactly the same OTR_{max} values with different cultivations. At the same time, P/V increases with lower filling volumes (Büchs et al., 2000; Montes-Serrano et al., 2022). For 96-well MTPs, this was shown by Montes-Serrano et al. (2022). However, they also showed that P/V is not the sole criterium influencing the conditions in the fluid. Shear rates were simulated by computational fluid dynamics (CFD) within their publication. These increase with increasing well size whereas P/V decreases with increasing well size. Therefore, the authors conclude that no direct inference from P/V on culture conditions can be made. Similar results were found by Peter et al. (2006) for shake flasks. They showed that the filling volume has no impact on hydromechanical stress whereas it was previously shown that P/V and the filling volume behave anti-proportionally (at constant shaking frequency and shaking diameter) (Büchs et al., 2000; Peter et al., 2006). For the data shown here, it is therefore also explainable why the same OTR curves result from different filling volumes. From the data, the thesis can be set up that the change in P/Vø by varying the filling volume is not high enough to evoke differences in culture behavior by OTR monitoring. The cultivations with 200 and 300 µL slightly differ from the other ones especially at the beginning of the cultivation, when the OTR values are lowest. In these two conditions, the gas volume is large compared to the oxygen consumed by the cells. This leads to an imprecise measurement of the partial pressure decrease in the wells. Therefore, these filling volumes are not recommended without adapting the measurement time. To increase the measurement precision for lower filling volumes, longer measurement phases are necessary (Dinger et al., 2022).

Regarding Figure 11 B, in which the same experiment with square well MTPs is shown, similar results are seen. The OTR curves of the cultivations with filling volumes of 400 to 900 μ L are again essentially equal. The ones with 200 and 300 μ L are again not comparable to the other results for the reasons mentioned above. Moreover, 1 mL filling volume is not suitable for square well MTPs. It leads to unpredictable and unreproducible results as can be seen by the large standard deviations indicated by the red shade. When shaking MTPs it is important to ensure full mixing so that the cells remain in suspension. Enough force must be generated to ensure that the surface of the liquid contacts the bottom of the well. This can be calculated using the liquid angle (Duetz et al., 2000; Duetz, 2007). The calculations show that complete mixing should no longer be possible from 800 μ L upwards for square 96-deep-well MTPs under the

cultivation conditions used in this study. However, the calculations are based on wells with a flat bottom. Round bottoms were used in this experiment. In addition, phenomena such as frictional forces are not considered in calculations and the geometry of the wells leads to baffling effects which are not predictable. It can therefore be assumed that the force in wells with 1 mL filling volume is no longer sufficient to achieve complete mixing, which leads to unreproducible results. When comparing all cultivations in round and square well MTPs with filling volumes between 400 and 900 µL (see App. Figure 10), it becomes obvious that the use of round and square geometries leads to very similar results. The OTR increases in both cases for about 4 days ending in the maximal reached OTR of about 2.7 mmol L-1 h-1. Only the shape of the peak is different (App. Figure 10). The reason for the different shapes cannot be explained in detail up to now but may be due to different power inputs. Square well MTPs are known for higher stress on the cells as the corners function as baffles (Hermann et al., 2003). However, as these experiments show, they barely influence the OTRs of the tested CHO DP12 cells.

5.4 Application example: different amounts of the media component glutamine

The first application example of the µTOM device refers to the analysis of media components. The common media in use are commercial and the composition is unknown. Therefore, an analysis of single media components is difficult. However, the amino acid glutamine has to be added to almost any of those media as it is not stable over time. Therefore, glutamine concentrations can be easily adjusted and the impact can be analyzed. Varying glutamine concentrations were chosen as an example for media component analysis. The effect of different initial glutamine amounts in the cell culture medium TCX6D was examined. Initial glutamine concentrations of 0 to 20 mM in steps of 1 mM were tested with the cell line CHO DP12. The corresponding OTR curves are illustrated in Figure 12.

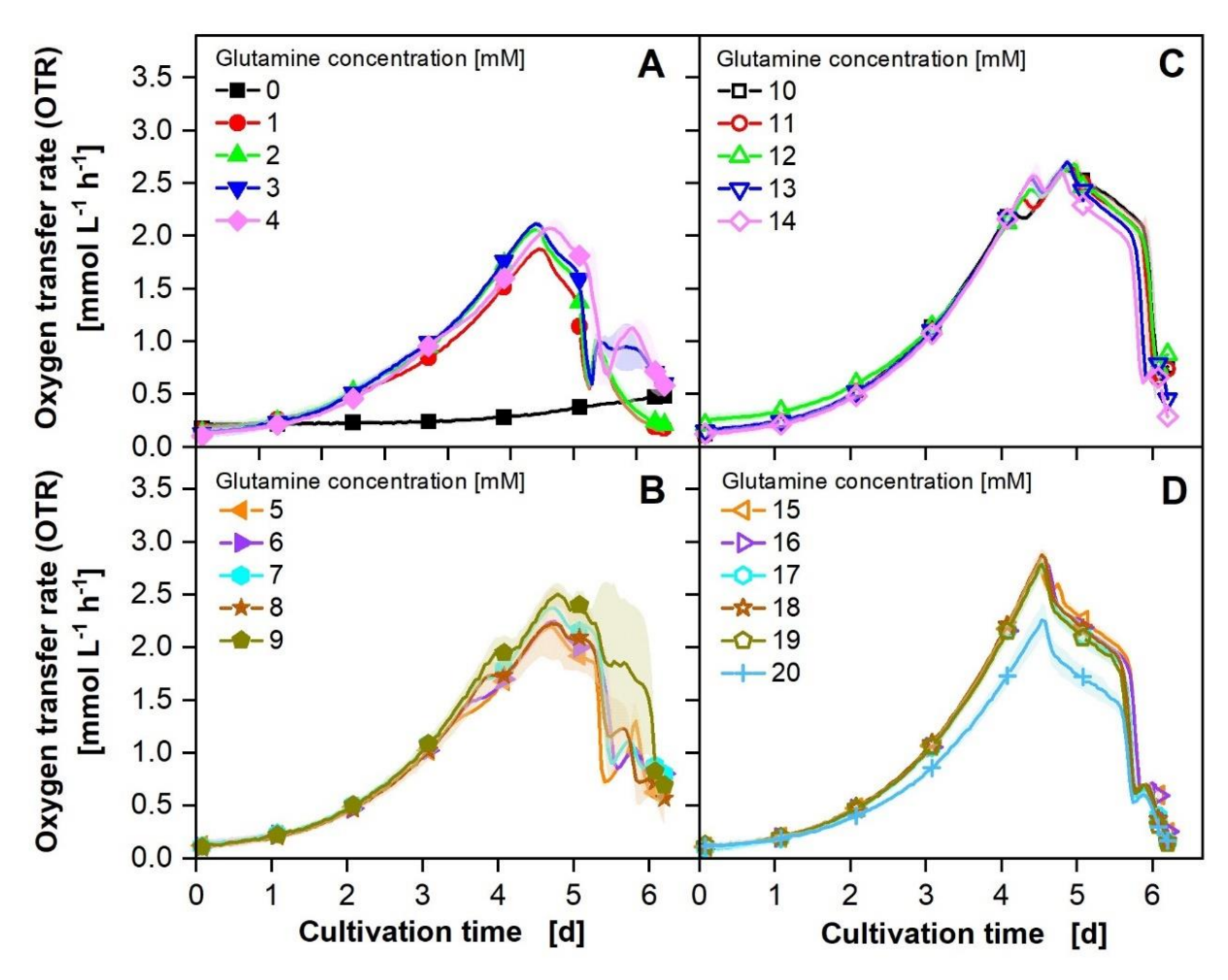


Figure 12: Oxygen transfer rate (OTR) of CHO DP12 cells with varying initial glutamine concentrations. The low standard deviations (N = 3) are shown as shaded areas. For clarity, only every 24^{th} measuring point over time is marked as a symbol. Culture conditions μ TOM device: round 96-deep-well microtiter plate, temperature (T) = 36.5° C, shaking frequency (n) = 850 rpm, shaking diameter (d₀) = 3 mm, filling volume (V_L) = 1 mL, 5 % CO₂, humidified, medium: TCX6D + varying concentrations of glutamine; starting cell density: $5x10^{5}$ cells mL⁻¹.

As can be seen in Figure 12 A, the OTR curve of the cultivation without any glutamine (black line and closed squares) does not increase for the first 4 cultivation days. Afterward, it rises to about 0.5 mmol L⁻¹ h⁻¹ until the end of the monitored time of 6 cultivation days. The cells survive without glutamine but there is hardly any growth. Glutamine can be synthesized by mammalian cells but it is, however, often intended to be an essential amino acid for CHO cells. It has various functions, e.g. in protein synthesis, as an amino acid precursor, and as a carbon and nitrogen source (Zhang et al., 2017). The absence of glutamine was reported to lead to a delay in the start of the exponential growth phase (Ritacco et al., 2018). A delay in growth is also seen for the CHO DP12 cultivation without glutamine from Figure 12 A. When using 1 to 4 mM of

glutamine, the OTR curves increase steadily until about day 4.5. This is in contrast to the kinks in the OTR curves described earlier (Chapter 3.2 and 3.3) where two phases of increase with different slopes are visible and which was related to depletion of glutamine. The OTR reaches a maximum of about 2 mmol L⁻¹ h⁻¹. The two decreasing phases are comparable to the standard cultivations described before (Chapter 3). There is a first decreasing phase before the OTR drops sharply because of glucose depletion around day 5 of cultivation. The use of 5 to 9 mM (Figure 12 B) glutamine leads to OTR curves that are comparable to the standard cultivations described in Chapter 3.3 with two increasing and two decreasing phases. The maximum OTR is about 2.2 to 2.5 mmol L⁻¹ h⁻¹. With higher glutamine concentrations (10 to 14 mmol L¹ h⁻¹, Figure 12 C) there are two distinct peaks visible in the OTR curves. The time of their appearance is slightly shifted backward with increasing glutamine concentrations. Afterward, the typical two decreasing phases occur. Two clear peaks in OTR progression are related to a second substrate limitation as described in Anderlei and Büchs (2001). Up from 15 mM glutamine to 19 mM, the second peak disappears resulting in one increasing OTR phase to a maximum of around 3 mmol L⁻ ¹ h⁻¹. A glutamine concentration of 20 mM leads to a slower increase in OTR and to a maximum of about only 2.3 mmol L⁻¹ h⁻¹. In comparison to the other curves in Figure 12, some kind of toxic effect occurs at 20 mM of glutamine. With the metabolization of glutamine to glutamate and α-ketoglutarate ammonium is produced (Mazurek, 2011; Pereira et al., 2018). Ammonium can be toxic to mammalian cells. For CHO cells, it was reported in two different studies that 5.1 mM of ammonium can lead to an inhibition of cell growth or that 8 mM can lead to a reduction of 50 % in growth. Therefore, it is recommended to balance the initial amino acid concentrations in the medium – especially glutamine – as they lead to ammonium production (Pereira et al., 2018). Common glutamine concentrations in use are between 2 and 8 mM (Bort et al., 2010). Research has demonstrated that low glutamine concentrations (about 2.5 mM) are optimal for cultivation (Bort et al., 2010; Parampalli et al., 2007). However, this study showed that growth is not decreased up to 19 mM of glutamine. In contrast, the OTR increased to a higher maximum with concentrations beyond 10 mM indicating higher growth. For further assertions and interpretations, ammonium concentrations should be measured.

One additional aspect that was analyzed for this experiment is the final antibody concentration. It is depicted in Figure 13.

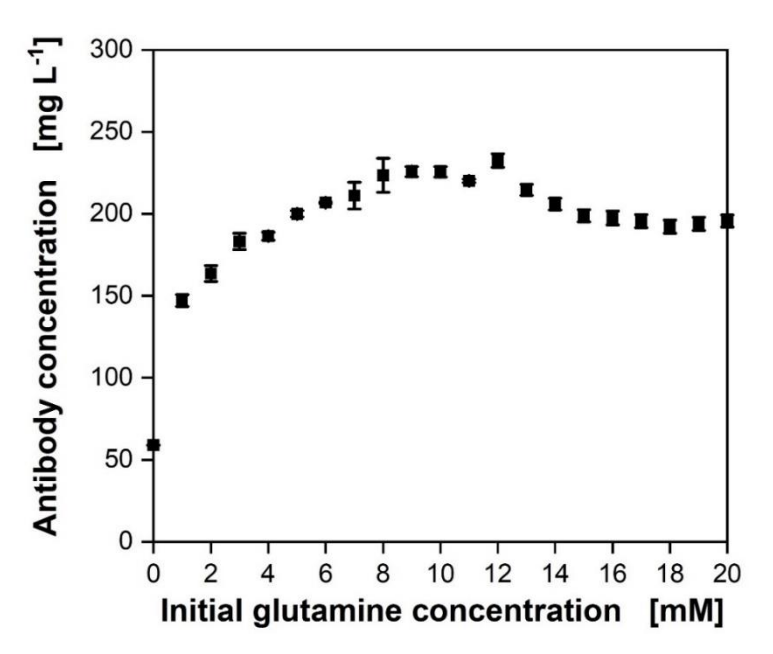


Figure 13: Final antibody concentrations for CHO DP12 cultivations with different initial amounts of glutamine. The standard deviations of three biological replicates are shown as error bars.

The antibody concentration at the end of cultivation (after 6 days) increases with increasing initial glutamine concentrations up to 7 mM to about 225 mg L⁻¹. It is on a nearly constant level for higher initial glutamine concentrations up to 13 mM. For higher concentrations, it is again constant with about 200 mg L⁻¹. Therefore, higher initial concentrations of glutamine than our standard conditions of 8 mM did not lead to severe reductions in the final antibody titer. In the literature, it was reported that high amounts of ammonium reduce product titer (Pereira et al., 2018; Ritacco et al., 2018). However, in this experiment, the high glutamine concentrations obviously did not lead to conditions where production was influenced. Another aspect studies have indicated is that product quality, especially glycoforms, can be affected (Pereira et al., 2018). This needs further investigation in future studies.

All in all, it could be shown that the μTOM device is a valuable tool for monitoring different media conditions in high-throughput. By monitoring the OTR, important information on culture behavior is available without any sampling. There is potential for further investigation from two perspectives: on the one hand, the question of glutamine

concentrations and its impact on cell growth can be further examined. On the other hand, the μ TOM device can be a useful tool for the analysis of any medium component and will be a valuable tool for media optimization.

5.5 Application example: kill curve experiments

5.5.1 Online monitoring of kill curve experiments in shake flasks

Kill curve experiments are traditionally conducted in shake flasks or tubes. Therefore, they were performed in 100 mL glass shake flasks with the antibiotic puromycin and CHO-K1 cells in the first experiment. Due to the capacity (number of flasks), two antibiotic concentrations were selected – a low (2 μg mL⁻¹) and a high (9 μg mL⁻¹) concentration. Additionally, a negative control was cultured without puromycin. All conditions were cultivated in four replicates. Two flasks per condition were connected to the TOM device to monitor the OTR online and two flasks were used for offline sampling. The culture volume per flask was set to 20 mL due to two reasons: 1) The offline flasks were sampled every two days. It must, therefore, be ensured that the liquid volume in the flasks is sufficient until the end of the experiment. 2) To obtain reliable OTR data from the CHO cultivation, the filling volume must be at least 20 % of the nominal flask volume due to the low respiration activity (Ihling et al., 2021). The results of this experiment are depicted in Figure 14.

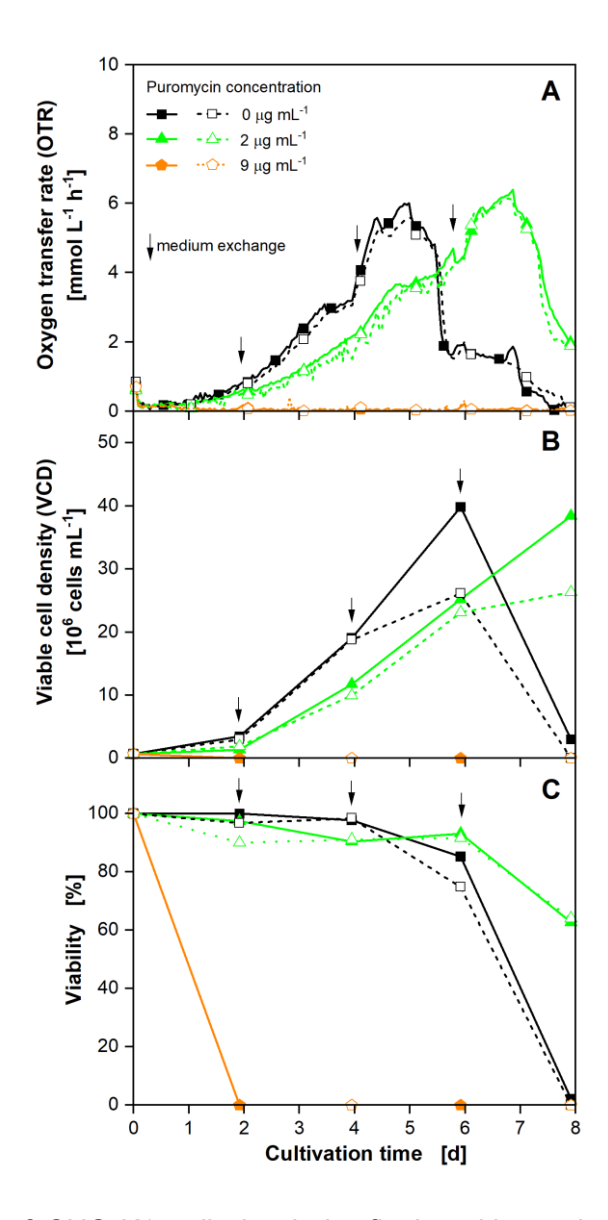


Figure 14: Kill curves of CHO-K1 cells in shake flasks with varying concentrations of the antibiotic puromycin. The experiment was performed in four replicates, in total. The medium was exchanged every 2nd day (indicated by black arrows) by cell separation through centrifugation and resuspension in fresh medium with supplemented puromycin. (A) Depicted is the oxygen transfer rate (OTR) determined by a Kuhner TOM device. For clarity, only every twelfth measuring point over time is marked as a symbol. The single outlier in the OTR data after every medium exchange due to temperature adaptations was removed from the data. For original data please refer to App. Figure 11. The two online monitored biological replicates are indicated by solid lines and filled symbols or dashed lines and open symbols. (B) Two further biological replicates were cultivated offline. The biological replicates of the offline analysis are depicted as solid and filled symbols or dashed lines and open symbols. The viable cell density (VCD) was determined at each medium exchange by the Neubauer Chamber method from offline shake flasks. (C) Viability was calculated from the same samples. Cultivations were performed in a Kuhner TOM device. Culture conditions: 100 mL glass flasks, temperature (T) = 36.5° C, shaking frequency (n) = 140 rpm, shaking diameter (d₀) = 50 mm, filling volume $(V_L) = 20 \text{ mL}$, 5 % CO_2 , 70 % rel. hum., medium: TCX6D + 8 mM glutamine + varying concentrations of puromycin; starting cell density: 5x10⁵ cells mL⁻¹.

The OTR of the reference culture without antibiotics increases until cultivation day 5 to a maximum of about 6 mmol L-1 h-1 (Figure 14 A, black lines). This high OTR occurs because of the regular medium exchange (indicated by black vertical arrows) every second day, in contrast to normal batch cultivations (Chapter 3.3). The sharp drop in the OTR between days 5 and 6 is due to glucose depletion, as described before (Chapter 3.3). The VCD (Figure 14 B), as well as the viability (Figure 14 C), reflect the observations from the OTR. The VCD increases over the first six cultivation days, before it drops sharply (black lines and squares). The deviations in the two replicates are probably caused by the Neubauer Chamber cell count method. This is known as quite an error-prone method because of the manual counting. Viability remains constant for five cultivation days before it drops.

The OTR curves of cultivations with 2 µg mL⁻¹ of puromycin resemble the curves of the reference cultivations but they are time-shifted (Figure 14 A, green line). The maximum OTR of likewise about 6 mmol L⁻¹ h⁻¹ is reached after 7 days instead of 5 days. This indicates that the metabolic activity of the cells is somehow influenced, but the cells are not killed. The offline data (Figure 14 B, C) show the same results. The VCD increases slower than for the reference culture and the viability drops later. The sharp drop in the OTR data reveals that the CHO cells die after 7 days due to glucose depletion. This conclusion could not be drawn based solely on offline data, which are usually taken once a day. With incomparably more effort, e.g. hourly sampling and offline analyses, a similar output could be expected.

The OTR curves of the cultures with 9 µg mL⁻¹ puromycin heavily differ from the other ones (Figure 14 A, orange lines). The OTR is at 0 mmol L⁻¹ h⁻¹ after only two cultivation days. This reveals that there is no metabolic activity anymore and, therefore, no living cells. These results are again reflected by the offline data (Figure 14 B, C).

All in all, the results of the first experiment show that the influence of different puromycin concentrations can be examined by online monitoring of the respiration activity. It is, therefore, suitable for performing kill curve experiments. Nevertheless, the minimal antibiotic concentration that kills all untransfected cells could not be determined in this preliminary experiment. This could be done by choosing more antibiotic concentrations between 2 and 9 µg mL⁻¹ in a second experiment. However,

this would be laborious and expensive because: 1) the medium exchange is elaborate because the shake flasks cannot be centrifuged and the cell suspension must, therefore, be transferred to centrifugation tubes every time 2) a lot of resources, like medium, tubes, cells, time, space in the incubator, etc. are needed. Therefore, the experiments were transferred to the μ TOM device in 96-deep-well MTPs.

5.5.2 Online monitored kill curve experiments in 96-deep-well MTPs

Firstly, the kill curve experiment with CHO-K1 cells and puromycin from Figure 14 was transferred to the round 96-deep-well MTP. Twelve different conditions could be cultivated in 8 replicates at once (see Figure 1). Antibiotic concentrations from 0 to 10 µg mL⁻¹ in steps of 1 µg mL⁻¹ and a negative control (NC), meaning only medium without cells, were used. The medium was exchanged every second day by centrifugation of the MTP, discarding the supernatant, and resuspension of the cells in fresh medium with the corresponding antibiotic concentration. Before every medium exchange, one well per condition was sampled for offline analysis of VCD and viability (Figure 15 B, C).

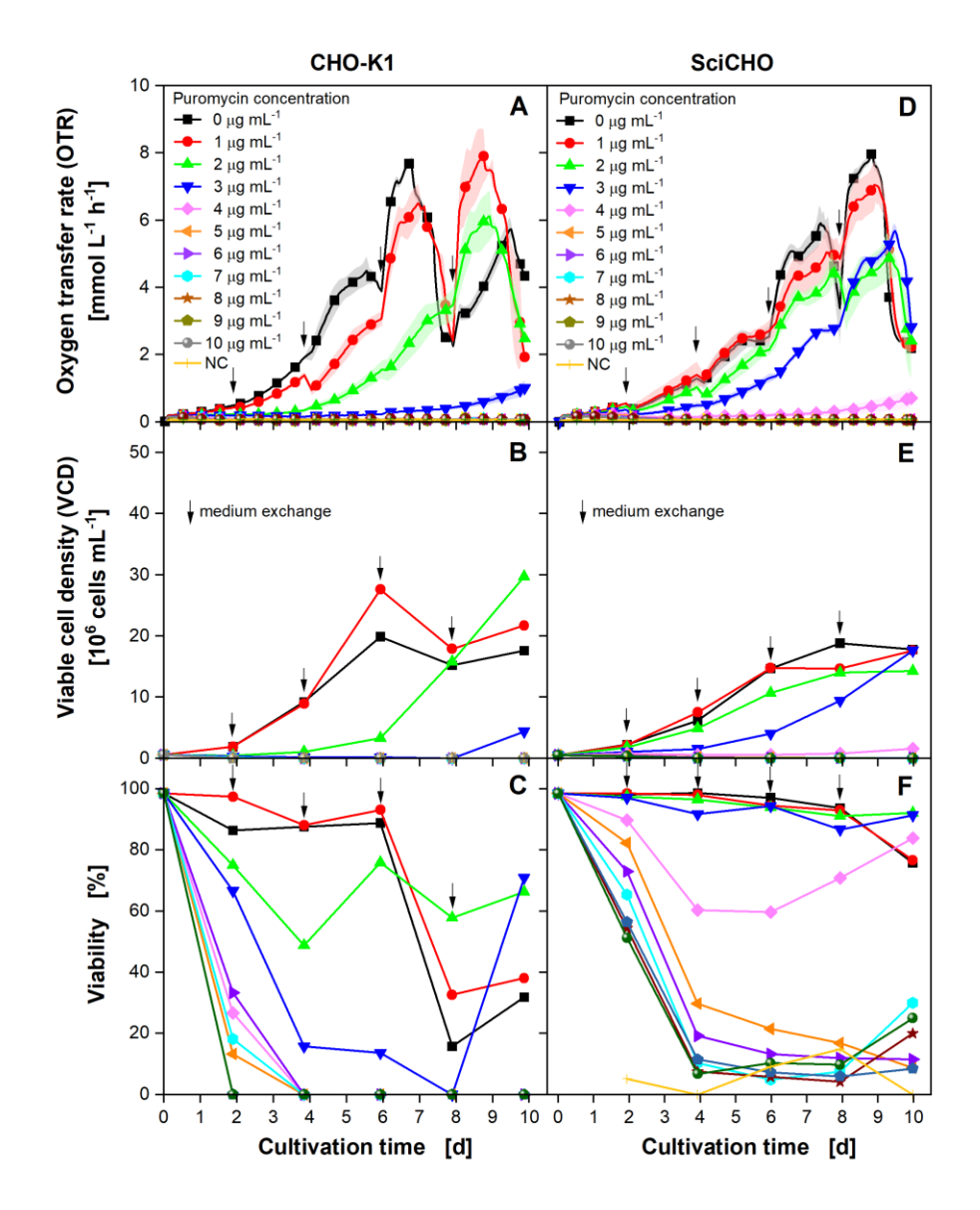


Figure 15: Kill curves of CHO-K1 cells and sciCHO cells in round 96-deep-well microtiter plates with varying concentrations of the antibiotic puromycin. The experiments were performed in eight replicates, according to the experimental strategy illustrated in Figure 1. The medium was exchanged every 2nd day (indicated by black vertical arrows) by cell separation through centrifugation and resuspension in fresh medium with supplemented puromycin. With every medium exchange, one well per condition was sampled for offline analysis resulting in a single sample per day. (A, D) Depicted is the mean oxygen transfer rate (OTR) of 3-4 replicates. The standard deviations are shown as shaded areas. For clarity, only every twelfth measuring point over time is marked as a symbol. The outlier in the OTR data after every medium exchange due to temperature adaptations was removed from the data. For original data, please refer to App. Figure 11 B, C. The viable cell density (VCD) was determined at each medium exchange by the Neubauer Chamber method for CHO-K1 cells and by CEDEX for sciCHO cells from one sampled well. (C, F) Viability was calculated from the same samples. Cultivations were performed in a µTOM device. Culture conditions: round 96-deep-well microtiter plate, temperature (T) = 36.5°C, shaking frequency (n) = 850 rpm, shaking diameter $(d_0) = 3 \text{ mm}$, filling volume $(V_L) = 1 \text{ mL}$, 5 % CO_2 , humidified, medium: TCX6D + 8 mM glutamine + varying concentrations of puromycin; starting cell density: 5x10⁵ cells mL⁻¹.

In Figure 15 A, the OTR of four replicates per condition is shown. These are the data from the wells that were not sampled and, therefore, ran until the end of cultivation. The graph of the cultures without puromycin (black line and squares) rises until glucose is depleted. After the medium exchange on day 8, the metabolic activity rises again. The graph for the cultivation with 1 µg mL⁻¹ puromycin shows a similar curve at a slightly lower level (red line and circles). For 2 µg mL⁻¹ (green line and upward triangles), the graph is time-shifted relative to the reference curve, as already observed in the shake flask cultivation (see Figure 14). The cultures treated with 3 µg mL⁻¹ puromycin (blue line and downward triangles) show a much reduced metabolic activity, in contrast to the reference, but there is still detectable respiration activity. This means that not all cells could be killed with this antibiotic concentration. All cultures with higher antibiotic concentrations than 3 µg mL⁻¹ puromycin show similar OTR data. After two days at the latest, the OTR is at about 0 mmol L⁻¹ h⁻¹. Thus, there are no living cells anymore. With this experiment, the lowest concentration that kills all untransfected cells could be determined as 4 µg mL⁻¹. This is in accordance with the literature, where exactly the same cell line and puromycin as an antibiotic were used (Hertel et al., 2022). Comparing the OTR curves to the corresponding VCD and viability graphs, the same results can be found. The viability is at 0 % for 4 µg mL⁻¹ or higher concentrations and there are no cells detectable at the end. For the cultivation with 3 µg mL⁻¹ puromycin, the offline measurements are however imprecise because there are very few cells. This makes cell counting with the Neubauer Chamber inaccurate and leads to outliers like the high viability at day 10 (Figure 15 C, blue line and downward triangles).

A second experiment was carried out to confirm that the kill curve experiment in MTPs by monitoring the OTR can be expanded to other CHO cell lines. The experimental setup was analogous to the first one, but sciCHO cells were used. The sciCHO cell line was derived from a non-engineered CHO-K1 subclone and was tested and optimized for stable and transient transfection (see Chapter 3.3). The OTR curves of this experiment are depicted in Figure 15 D. Concerning the kill curve experiment, the curve progressions are similar to the first experiment with CHO-K1 cells. The cultures treated with 1 (red line and circles), 2 (green line and upward triangles), and 3 (blue line and downward triangles) µg mL-1 puromycin show slower metabolic activity than the reference culture without puromycin (black line and squares). The cultivation with

4 µg mL⁻¹ (pink line and diamonds) shows a very low OTR, but there is still metabolic activity detected. Conclusively, 4 µg mL⁻¹ puromycin is not sufficient for sciCHO cells to kill all untransfected cells. The first concentration at which all the cells are killed is 5 μg mL⁻¹ (orange line and leftward triangles). This emphasizes that antibiotics have different effects on different cell lines, even if they are closely related. For this experiment, VCD and viability were measured by the CEDEX. The VCD (Figure 15 E) is, in general, lower than for the CHO-K1 cells (Figure 15 B) and increases to a lesser extent. That was expected from the OTR curves. The VCD verifies that 5 µg mL⁻¹ is the lowest puromycin concentration at which no cells survive. The viability (Figure 15 F) is above 60 % for all cultivations treated with 0-4 µg mL⁻¹ puromycin. For all other samples, the viability never drops to 0 %. This is not due to living cells, but due to the measurement device. The CEDEX has a lower detection limit of 4x10⁵ cells mL⁻¹. If the concentration is lower, the accuracy drops, and especially the measured viability is affected. If only one particle is incorrectly recognized as a viable cell, viability is influenced. This is also emphasized by the negative control (yellow line and crosses, Figure 15 F), in which a viability of up to 20 % is measured, even though there have never been cells in the corresponding wells.

5.5.3 Transfer of the MTP kill curve method to a second antibiotic

To confirm the general applicability of performing kill curve experiments in online monitored 96-deep-well MTPs, a second antibiotic was tested. For this purpose, hygromycin B was chosen. The setup for the experiment was similar to the ones before with puromycin, but this time the two cell lines were cultivated simultaneously in one MTP (see App. Figure 12). Hygromycin B concentrations from 100-250 µg mL⁻¹ for CHO-K1 cells and from 100-350 µg mL⁻¹ for sciCHO cells in steps of 50 µg mL⁻¹ were tested. Additionally, a reference culture for both cell lines without hygromycin B was cultivated. Figure 16 shows the OTR curves of the cultivations.

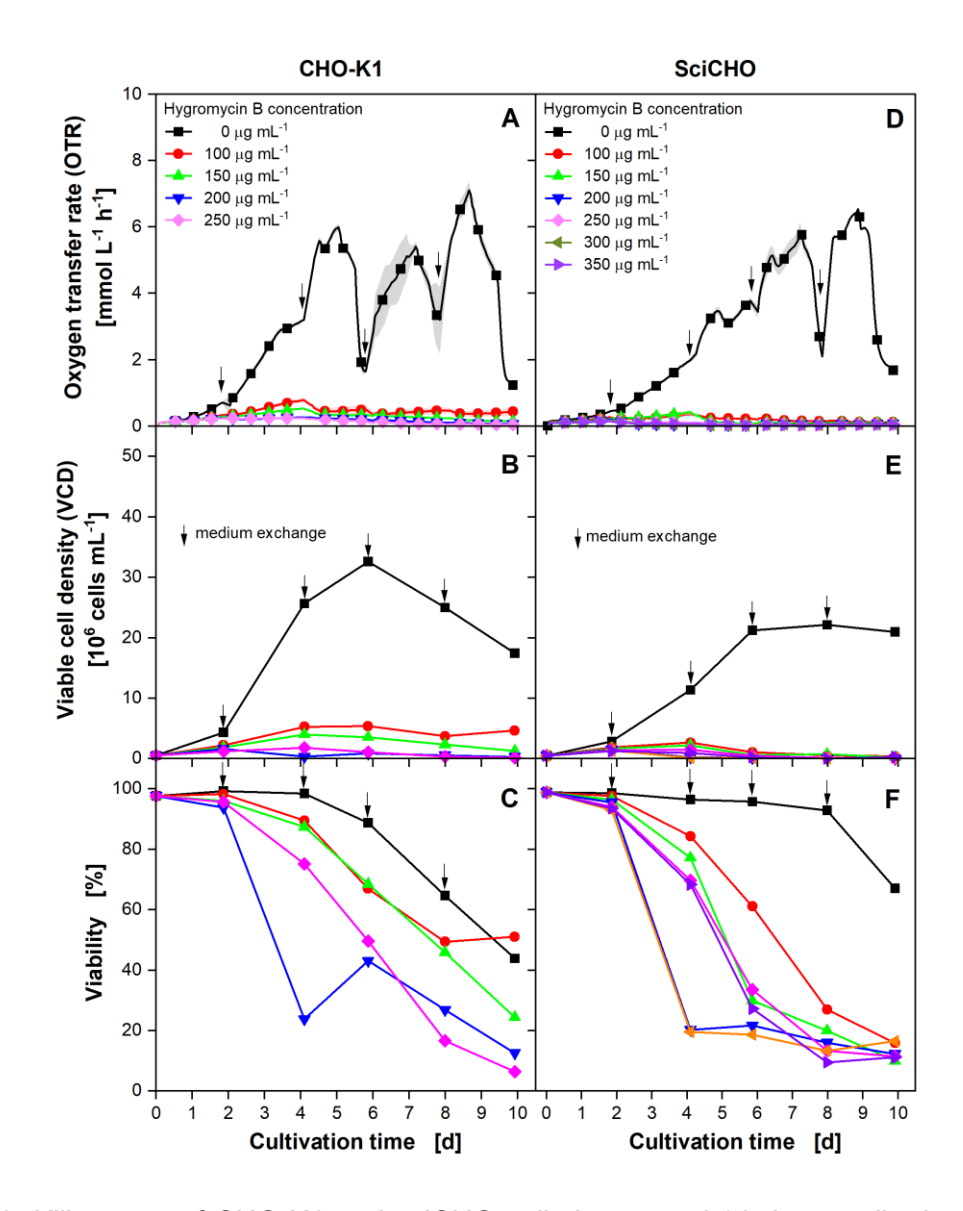


Figure 16: Kill curves of CHO-K1 and sciCHO cells in a round 96-deep-well microtiter plate with varying concentrations of the antibiotic hygromycin B. The experiments were performed in eight replicates on a single microtiter plate (see also App. Figure 12). The medium was exchanged every 2nd day (indicated by vertical black arrows) by cell separation through centrifugation and resuspension in fresh medium with supplemented hygromycin B. With every medium exchange, one well per condition was sampled for offline analysis resulting in a single sample per day. (A, D) Depicted is the mean oxygen transfer rate (OTR) of 3-4 replicates. The standard deviations are shown as shaded areas. For clarity, only every twelfth measuring point over time is marked as a symbol. The outlier in the OTR after every medium exchange due to temperature adaptations was removed from the data. For original data please refer to App. Figure 11 D, E. (B, E) The viable cell density (VCD) was determined at each medium exchange by CEDEX from one sampled well. (C, F) Viability was calculated from the same samples. Cultivations were performed in a µTOM device. Culture conditions: round 96-deep-well microtiter plate, temperature (T) = 36.5°C, shaking frequency (n) = 850 rpm, shaking diameter $(d_0) = 3 \text{ mm}$, filling volume $(V_L) = 1 \text{ mL}$, 5 % CO_2 , humidified, medium: TCX6D + 8 mMglutamine + varying concentrations of hygromycin B; starting cell density: 5x10⁵ cells mL⁻¹.

The OTR curve of the reference culture without hygromycin B (black line and squares) differs strongly from all the other ones. It shows a high OTR increase and drops after 5 days because of glucose depletion. The cultures treated with 100 (red line and circle) or 150 (green line and upward triangle) µg mL⁻¹ hygromycin B show a slight increase in the OTR signal up to day 4. Afterward, it drops slightly and remains on a constant level until the end of cultivation, meaning there is still a low metabolic activity. For 200 (blue line and downward triangles) and 250 (pink line and diamond) µg mL⁻¹ hygromycin B, the OTR is on a very low level (< 0.2 mmol·L⁻¹·h⁻¹) for the first 6 days of cultivation. Afterward, it drops to 0 mmol L⁻¹ h⁻¹. Thus, the lowest concentration that kills all cells is 200 µg mL⁻¹ hygromycin B. Analyzing the OTR curves for the sciCHO cells in Figure 16 D, it becomes visible that all OTR curves from cultures treated with hygromycin B drop to 0 mmol L⁻¹ h⁻¹ during the cultivation time. Therefore, the concentration sought here is $\leq 100 \, \mu g \, mL^{-1}$. The offline data confirm the online analysis for those cultivations depicted in Figure 16 B, C, E, and F. In summary, kill curve experiments could be performed for two different CHO cell lines with two antibiotics each. For every combination of cell line and antibiotic, a minimal concentration that kills all untransfected cells could be found. The results are summarized in Table 2.

Table 2: Summarized antibiotic concentrations, at which all untransfected cells were killed in the experiments performed in this study.

Cell line Antibiotics	CHO-K1	SciCHO
Puromycin InvivoGen (QLL-43-02)	4 μg mL ⁻¹	5 μg mL ⁻¹
Hygromycin B Roth (169283353)	200 μg mL ⁻¹	≤ 100 µg mL ⁻¹

The concentration of either puromycin or hygromycin B is different for the two cell lines, which emphasizes that the effectiveness of one antibiotic varies between different cells (Lanza et al., 2013). On top of this, the courses of the OTR curves highlight that antibiotics have highly different effects on cell cultures. While cells treated with low amounts of puromycin show only slower metabolic activities, cells treated with low

amounts of hygromycin B can hardly survive. The different modes of action of antibiotics are stated several times in the literature. In short, hygromycin B inhibits protein synthesis by disrupting translocation and promoting mistranslation, while puromycin inhibits protein synthesis by ribosome-catalyzed incorporation into the C-terminus of elongating nascent chains (Delrue et al., 2018; Mortensen and Kingston, 2009; Schiøtz et al., 2011; Yeo et al., 2017).

Using the μ TOM device, it is possible to perform 96 kill curve experiments simultaneously in one MTP. In contrast, 96 experiments in commonly used tubes or shake flasks would require a considerable amount of additional work, and material, and are almost impossible to handle in the laboratory for several reasons: 1. There must be sufficient incubation capacity for all cultivation vessels. 2. All cultures would have to be centrifuged and sampled individually. 3. The cells would have to be counted manually using the Neubauer Chamber or a high-capacity cell counting device would have to be available. 4. There would be an extremely high medium consumption and, therefore, high costs. In the MTP, 5 mL of medium is used for one well (corresponding to one antibiotic concentration without any replicates), including all media changes every two days. For one shake flask (or tube) with a filling volume of 20 mL, a total of 100 mL of medium would be required for the same experimental outcome. This means that using the μ TOM for kill curve experiments can reduce media consumption by 95 %. Generally, it is expected that the advantages of the μ TOM kill curve method can be exploited for various cell types, for example with different metabolic rates.

5.6 Summary

To summarize, the μ TOM device was shown to be suitable for online monitoring of CHO cell cultures. Compared to the two published devices M24 and μ RAMOS (Chen et al., 2009; Ihling et al., 2023), the 96-deep-well MTPs used in the μ TOM allow for a reduction of the filling volume to at least 400 μ L per well (M24 = 5mL, μ RAMOS = 2mL). At the same time, the number of wells and, thus, the number of parallel cultures increases. The transfer of CHO cultivations from the well-established TOM device for shake flasks to the μ TOM device based on OTR_{max} as a scale-down parameter showed highly comparable results. The OTR curves for both devices are

essentially equal for CHO-K1 and CHO DP12 cells, which indicates the same environmental conditions in both devices. On top of this, cultivations of the CHO-K1 cells in the TOM and μ TOM devices were nearly identical over a period of about three months, verifying a high reproducibility. Moreover, results demonstrate that the CHO DP12 cells can be cultivated in square 96-deep-well MTPs as well. Results are comparable to round well MTPs.

The second part of this chapter dealt with application examples of the μ TOM device. At first, different amounts of the media component glutamine were analyzed. Varying concentrations of glutamine were clearly visible in the progression of the OTR curves of CHO DP12 cells. Thus, the μ TOM device was shown to be in general a valuable tool for analyzing media components. Glutamine concentrations from 1-19 mM resulted in well-growing cells. Without any glutamine, growth was delayed for at least 5 cultivation days. At 20 mM some kind of toxic effect appeared. The final antibody titer was at the maximum for this cell line for initial glutamine concentrations between 7 and 20 mM. For a deeper insight into the biological interpretation of the results, further investigation is necessary but was not part of this thesis. The goal of figuring out whether the μ TOM is suitable for media component screening was achieved.

The second example of application engaged with kill curve experiments. The influence of the antibiotic puromycin on CHO-K1 cells could be successfully monitored through online monitoring of the OTR with the TOM device as a proof of concept. Kill curve experiments were then transferred to the μ TOM device. By testing 10 different antibiotic concentrations at once, the minimal concentration that kills all untransfected cells could be determined in one step, without requiring any sampling and offline analysis. In contrast to similar experiments in shake flasks, 95 % of medium reduction could be achieved. Furthermore, the general validity of performing kill curve experiments in the μ TOM was demonstrated by using a second CHO cell line (sciCHO) and a second antibiotic (hygromycin B) for both cell lines. In future investigations, dedicated wells are no longer required for verification by offline samples. In this case, 32 different conditions could be analyzed in triplicates in only one experiment.

All in all, the presented results highlight the wide application field of OTR online monitoring for CHO cell cultures in 96-deep-well MTPs.

6 Scale-up of CHO cells from MTPs to a STR

6.1 Background

It is becoming increasingly important in the pharmaceutical industry to focus on timeand cost-saving methods during process development. Process development in large scales is elaborate. Thus, it is normally executed on lab-scale and the process is later scaled up to production scale (Heath and Kiss, 2007). Furthermore, it is often not feasible to explore the influences of all process parameters in large-scale experiments (Li et al., 2006). Therefore, scale-up and scale-down approaches are very common. The main goal of scaling up processes is to increase the working volume while keeping the product yield and quality as well as cell density and viability similar. On the other hand, scale-down models aim to mimic typical phenomena in large-scale vessels (Li et al., 2006; Xing et al., 2009). Most of the scale approaches in the literature for mammalian cells focus on the scale transfers between differently sized STRs, for example in Gaugler et al. (2024), Li et al. (2006), Pan (2018), Tyupa et al. (2021), Xing et al. (2009) and Xu et al. (2017). Studies are summarized by Lemire et al. (2021). They also describe the most important key process parameters that must be considered when scaling up. These comprise aeration, oxygen supply, CO₂ stripping, mixing time, and hydrodynamic shear stress including power input. Ideally, all these parameters should be kept constant between different scales. However, as this is technically not possible, one parameter must be chosen as the scale-up/-down criterion. The most commonly used parameters in cell culture experiments are a constant k_La value, a constant volumetric aeration rate, impeller tip speeds, or a constant P/V (Lemire et al., 2021). A constant k_La value considers oxygen supply and a constant volumetric aeration rate is based on sufficient CO₂ stripping (Lemire et al., 2021). When using a constant P/V as scale-up parameter, gas transfer and mixing phenomena are considered. P/V is a crucial parameter for mammalian cell cultures as it is a variable to quantify hydromechanical stress. This is particularly important in STRs as P/Vø and P/Vmax occurring behind the stirrer blades have to be distinguished (Nienow, 2006; Nienow et al., 2013) (see also Chapter 4).

Nowadays, miniaturized STRs are a common choice for small-scale experiments. The minimal cylindric vessels comprise 250 mL whereas vessels with squared geometry

have minimal filling volumes of approximately 10 mL (Hsu et al., 2012; Moses et al., 2012; Rameez et al., 2014). However, there are other options like shake flasks or MTPs as was described in Chapters 3 and 5. For microbial systems, scale-up approaches from small shaken devices to larger STRs are a common method and reviewed by Marques et al. (2010). To my knowledge, these approaches are barely stated in the literature for mammalian cell systems. Scale transfer between MTPs, shake flasks and STRs was only found within the three publications briefly described in the following. None of them considered MTPs as small as 96-well MTPs and with different geometries. Micheletti et al. (2006) performed a scale translation from shaken 24-well MTPs (800 µL) to conical flasks (100 mL) and a STR (3.5 L) with VPM8 hybridoma cells. They used a constant P/V as a scale-up parameter and found that the MTP cultivations were not completely comparable to larger scales. The growth rate was reduced while lactate concentrations were increased. The titer in MTPs was almost twice as high as in the STR and shake flasks (Micheletti et al., 2006). In another study, a comparison of MTPs (2-4 mL), a miniature bioreactor (500 mL), and a STR (5 L) was performed in fed-batch mode with CHO cells. Here, a matched mixing time was used as the scale-up parameter. The results of the cultivation in all devices were very comparable as long as they were in batch mode. Slight deviations occurred in fedbatch mode (Sani, 2015). Markert and Joeris (2017) set up an automated MTP-based system (6-48 wells) for CHO-K1 cell cultures and compared the results to 1000 L STRs. The results shown are very comparable between the scales (VCD, product-, and lactate concentration). Unfortunately, however, no cultivation conditions were specified for the different scales (Markert and Joeris, 2017). Some other approaches focus on the comparability between shaken tubes and STRs (Gomez et al., 2017; Rouiller et al., 2016; Tissot et al., 2011).

For small-scale shaken systems, the low information content is often criticized. However, it could be shown previously in this thesis that OTR monitoring is simple to implement for shake flasks and MTPs (Chapters 3 and 5). Therefore, OTR monitoring is a valuable tool for mammalian cells and seems to be promising for scale-up approaches. Thus, the question arises whether it is possible to scale up mammalian cell cultivations from MTP scale to a STR cultivation using OTR online monitoring.

Cell culture media and cultivations foam strongly in agitated systems. Therefore, antifoam agents are mandatory in STR cultivations. At the latest, since the

development of chemically defined media, this issue is of great interest. There is a huge number of antifoam agents commercially available (Routledge, 2012). Chemical agents are classified by their formulations. They consist of solid hydrophobic particles, an oil, or a mixture of those (Velugula-Yellela et al., 2018). The mechanisms of disrupting the foam are different and are summarized in Routledge (2012). Most commercially available media contain Pluronic F68 – often in concentrations of about 0.1 % (Ma et al., 2004; Tharmalingam and Goudar, 2015; Zhang et al., 1992). The mode of action of Pluronic F68 was investigated in several studies. For example, it incorporates into CHO cell membranes, changes the membrane fluidity, and lowers the interfacial tension at the vapor-liquid interface, all resulting in protection of the cells from foam or bubble bursting (Tharmalingam and Goudar, 2015). Beyond that, Pluronic F68 is used to reduce foam building. However, it was also demonstrated that high concentrations can have inhibiting effects on cell growth (Hu et al., 2008). Some other studies dealt with the influence of different antifoam agents on CHO cells. Velugula-Yellela et al. (2018) tested the influence of the Antifoams 204, C, EX-Cell, SE15 and Y-30. While Antifoam 204 and Y-30 are toxic for CHO cells, VCDs are similar to each other for the other three antifoams. Flynn et al. (2024) also found that Antifoam 204 is toxic for CHO cells. In contrast, Antifoam C leads to a reduction in growth, and Antifoam SE-15 shows no inhibition. Furthermore, Antifoam SE-15 was demonstrated to reduce foam completely within 2 minutes (Flynn et al., 2024). It is known that antifoams influence the k_La value and the DOT (Routledge, 2012). However, no detailed investigation of the effect of different antifoams in various concentrations on CHO cells is available. As this is important information when using the OTR as a database for scale-up processes in STRs, the influence of some antifoam agents was studied.

This chapter first evaluates the influence of different antifoam agents on the OTR of CHO DP12 cells. Afterward, the aim is to explore the possibility of scaling up cultivations from the small shaken systems (MTP and shake flasks) to a 1.5 L STR.

6.2 Influence of antifoam on the OTR of CHO cell cultures

The use of antifoam agents in STRs is unavoidable for mammalian cell cultivations. As this represents a difference to the shaken systems, the influence of different antifoam agents on the OTR of the cultivation was tested in advance. This was carried out in MTPs with the μ TOM device using different amounts of antifoam (dilutions of 1:50 to 1:10000). The results are shown in Figure 17.

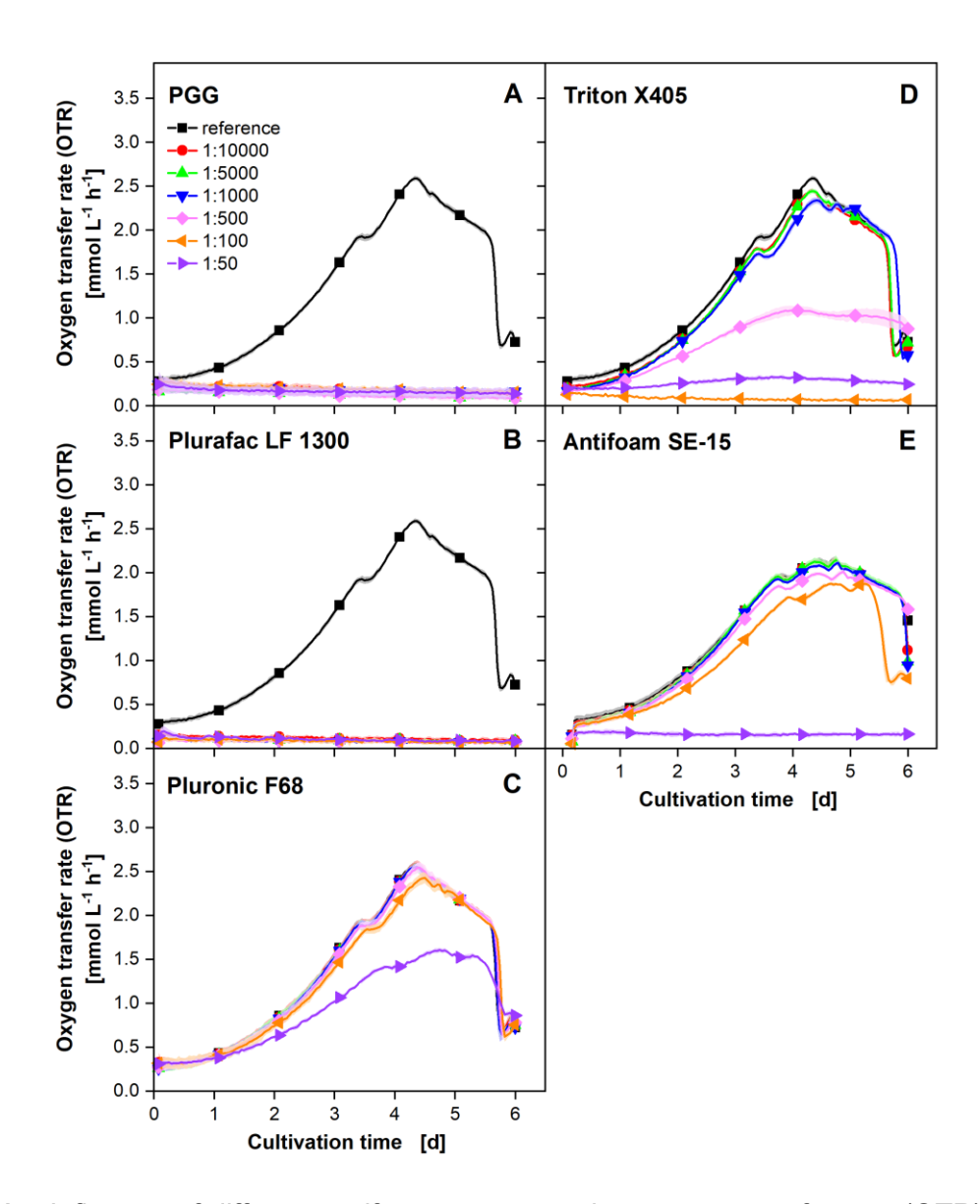


Figure 17: Influence of different antifoam agents on the oxygen transfer rate (OTR) of CHO DP12 cells. Depicted is the OTR as the mean value of 3 replicates. Standard deviations are shown as shaded areas. For clarity, only every 24^{th} measuring point over time is marked as a symbol. Antifoam agents were tested in dilutions from 1:50 to 1:10000. Tested antifoams are A) Polypropylenglycol (PGG), B) Plurafac LF 1300, C) Pluronic F68, D) Triton X405, and F) Antifoam SE-15. Culture conditions μ TOM device: round 96-deep-well microtiter plate, temperature (T) = 36.5° C, shaking frequency (n) = 850 rpm, shaking diameter (d₀) = 3 mm,

filling volume (V_L) = 0.8 mL, 5 % CO₂, humidified, medium: TCX6D + 8 mM; starting cell density: $5x10^5$ cells mL⁻¹.

In Figure 17 A and B, the OTR progressions of the cultivations with the antifoam agents PGG and Plurafac LF 1300 are depicted. Both are non-ionic surfactants and are known as strong antifoam agents (Karakashev and Grozdanova, 2012; Koch et al., 1995). The reference CHO DP12 cultivation without any antifoam agent shows the same OTR progression as described previously (Chapter 3.3). As soon as PGG or Plurafac LF 1300 are added, an OTR of nearly 0 mmol L⁻¹ h⁻¹ results. Thus, it can be seen that both antifoam agents have a toxic effect on CHO cells and are therefore not suitable for cultivations. Other studies with CHO cells and antifoams also found that some of them are toxic, for example, Antifoam 204 (Flynn et al., 2024; Velugula-Yellela et al., 2018). The OTR progressions of the cultivations with Pluronic F68 are shown in Figure 17 C. The progression of all curves with the antifoam in dilutions from 1:100 to 1:10000 is highly comparable to the progression of the reference culture. Thus, the antifoam does not affect the OTR. Solely, the increase of the OTR at a dilution of 1:50 is slowed compared to the other ones and the maximal OTR is at only 1.5 mmol L⁻¹ h⁻¹. In literature, some studies also revealed the toxicity of Pluronic F68 in high concentrations (Hu et al., 2008). Pluronic is an essential component of cell culture media and is also present in TCX6D. It has various functions in protecting CHO cells (Tharmalingam and Goudar, 2015; Zhang et al., 1992). However, it is not as effective as other antifoam agents in destroying existing foam (unpublished data). Therefore, two other antifoams were tested. One of these is Triton X405 (Figure 17 D). For this, slight influences on OTR progression are visible for dilutions from 1:1000 to 1:10000. The OTR curve is slightly shifted downwards compared to the reference culture. Triton X405 in dilutions from 1:50 to 1:500 leads to heavily reduced growth rates, reduced maximum OTR values, or even no growth at all. As Triton X405 impacts the OTR already in low concentrations slightly and has severe influence in higher concentrations, this one was not chosen for the STR cultivations. For Antifoam SE-15 (Figure 17 E), the OTR curves with dilutions up to 1:1000 show nearly identical progressions to the reference cultivation. In a dilution of 1:500, the OTR curve is slightly shifted downwards from cultivation days 3 to 5. In a dilution of 1:100, the increase of the OTR has slowed and the maximal reached OTR is about 0.3 mmol L-1 h-1 lower than for the other cultures. In the lowest tested dilution (1:50) the OTR does not increase. It stays almost on a constant level over the whole cultivation time indicating that the cells do not grow because of toxic effects of the antifoam. Antifoam SE-15 was previously already found to be a very good antifoam agent as it was able to remove all foam within two minutes. Furthermore, it had no impact on cell growth and antibody production (Flynn et al., 2024). This experiment showed that there was almost no influence on the OTR in a certain concentration range. Therefore, antifoam SE-15 was used for the STR cultivations. The dilution was not lower than 1:1000 meaning that the influence of the antifoam on the OTR should be negligible.

6.3 Scale-up from small shaken vessels to a STR based on OTR_{max}

The comparability between MTPs and shake flask cultivations was shown in Chapter 5. In this chapter, the question is addressed of whether a scale-up to a STR is also possible. The aim here is to reproduce the results shown in Figure 10 in a STR. Therefore, a scale-up parameter is needed. In the first approach, OTR_{max} was used as a scale-up parameter as this was already successfully utilized for the scale transfer between MTP and shake flasks. For calculations, OTR_{max} for the STR was fixed to 3.75 mmol L⁻¹ h⁻¹ because the maximal OTR measured in the shake flask was about 3 mmol L⁻¹ h⁻¹ (see Figure 10) and the DOT should not fall below 20 % (Lemire et al., 2021). With this assumption, the k_La value was calculated according to Equation (13) and then used to calculate P/V with Equation (14). The resulting P/V is 0.33 kW m⁻³. The Ne for one Rushton turbine is 5.4 in a turbulent flow regime (Re > 10⁴) (Bates et al., 1963). Using this and the calculated target P/V, the stirrer speed for the experiment can be calculated by using Equation (16). All values needed for calculation are depicted in App. Table 2. The resulting stirrer speed is 359 rpm. Therefore, a stirring speed of 360 rpm was used for the first scale-up experiment depicted in Figure 18. The assumption of a turbulent flow regime was checked by determining Re. As this is >10⁴ (1.2x10⁴) for the described stirring conditions, the assumption of a turbulent flow regime was valid.

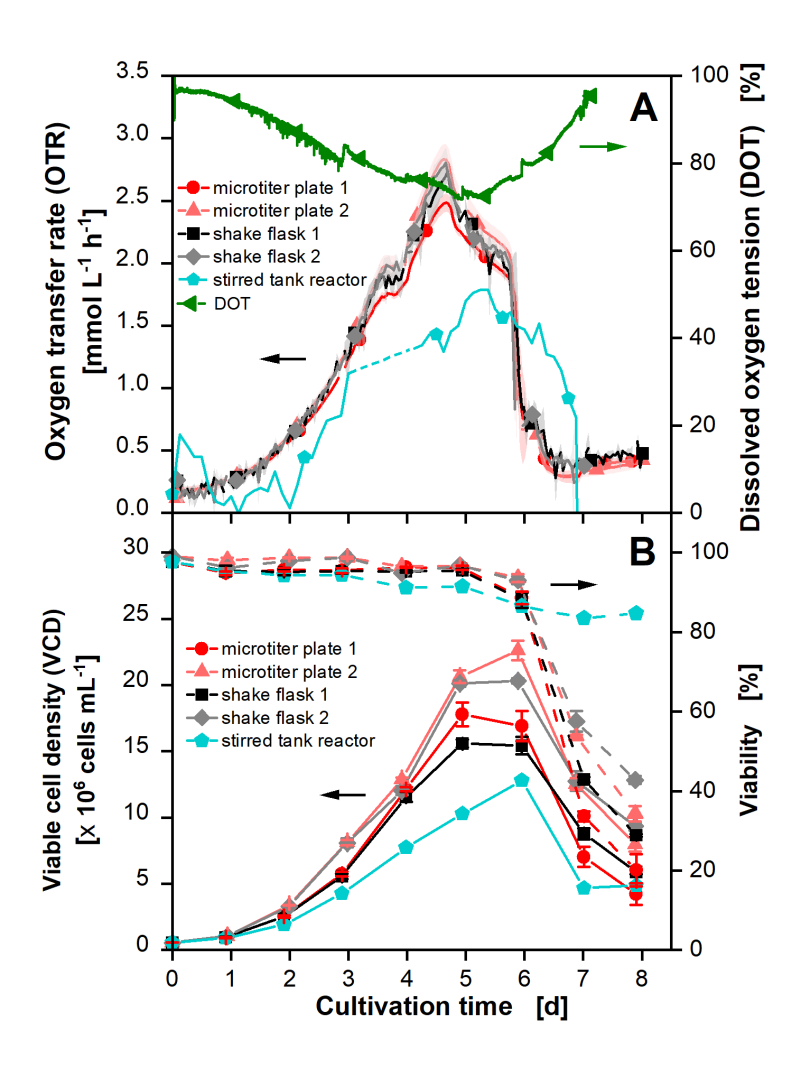


Figure 18: OTR_{max}-based scale-up of CHO DP12 cell cultivations. Cultures were cultivated in round 96-deep-well plates (dark and light red lines/circles and upward triangle), shake flasks (black and gray lines/squares and diamonds), and a stirred tank reactor (STR, blue line and pentagon). A) Depicted is the oxygen transfer rate (OTR). The curves of the microtiter plate and shake flask cultivations are already shown in Figure 10 and plotted here again for improved comparability. The data for the STR are interpolated over 3 hours. The calculated OTR values between days 3 and 4 are distorted by a short-term failure of aeration and stirring and were therefore excluded from the data. For original data refer to App. Figure 13. The dissolved oxygen tension (DOT) (green line and sideward triangle) of the stirred tank reactor is also plotted. For clarity, only one measuring point per day is shown. B) Displayed are the viable cell densities (VCD) and viabilities for all cultivations. Culture conditions TOM and µTOM device: refer to Figure 10. Culture conditions stirred tank reactor: 1.5 L reactor, temperature (T) = 36.5° C, stirrer speed $(n_{ST}) = 360 \text{ rpm}$ (Rushton turbine), volume $(V_L) = 600 \text{ mL}$, 5 % CO_2 , aeration = 0.2 vvm (sparged), medium: TCX6D + 8 mMglutamine; starting cell density: 5x10⁵ cells mL⁻¹.

OTR determination in shaken systems works according to the RAMOS principle, i.e. the OTR is calculated from the slope of the oxygen partial pressure decrease in the measuring phase of the system and is therefore independent of absolute oxygen concentration values. Additionally, the measurement precision can be tuned by

prolonging the measurement phase (Anderlei et al., 2004). This makes the OTR determination more precise compared to the off-gas analysis which uses absolute oxygen concentration values. Looking at Figure 18, this difference in accuracy becomes obvious when comparing the OTR curves of the already described cultivations in MTPs and shake flasks (see Chapter 3.3) with the one of the STR (blue line and pentagons). However, it is apparent that the shape of the curves is similar but the increase of the STR-OTR curve is slower than the other ones. Additionally, the maximum reached OTR for the STR is only about 1.8 mmol L⁻¹ h⁻¹ compared to about 2.8 mmol L⁻¹ h⁻¹ for the shaken devices. The calculated OTR values between days 3 and 4 are distorted by a short-term failure (<10 minutes) of aeration and stirring and were therefore excluded from the data. Oxygen availability was not influenced as the DOT did not drop below 70 % (green line and sideward triangle). For calculations of the stirrer speed with the scale-up parameter OTR_{max}, the requirement was made that DOT should not drop below 20 %. The DOT dropped only to 70% which shows that the k_La value was higher than assumed initially. The underestimation is probably because the calculation has been established for large-scale STRs where surface to volume aeration is lower than in smaller STRs and surface aeration may play a role (Maier, 2002).

The VCD and viability in Figure 18 B show the same trend as the OTR curves. The increase of the VCD is slower for the STR than for the shaken devices. At the same time, viability stays above 80 % for at least 8 cultivation days compared to 6 for the shaken devices. Also, the peak VCD with about 12x10⁶ cells mL⁻¹ is the lowest for STR cultivation. A slowed depletion of nutrients was also observed. Glucose was depleted one day later for the STR than for the shaken devices. The lactate switch occurred later as well (see App. Figure 14 B and C). Finally, the antibody concentration did not reach the expected maximum of 250 mg L⁻¹ (see App. Figure 14 D). All these observations were already discussed for shake flask cultivations with increased P/V and respective energy dissipation rates in Chapter 4. Glucose and glutamine depletion, the lactate switch and the specific growth rate correlated linearly with logarithmically plotted average energy dissipation. Therefore, it was concluded that the cultivation conditions chosen here with the scale-up parameter OTR_{max} led to conditions with too high power input. The cells were subjected to hydromechanical stress leading to a change in nutrient consumption and slowed growth. Thus, OTR_{max} based scale-up is

not suitable when scaling up cell cultures from shaken devices to a STR but the hydromechanical stress in the form of P/V must be considered.

6.4 Scale-up of CHO cell cultivations to a STR with constant P/Vø

Due to the findings in Chapter 4, P/Vø was used as a scale-up parameter for the second experiment. The aim was to match the P/Vø of 0.12 kW m⁻³ in STR that prevails in the shake flasks under the shaking conditions in this study (see Chapter 4). Therefore, Equation (16) was used to calculate the stirring speed with a $P/V_{\varnothing} = 0.12 \text{ kW m}^{-3}$ and the parameters used before. The resulting stirrer speed is about 250 rpm. In STRs, the magnitude of P/V varies depending on the locality. There are regions with higher local P/V behind the stirrer blades and regions with lower P/V. Each cell experiences different power inputs which are combined in the P/Vø. To not expose the cells to a too high P/V at the beginning of cultivation, the decision was made to not exceed the maximal local P/V. The cells must adapt to new conditions (fresh medium and stirred conditions). Therefore, the cells should be specially protected at the beginning of cultivation. In the literature, different estimations of the deviation of P/V_{max} from P/Vø are made. Kresta and Wood (1991) for example showed that P/V_{max} is about 10-fold higher than P/Vø. Therefore, a second criterium was set for the beginning phase (as long as DOT was above 80 %) of the cultivation. The upper limit of P/V (P/V_{max}) should not exceed P/Vø of 0.12 kW m⁻³ of the shake flask. This was used to calculate the stirrer speed with Eq. 8 (n = 117 rpm). The stirring speed was consequently started at 100 rpm and then increased to 250 rpm. After reaching 250 rpm, no further increase was performed to keep P/Vø in the STR in the range of $P/V \emptyset$ of the shake flasks. The Re-number is only slightly below 10^4 (Re = 0.84×10^4) for 250 rpm which is why a turbulent flow regime can be assumed. The OTR, VCD, and viability curves of the scale-up with constant P/V as a scale parameter are depicted in Figure 19. The results from Figure 10 are shown again for better comparability.

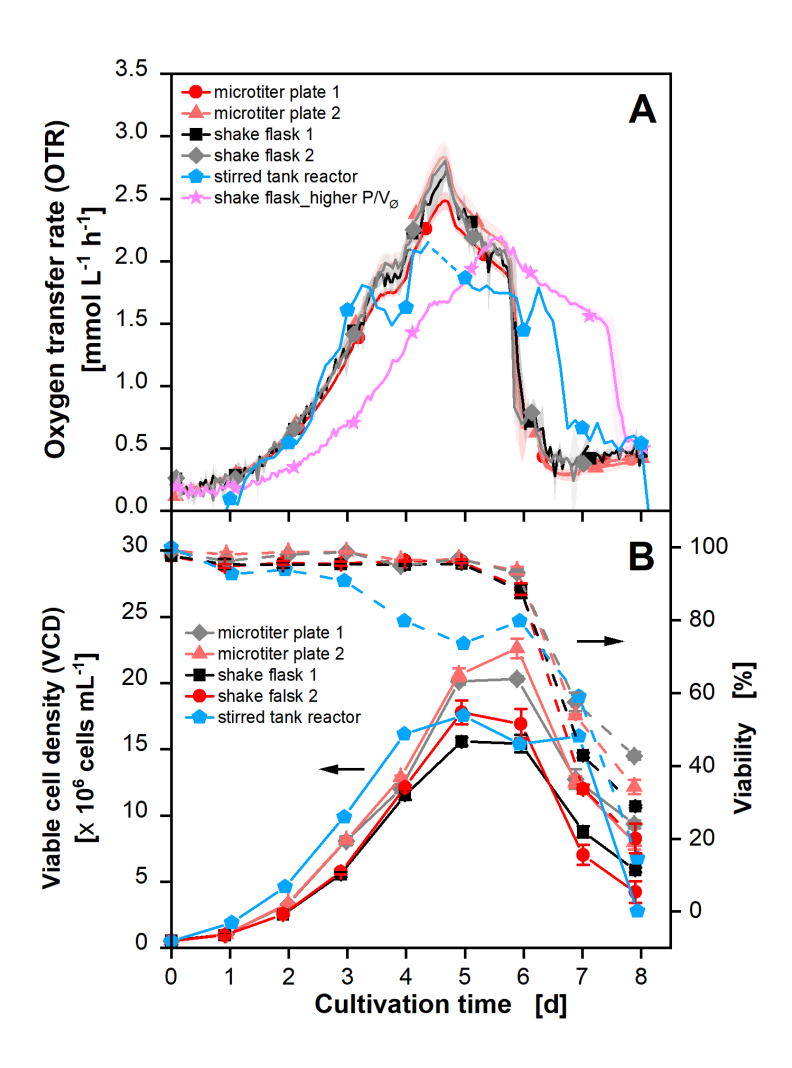


Figure 19: Scale-up of CHO DP12 cell cultivations with constant P/Vø. Cultivation in round 96deep-well plates (dark and light red lines/circles and upward triangle), shake flasks (black and gray lines/squares and diamonds), and a stirred tank reactor (blue line and pentagon). A) Depicted is the oxygen transfer rate (OTR). The curves of the microtiter plate and shake flask cultivations are already shown in Figure 10 and plotted here again for improved comparability. Additionally, the curve of the shake flask cultivation with $P/V = 1.45 \text{ W kg}^{-1}$ from Figure 5 is shown. The data for the STR are interpolated over 3 hours. The calculated OTR values between days 4 and 5 are distorted by a problem with the off-gas cooler and were therefore excluded from the data. For original data refer to App. Figure 13. For clarity, only one measuring point per day is shown. B) Displayed are the viable cell density (VCD) and viability for all cultivations. Culture conditions TOM and µTOM device: refer to Figure 10 Culture conditions stirred tank reactor: 1.5 L reactor, temperature (T) = 36.5° C, speed $(n_{ST}) = 100-250 \text{ rpm}$ (Rushton turbine), filling volume $(V_L) = 600 \text{ mL}$, 5 % CO_2 , aeration = 0.2 vvm (sparged), medium: TCX6D + 8 mM glutamine; starting cell density: 5x10⁵ cells mL⁻¹.

The OTR curves of all five cultivations in Figure 19 are identical during the first increasing phase (ca. 3 days) until glutamine is depleted (indicated by the kink in the OTR progression as described in Chapter 3.3). Afterward, the second increasing phase starts. The decreasing phase starting at day 4.5 is approximately one day

prolonged for the STR compared to the shaken devices. Therefore, the gradual OTR drop due to glucose depletion appeared on day 7 for the STR instead of day 6 as was seen for the shaken devices. Calculated OTR data between days 4.5 and 5.5 were distorted due to a technical problem with the off-gas cooler. Undefined excess water in the off-gas stream falsified the calculated OTR data and were therefore excluded from the graph. The DOT measurement is displayed in App. Figure 13. The DOT drops to a minimum of about 50 % which is absolutely tolerable as oxygen concentrations are usually maintained between 10% and 80% for CHO cell cultures (Lemire et al., 2021).

The deviations between OTR progression of STR and shake flasks can be explained when keeping the difference between P/Vø and P/Vmax for STRs in mind. P/Vmax was stated to be about 10 times higher than the P/Vø. Therefore, the results of the STR were compared to a shake flask cultivation with a ca. 10-fold higher P/V (1.45 kW m⁻³) from Chapter 4 and shown in Figure 19 (pink line and stars). The OTR drop due to glucose depletion at day 7 of the STR is in between those of the reference cultivations in the shaken devices (day 6) and the cultivation with increased P/Vø (day 8). The results can be confirmed by offline analyses, as shown in the following.

The VCD shown in Figure 19 B is comparable between the STR and the shaken devices. The viability of the STR is at a constant high level for the first three cultivation days before there is a slight decrease to around 80 % for the next three days. These deviations could be due to the method of VCD and viability determination. They were determined by using the manual Neubauer chamber method for the STR cultivation while the automated CEDEX device was used for the other cultivations. As the manual method is known as imprecise, this could have led to inaccuracies. The time of the severe viability decrease is again the same for all cultivations. Next to OTR, VCD, and viability, different offline parameters were analyzed for all cultivations and are depicted in Figure 20.

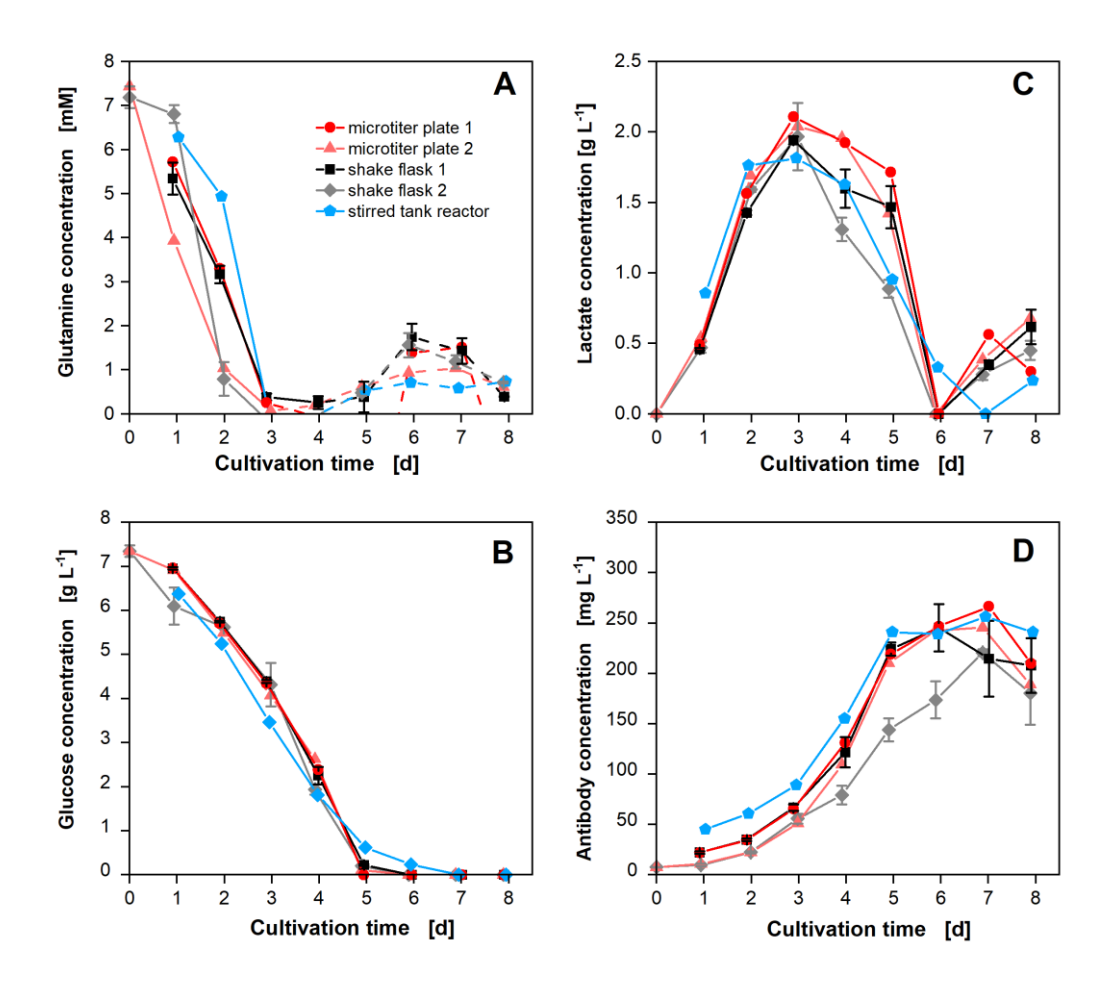


Figure 20: Offline measured metabolite and product concentrations of the cultivations shown in Figure 19. CHO DP12 cell cultivations were performed in round 96-deep-well plates (dark and light red lines/circles and upward triangle), shake flasks (black and gray lines/squares and diamonds), and a stirred tank reactor (blue line and pentagon). Depicted are A) glutamine concentrations B) glucose concentrations C) lactate concentrations and D) IgG antibody titer.

The glutamine concentrations in Figure 20 A demonstrate that the glutamine consumption was identical for all cultivations and is in accordance with the observations from Figure 19 where the kink in the OTR curve appears for all of them at almost the same time (approximately after 3.5 days). After depletion, the measured values increase again (dotted lines) which is only due to uncertainties and inaccurate measurements for very low or no glutamine concentrations of the spectrophotometric kit used for determining glutamine concentrations. Glucose (Figure 20 B) and lactate (Figure 20 C) consumption are in general also comparable between all cultivations in shaken devices and the STR even though the time of lactate depletion is slightly shifted backward for the STR. The most important aspect of a cultivation is the product production. Therefore, antibody concentrations were measured over the whole

cultivation time. As can be seen from Figure 20 D, a titer of about 250 mg L⁻¹ was reached in all five cultivations. This is the maximum known titer for this cell line stated by the supplier. All in all, results show that the scaling strategy using a constant P/V_{\varnothing} resulted in highly comparable cultivation conditions during the exponential growth phase across two systems with different power-input elements (shaken and stirred), spanning three orders of magnitude in scale.

6.5 Summary

This study addressed the question of whether a scale-up from small shaken devices to a STR is possible for CHO cells. The scale transfer between MTPs and shake flasks was already proven to be successful in Chapter 5. For STR cultivations, the use of an antifoam agent is required. This is a difference to the cultivations in shaken systems. Therefore, different types of antifoam were analyzed regarding their influence on the OTR. PGG and Plurafac LF 1300 were toxic to the cells. Pluronic F68 had little impact on the OTR. However, it is not the best antifoam agent to destroy existing foam. Triton X405 and Antifoam SE-15 are both highly effective antifoams. As Antifoam SE-15 had less influence on the OTR, this was used as an antifoam agent in the STR cultivations.

Two different approaches of scale-up processes were performed within this study. The transfer of cultivation to a STR by using an OTR_{max}-based scale-up strategy was not successful. This strategy focuses on sufficient oxygen supply within cultivation but does not concern hydrodynamics, shear forces or power input. The resulting hydromechanical stress was too high in the STR and oxygen supply is not an issue in mammalian batch cultivations as the cells grow slowly and oxygen is usually available in excess. Therefore, a constant P/Vø as scale-up parameter while ensuring a sufficient oxygen supply (DOT > 50 %) was shown to be suitable for a scale-up to a STR. With this strategy, hydrodynamics and different kinds of forces come into focus. A detailed analysis of P/Vø in shake flasks was consulted to perform a data-driven scale-up. The cultivation results (OTR progression) were to be expected for the STR when considering that an average and maximal local P/V are present in the STR but the difference is negligible in shaken devices. Offline parameters like VCD, viability,

glucose, lactate, and glutamine concentrations were highly similar in all three cultivation devices. Strikingly, also the antibody titer was the same for all cultivations when considering that the volumes were varied by three orders of magnitude across the scales. Therefore, a scaling strategy with constant P/V_{\varnothing} is more sensible for mammalian cells than a OTR_{max}-based strategy and improves comparability to shaken devices.

This study showed that a data-driven scale-up from 96-deep-well MTPs with a filling volume of a minimum of 400 μ L to a STR with 600 mL working volume was successful, meaning that the same cultivation conditions and the same final antibody titers were achieved.

7 Conclusion and outlook

Online monitoring of small-scale mammalian cell cultivations is seldom performed in routine process development. However, it provides valuable information about process behavior and is a beneficial tool for scaling up processes. CHO production processes are well-established in industry nowadays. Thus, Li et al. already stated in 2010 that the research focus is now on time- and cost-effectiveness in process development. They highlighted high-throughput techniques, online monitoring, and the usage of disposables as the three main areas of future research. The here presented thesis has made a decisive contribution to at least two of these aspects: online monitoring of the respiration activity in different scales combined with high throughput in 96-well MTPs.

Initially, different CHO cell lines were characterized by online monitoring of the OTR. A well-performing medium could be identified easily and without any sampling. Depletion of key metabolites is directly visible from the shape of the OTR curve progression. As OTR is correlated to VCD, online monitoring is an effective alternative without the need for sampling, while providing more information during cultivation. OTR monitoring was already shown to be a useful tool in process development. However, further development could even improve the information content. The correlation between VCD and glucose concentration to the OTR was previously described (Ihling et al., 2022a). A routine and automated application of these correlations would simplify processes. Real-time adjustments of the cultivation strategy would be facilitated. The implementation of different cultivation strategies like fed-batch or pulsed-batch fermentations – which would better reflect production processes – would be easier to realize. Furthermore, the combination of the OTR monitoring with others like DO and pH during cultivation would provide helpful information. Additionally, online monitoring of product concentrations (e.g. antibody titers) would be highly interesting as product concentration is often the determining factor in CHO cell cultivations.

The second part of this study analyzed the influence of hydromechanical stress levels on CHO DP12 cell cultures in shake flasks using OTR monitoring. The online data clearly demonstrated that the growth rate is slowed with increasing average energy dissipation rate. Glucose and glutamine depletion and the lactate switch correlate linearly with logarithmically plotted average energy dissipation rate. The final antibody titer was the same for all cultivations within laminar conditions. In turbulent conditions,

the final antibody titer was reduced by 40 %. This study showed that the influence of hydromechanical stress on CHO cells in shake flasks can be easily analyzed by using OTR monitoring. It already revealed important general relations between hydromechanical stress and the culture behavior of CHO cells. However, it would be worthwhile to repeat experiments with a high-producing CHO cell line. For future investigations, the analysis of antibody activity, glycosylation profiles, and further product quality aspects would be of high interest. As the established method is easily applicable and shake flasks are time- and cost-effective to handle, the application to other, more sensitive cells should be easy to implement.

The scale-down of CHO cell cultivations from shake flasks to 96-deep-well MTPs was examined in the third part of this study. OTR_{max} was used as the scale-down parameter. OTR progressions of shake flask and MTP cultivations were identical with the chosen cultivation conditions. In round well MTPs, the filling volumes could be reduced from 1 mL to 400 µL leading to the same results. 400 µL to 900 µL filling volumes are appropriate in square well MTPs. Even though the scale-down from shake flasks to MTPs was highly successful, there is potential for further investigation. On the one hand, a characterization of the different MTPs would provide valuable information, for example regarding shear rates and power input. This would facilitate the simulation of cultivation conditions from larger scales and make MTPs a useful tool as a scaledown model. On the other hand, it would be of keen interest to further decrease the filling volume while obtaining the same results. Two approaches are conceivable for that: firstly, the measuring phases of the µTOM device could be adapted for lower filling volumes. The measurement accuracy will be improved so that OTR determination of lower filling volumes is more precise. The second option would be the implementation of shaken low-well MTPs. The ratio of headspace to filling volume would improve and the precision of OTR measurement at lower filling volumes would increase.

Two application examples of the μ TOM device were shown within this thesis. One was from the research area of cell line engineering. Kill curve experiments were streamlined and, experimental procedure was reduced while throughput was increased at the same time. Beyond that, there are other applications conceivable in this research area. The monitoring technique could, for example, simplify clone selection steps when generating new cell lines. In general, the μ TOM is an advantageous tool for any kind of screening experiment. The second example provided the first proof that media

screening and optimization is possible for CHO cells. The influence of different initial glutamine concentrations was studied. From this single, simple experiment many further biological research questions have emerged. During metabolization of glutamine, ammonium is built as a by-product. This is toxic to the cells in high concentrations. Therefore, low glutamine concentrations are recommended for CHO cell cultivations. However, in the experiment presented here, high glutamine concentrations of up to 19 mM did not lead to toxic effects but even improved metabolic activity. For further investigation, ammonium concentrations as well as amino acid concentrations should be measured. Moreover, a detailed examination of productivity and product quality would be necessary. It would be also worth examining the phenomenon with other media and other, high-producing cell lines. New cultivation conditions could be implemented and similar studies with other media components like glucose could be investigated. Starting with this knowledge, OTR databased fed- or pulsed-batch strategies could be established.

Finally, a scale-up of the CHO cell cultivations from the small shaken devices to a STR was performed with the knowledge from previous studies in shake flasks and MTPs. For this, different antifoam agents were tested concerning their impact on the OTR. Antifoam SE-15 was proven to be the best antifoam with the smallest impact on OTR. However, there are many other possible antifoams available. They could be tested with little effort in the μ TOM device. Results could serve as a reference for further use of antifoams in mammalian cell cultivations.

The scale-up approach from small shaken devices to a STR was successful by using a constant power input as a scale-up parameter. This may lead to future experiments with CHO cells being carried out on a small shaken scale and subsequently being predictably reproduced in a STR. It is moreover conceivable that the shaken systems are used as scale-down models for larger systems e.g. to simulate heterogeneity effects at large scale. The data density of the STR cultivations could be further improved, for example, by using different probes such as capacitance, redox, or Raman sensors. All experiments in this study were performed in batch mode to prove the general feasibility of the methods. However, industrial production processes are usually performed in pulsed-batch, fed-batch, extended-batch, or perfusion mode. It would therefore be of high interest to transfer results on all scales from batch mode to one with feeding.

CHO cell culture processes are in general well-established even if there are still many details to be explored and processes can be streamlined. However, knowledge from these processes including the findings of this study is of high importance for the much less explored research areas of cell and gene therapy. Methods should be transferred to other mammalian cells like Human embryonic kidney (HEK) or stem cells which are the workhorses for cell and gene therapy studies.

In summary, this thesis established online monitoring of the oxygen transfer rate for fast-growing CHO cells in high-throughput in shake flasks and 96-well MTPs. The influence of hydromechanical stress on CHO cells was investigated and used as database for scale-up experiments into a STR. Therefore, the thesis decisively contributed to streamlining process development with CHO cell cultures and laid the foundation for improvements with other mammalian cell lines and processes.

8 Bibliography

- Aehle, M., Kuprijanov, A., Schaepe, S., Simutis, R., Lübbert, A., 2011. Simplified off-gas analyses in animal cell cultures for process monitoring and control purposes. Biotechnology letters 33 (11), 2103–2110. doi:10.1007/s10529-011-0686-5.
- Al-Rubeai, M., Singh, R.P., Goldman, M.H., Emery, A.N., 1995. Death mechanisms of animal cells in conditions of intensive agitation. Biotech & Bioengineering 45 (6), 463–472. doi:10.1002/bit.260450602.
- Anderlei, T., Büchs, J., 2001. Device for sterile online measurement of the oxygen transfer rate in shaking flasks. Biochemical Engineering Journal 7 (2), 157–162. doi:10.1016/S1369-703X(00)00116-9.
- Anderlei, T., Keebler, M.V., Cairó, J.J., Lecina, M., 2020. HEK293 cell-based bioprocess development at bench scale by means of online monitoring in shake flasks (RAMOS and SFR). Methods in molecular biology (Clifton, N.J.) 2095, 83–103. doi:10.1007/978-1-0716-0191-4_6.
- Anderlei, T., Zang, W., Papaspyrou, M., Büchs, J., 2004. Online respiration activity measurement (OTR, CTR, RQ) in shake flasks. Biochemical Engineering Journal 17 (3), 187–194. doi:10.1016/S1369-703X(03)00181-5.
- Aviner, R., 2020. The science of puromycin: From studies of ribosome function to applications in biotechnology. Computational and structural biotechnology journal 18, 1074–1083. doi:10.1016/j.csbj.2020.04.014.
- Bareither, R., Pollard, D., 2011. A review of advanced small-scale parallel bioreactor technology for accelerated process development: current state and future need. Biotechnology progress 27 (1), 2–14. doi:10.1002/btpr.522.
- Bates, R.L., Fondy, P.L., Corpstein, R.R., 1963. Examination of Some Geometric Parameters of Impeller Power. Ind. Eng. Chem. Proc. Des. Dev. 2 (4), 310–314. doi:10.1021/i260008a011.
- Bebbington, C.R., Renner, G., Thomson, S., King, D., Abrams, D., Yarranton, G.T., 1992. High-level expression of a recombinant antibody from myeloma cells using a

- glutamine synthetase gene as an amplifiable selectable marker. Biotechnology (Nature Publishing Company) 10 (2), 169–175. doi:10.1038/nbt0292-169.
- Bort, J.A.H., Stern, B., Borth, N., 2010. CHO-K1 host cells adapted to growth in glutamine-free medium by FACS-assisted evolution. Biotechnology journal 5 (10), 1090–1097. doi:10.1002/biot.201000095.
- Büchs, J., Maier, U., Milbradt, C., Zoels, B., 2000. Power consumption in shaking flasks on rotary shaking machines: I. Power consumption measurement in unbaffled flasks at low liquid viscosity. Biotech & Bioengineering 68 (6), 589–593. doi:10.1002/(SICI)1097-0290(20000620)68:6<589:AID-BIT1>3.0.CO;2-J.
- Büchs, J., Zoels, B., 2001. Evaluation of Maximum to Specific Power Consumption Ratio in Shaking Bioreactors. J. Chem. Eng. Japan / JCEJ 34 (5), 647–653. doi:10.1252/jcej.34.647.
- Chalmers, J.J., 2015. Mixing, aeration and cell damage, 30+ years later: what we learned, how it affected the cell culture industry and what we would like to know more about. Current Opinion in Chemical Engineering 10, 94–102. doi:10.1016/j.coche.2015.09.005.
- Chalmers, J.J., Ma, N., 2015. Hydrodynamic damage to animal cells, in: Animal Cell Culture, 2015th ed. Springer International Publishing, Cham, pp. 169–183.
- Chen, A., Chitta, R., Chang, D., Amanullah, A., 2009. Twenty-four well plate miniature bioreactor system as a scale-down model for cell culture process development. Biotech & Bioengineering 102 (1), 148–160. doi:10.1002/bit.22031.
- Crommelin, D.J.A., Mastrobattista, E., Hawe, A., Hoogendoorn, K.H., Jiskoot, W., 2020. Shifting Paradigms Revisited: Biotechnology and the Pharmaceutical Sciences. Journal of Pharmaceutical Sciences 109 (1), 30–43. doi:10.1016/j.xphs.2019.08.010.
- Daub, A., Böhm, M., Delueg, S., Mühlmann, M., Schneider, G., Büchs, J., 2014. Characterization of hydromechanical stress in aerated stirred tanks up to 40 m(3) scale by measurement of maximum stable drop size. Journal of biological engineering 8 (1), 17. doi:10.1186/1754-1611-8-17.

- Delrue, I., Pan, Q., Baczmanska, A.K., Callens, B.W., Verdoodt, L.L.M., 2018. Determination of the selection capacity of antibiotics for gene selection. Biotechnology journal 13 (8), e1700747. doi:10.1002/biot.201700747.
- Dinger, R., Lattermann, C., Flitsch, D., Fischer, J.P., Kosfeld, U., Büchs, J., 2022. Device for respiration activity measurement enables the determination of oxygen transfer rates of microbial cultures in shaken 96-deepwell microtiter plates. Biotechnology and bioengineering 119 (3), 881–894. doi:10.1002/bit.28022.
- Duetz, W.A., 2007. Microtiter plates as mini-bioreactors: miniaturization of fermentation methods. Trends in Microbiology 15 (10), 469–475. doi:10.1016/j.tim.2007.09.004.
- Duetz, W.A., Rüedi, L., Hermann, R., O'Connor, K., Büchs, J., Witholt, B., 2000. Methods for intense aeration, growth, storage, and replication of bacterial strains in microtiter plates. Applied and Environmental Microbiology 66 (6), 2641–2646. doi:10.1128/AEM.66.6.2641-2646.2000.
- Dumont, J., Euwart, D., Mei, B., Estes, S., Kshirsagar, R., 2016. Human cell lines for biopharmaceutical manufacturing: history, status, and future perspectives. Critical reviews in biotechnology 36 (6), 1110–1122. doi:10.3109/07388551.2015.1084266.
- Ferguson, E.C., Rathmell, J.C., 2008. New roles for pyruvate kinase M2: working out the Warburg effect. Trends in Biochemical Sciences 33 (8), 359–362. doi:10.1016/j.tibs.2008.05.006.
- Flitsch, D., Krabbe, S., Ladner, T., Beckers, M., Schilling, J., Mahr, S., Conrath, U., Schomburg, W.K., Büchs, J., 2016. Respiration activity monitoring system for any individual well of a 48-well microtiter plate. Journal of biological engineering 10, 14. doi:10.1186/s13036-016-0034-3.
- Flynn, J., Breen, L., Narayanan, S., Butler, M., 2024. Measurement and control of foam generation in a mammalian cell culture. Biotechnology progress 40 (4), e3450. doi:10.1002/btpr.3450.
- Forsten, E., Finger, M., Scholand, T., Deitert, A., Kauffmann, K., Büchs, J., 2023. Inoculum cell count influences separation efficiency and variance in Ames plate incorporation and Ames RAMOS test. The Science of the total environment 905, 167035. doi:10.1016/j.scitotenv.2023.167035.

- Forsten, E., Gerdes, S., Petri, R., Büchs, J., Magnus, J., 2024. Unraveling the impact of pH, sodium concentration, and medium osmolality on Vibrio natriegens in batch processes. BMC biotechnology 24 (1), 63. doi:10.1186/s12896-024-00897-8.
- Fu, T., Zhang, C., Jing, Y., Jiang, C., Li, Z., Wang, S., Ma, K., Zhang, D., Hou, S., Dai, J., Kou, G., Wang, H., 2016. Regulation of cell growth and apoptosis through lactate dehydrogenase C over-expression in Chinese hamster ovary cells. Appl Microbiol Biotechnol 100 (11), 5007–5016. doi:10.1007/s00253-016-7348-4.
- Gamboa-Suasnavart, R.A., Valdez-Cruz, N.A., Gaytan-Ortega, G., Reynoso-Cereceda, G.I., Cabrera-Santos, D., López-Griego, L., Klöckner, W., Büchs, J., Trujillo-Roldán, M.A., 2018. The metabolic switch can be activated in a recombinant strain of Streptomyces lividans by a low oxygen transfer rate in shake flasks. Microb Cell Fact 17 (1), 189. doi:10.1186/s12934-018-1035-3.
- Gaugler, L., Hofmann, S., Schlüter, M., Takors, R., 2024. Mimicking CHO large-scale effects in the single multicompartment bioreactor: A new approach to access scale-up behavior. Biotech & Bioengineering 121 (4), 1244–1256. doi:10.1002/bit.28647.
- Godoy-Silva, R., Chalmers, J.J., Casnocha, S.A., Bass, L.A., Ma, N., 2009a. Physiological responses of CHO cells to repetitive hydrodynamic stress. Biotech & Bioengineering 103 (6), 1103–1117. doi:10.1002/bit.22339.
- Godoy-Silva, R., Mollet, M., Chalmers, J.J., 2009b. Evaluation of the effect of chronic hydrodynamical stresses on cultures of suspensed CHO-6E6 cells. Biotech & Bioengineering 102 (4), 1119–1130. doi:10.1002/bit.22146.
- Gomez, N., Ambhaikar, M., Zhang, L., Huang, C.-J., Barkhordarian, H., Lull, J., Gutierrez, C., 2017. Analysis of Tubespins as a suitable scale-down model of bioreactors for high cell density CHO cell culture. Biotechnology progress 33 (2), 490–499. doi:10.1002/BTPR.2418.
- Hansen, S., Hariskos, I., Luchterhand, B., Büchs, J., 2012. Development of a modified Respiration Activity Monitoring System for accurate and highly resolved measurement of respiration activity in shake flask fermentations. J Biol Eng 6 (1), 11. doi:10.1186/1754-1611-6-11.
- Hanson, M.A., Ge, X., Kostov, Y., Brorson, K.A., Moreira, A.R., Rao, G., 2007. Comparisons of optical pH and dissolved oxygen sensors with traditional

- electrochemical probes during mammalian cell culture. Biotech & Bioengineering 97 (4), 833–841. doi:10.1002/bit.21320.
- Hartley, F., Walker, T., Chung, V., Morten, K., 2018. Mechanisms driving the lactate switch in Chinese hamster ovary cells. Biotech & Bioengineering 115 (8), 1890–1903. doi:10.1002/bit.26603.
- Heath, C., Kiss, R., 2007. Cell culture process development: advances in process engineering. Biotechnology progress 23 (1), 46–51. doi:10.1021/bp060344e.
- Hemmerich, J., Noack, S., Wiechert, W., Oldiges, M., 2018. Microbioreactor systems for accelerated bioprocess development. Biotechnology journal 13 (4), e1700141. doi:10.1002/biot.201700141.
- Henzler, H.-J., Biedermann, A., 1996. Modelluntersuchungen zur Partikelbeanspruchung in Reaktoren. Chemie Ingenieur Technik 68 (12), 1546–1561. doi:10.1002/cite.330681205.
- Hermann, R., Lehmann, M., Büchs, J., 2003. Characterization of gas-liquid mass transfer phenomena in microtiter plates. Biotech & Bioengineering 81 (2), 178–186. doi:10.1002/bit.10456.
- Hernández Rodríguez, T., Pörtner, R., Frahm, B., 2013. Seed train optimization for suspension cell culture. BMC Proc 7 (S6). doi:10.1186/1753-6561-7-S6-P9.
- Hertel, O., Neuss, A., Busche, T., Brandt, D., Kalinowski, J., Bahnemann, J., Noll, T., 2022. Enhancing stability of recombinant CHO cells by CRISPR/Cas9-mediated site-specific integration into regions with distinct histone modifications. Frontiers in bioengineering and biotechnology 10, 1010719. doi:10.3389/fbioe.2022.1010719.
- Ho, S.C.L., Tong, Y.W., Yang, Y., 2013. Generation of monoclonal antibody-producing mammalian cell lines. Pharmaceutical Bioprocessing 1 (1), 71–87. doi:10.4155/pbp.13.8.
- Hsu, W.-T., Aulakh, R.P.S., Traul, D.L., Yuk, I.H., 2012. Advanced microscale bioreactor system: a representative scale-down model for bench-top bioreactors. Cytotechnology 64 (6), 667–678. doi:10.1007/s10616-012-9446-1.

- Hu, W., Berdugo, C., Chalmers, J.J., 2011. The potential of hydrodynamic damage to animal cells of industrial relevance: current understanding. Cytotechnology 63 (5), 445–460. doi:10.1007/s10616-011-9368-3.
- Hu, W., Rathman, J.J., Chalmers, J.J., 2008. An investigation of small-molecule surfactants to potentially replace pluronic F-68 for reducing bubble-associated cell damage. Biotech & Bioengineering 101 (1), 119–127. doi:10.1002/bit.21872.
- Hunt, J.C.R., Vassilicos, J.C., 1991. Kolmogorov's contributions to the physical and geometrical understanding of small-scale turbulence and recent developments. Proc. R. Soc. Lond. A 434 (1890), 183–210. doi:10.1098/rspa.1991.0088.
- Ihling, N., Berg, C., Paul, R., Munkler, L.P., Mäkinen, M.E.-L., Chotteau, V., Büchs, J., 2023. Scale-down of CHO cell cultivation from shake flasks based on oxygen mass transfer allows application of parallelized, non-invasive, and time-resolved monitoring of the oxygen transfer rate in 48-well microtiter plates. Biotechnology journal, e2300053. doi:10.1002/biot.202300053.
- Ihling, N., Bittner, N., Diederichs, S., Schelden, M., Korona, A., Höfler, G.T., Fulton, A., Jaeger, K.-E., Honda, K., Ohtake, H., Büchs, J., 2018. Online measurement of the respiratory activity in shake flasks enables the identification of cultivation phases and patterns indicating recombinant protein production in various Escherichia coli host strains. Biotechnology progress 34 (2), 315–327. doi:10.1002/btpr.2600.
- Ihling, N., Munkler, L.P., Berg, C., Reichenbächer, B., Wirth, J., Lang, D., Wagner, R., Büchs, J., 2021. Time-resolved monitoring of the oxygen transfer rate of Chinese Hamster Ovary cells provides insights into culture behavior in shake flasks. Frontiers in bioengineering and biotechnology 9, 725498. doi:10.3389/fbioe.2021.725498.
- Ihling, N., Munkler, L.P., Paul, R., Berg, C., Reichenbächer, B., Kadisch, M., Lang, D., Büchs, J., 2022a. Non-invasive and time-resolved measurement of the respiration activity of Chinese hamster ovary cells enables prediction of key culture parameters in shake flasks. Biotechnology journal 17 (8), e2100677. doi:10.1002/biot.202100677.
- Ihling, N., Munkler, L.P., Paul, R., Lang, D., Büchs, J., 2022b. Introducing oxygen transfer rate measurements as a novel method for time-resolved cytotoxicity

- assessment in shake flasks. Environ Sci Eur 34 (1), 1–15. doi:10.1186/s12302-022-00673-5.
- Jang, M., Kim, S.S., Lee, J., 2013. Cancer cell metabolism: implications for therapeutic targets. Experimental & molecular medicine 45 (10), e45. doi:10.1038/emm.2013.85.
- Kambayashi, T., Noguchi, T., Nojima, A., Kono, S., Taniguchi, S.-I., Ozaki, Y., 2020. Glucose Monitoring in Cell Culture with Online Ultrasound-Assisted Near-Infrared Spectroscopy. Analytical chemistry 92 (4), 2946–2952. doi:10.1021/acs.analchem.9b03354.
- Karakashev, S.I., Grozdanova, M.V., 2012. Foams and antifoams. Advances in Colloid and Interface Science 176-177, 1–17. doi:10.1016/j.cis.2012.04.001.
- Kaufman, R.J., Sharp, P.A., 1982. Amplification and expression of sequences cotransfected with a modular dihydrofolate reductase complementary dna gene. Journal of molecular biology 159 (4), 601–621. doi:10.1016/0022-2836(82)90103-6.
- Keane, J.T., Ryan, D., Gray, P.P., 2003. Effect of shear stress on expression of a recombinant protein by Chinese hamster ovary cells. Biotech & Bioengineering 81 (2), 211–220. doi:10.1002/bit.10472.
- Kim, D.Y., Chaudhry, M.A., Kennard, M.L., Jardon, M.A., Braasch, K., Dionne, B., Butler, M., Piret, J.M., 2013. Fed-batch CHO cell t-PA production and feed glutamine replacement to reduce ammonia production. Biotechnology progress 29 (1), 165–175. doi:10.1002/btpr.1658.
- Kim, J.Y., Kim, Y.-G., Lee, G.M., 2012. CHO cells in biotechnology for production of recombinant proteins: current state and further potential. Appl Microbiol Biotechnol 93 (3), 917–930. doi:10.1007/s00253-011-3758-5.
- Klausing, S., Krämer, O., Noll, T., 2013. Enhancing cell growth and antibody production in CHO cells by siRNA knockdown of novel target genes. BMC Proc 7 (S6). doi:10.1186/1753-6561-7-S6-P92.
- Klöckner, W., Büchs, J., 2012. Advances in shaking technologies. Trends in biotechnology 30 (6), 307–314. doi:10.1016/j.tibtech.2012.03.001.

- Koch, V., Rüffer, H.-M., Schügerl, K., Innertsberger, E., Menzel, H., Weis, J., 1995. Effect of antifoam agents on the medium and microbial cell properties and process performance in small and large reactors. Process Biochemistry 30 (5), 435–446. doi:10.1016/0032-9592(94)00029-8.
- Kolmogorov, A.N., 1941. Dissipation of energy in the locally isotropic turbulence. Compt. Rend. Acad. Sci. USSR (32), 1. doi:10.1098/rspa.1991.0076.
- Kolmogorov, A.N., 1962. A refinement of previous hypotheses concerning the local structure of turbulence in a viscous incompressible fluid at high Reynolds number. Journal of Fluid Mechanics 13 (1), 82–85. doi:10.1017/S0022112062000518.
- Kottmeier, K., Müller, C., Huber, R., Büchs, J., 2010. Increased product formation induced by a directed secondary substrate limitation in a batch Hansenula polymorpha culture. Appl Microbiol Biotechnol 86 (1), 93–101. doi:10.1007/s00253-009-2285-0.
- Kresta, S.M., Wood, P.E., 1991. Prediction of the three-dimensional turbulent flow in stirred tanks. AIChE Journal 37 (3), 448–460. doi:10.1002/aic.690370314.
- Kunas, K.T., Papoutsakis, E.T., 1990. Damage mechanisms of suspended animal cells in agitated bioreactors with and without bubble entrainment. Biotech & Bioengineering 36 (5), 476–483. doi:10.1002/bit.260360507.
- Kunert, R., Reinhart, D., 2016. Advances in recombinant antibody manufacturing. Appl Microbiol Biotechnol 100 (8), 3451–3461. doi:10.1007/s00253-016-7388-9.
- Lai, T., Yang, Y., Ng, S.K., 2013. Advances in Mammalian cell line development technologies for recombinant protein production. Pharmaceuticals (Basel, Switzerland) 6 (5), 579–603. doi:10.3390/ph6050579.
- Lalonde, M.-E., Durocher, Y., 2017. Therapeutic glycoprotein production in mammalian cells. Journal of Biotechnology 251, 128–140. doi:10.1016/j.jbiotec.2017.04.028.
- Lanza, A.M., Kim, D.S., Alper, H.S., 2013. Evaluating the influence of selection markers on obtaining selected pools and stable cell lines in human cells. Biotechnology journal 8 (7), 811–821. doi:10.1002/biot.201200364.
- Lemire, L., Pham, P.L., Durocher, Y., Henry, O., 2021. Practical Considerations for the Scale-Up of Chinese Hamster Ovary (CHO) Cell Cultures, in: Pörtner, R. (Ed.), Cell

- Culture Engineering and Technology, vol. 10. Springer International Publishing, Cham, pp. 367–400.
- Lewis, N.E., Liu, X., Li, Y., Nagarajan, H., Yerganian, G., O'Brien, E., Bordbar, A., Roth, A.M., Rosenbloom, J., Bian, C., Xie, M., Chen, W., Li, N., Baycin-Hizal, D., Latif, H., Forster, J., Betenbaugh, M.J., Famili, I., Xu, X., Wang, J., Palsson, B.O., 2013. Genomic landscapes of Chinese hamster ovary cell lines as revealed by the Cricetulus griseus draft genome. Nat Biotechnol 31 (8), 759–765. doi:10.1038/nbt.2624.
- Li, F., Hashimura, Y., Pendleton, R., Harms, J., Collins, E., Lee, B., 2006. A systematic approach for scale-down model development and characterization of commercial cell culture processes. Biotechnology progress 22 (3), 696–703. doi:10.1021/BP0504041.
- Li, F., Vijayasankaran, N., Shen, A., Kiss, R., Amanullah, A., 2010. Cell culture processes for monoclonal antibody production. mAbs 2 (5), 466–479. doi:10.4161/mabs.2.5.12720.
- Ling, W.L.W., 2020. Current Considerations and Future Advances in Chemically Defined Medium Development for the Production of Protein Therapeutics in CHO Cells, in: Lee, G.M., Faustrup Kildegaard, H. (Eds.), Cell culture engineering. Recombinant protein production. Wiley-VCH, Weinheim, pp. 279–294.
- Lücke, J., Bädeker, M., 2023. Medizinische Biotechnologie in Deutschland 2023. Boston Consulting Group 2023.
- Ma, N., Chalmers, J.J., Aunins, J.G., Zhou, W., Xie, L., 2004. Quantitative studies of cell-bubble interactions and cell damage at different pluronic F-68 and cell concentrations. Biotechnology progress 20 (4), 1183–1191. doi:10.1021/bp0342405.
- Ma, N., Koelling, K.W., Chalmers, J.J., 2002. Fabrication and use of a transient contractional flow device to quantify the sensitivity of mammalian and insect cells to hydrodynamic forces. Biotech & Bioengineering 80 (4), 428–437. doi:10.1002/bit.10387.

- Maier, B., 2002. Auslegung und Betrieb von Rührkesselbioreaktoren unter erhöhtem Reaktordruck. Zugl.: Aachen, Techn. Hochsch., Diss., 2002. Shaker, Aachen, 146 pp.
- Markert, S., Joeris, K., 2017. Establishment of a fully automated microtiter plate-based system for suspension cell culture and its application for enhanced process optimization. Biotechnology and bioengineering 114 (1), 113–121. doi:10.1002/bit.26044.
- Markert, S., Musmann, C., Hülsmann, P., Joeris, K., 2019. Automated and enhanced clone screening using a fully automated microtiter plate-based system for suspension cell culture. Biotechnology progress 35 (2), e2760. doi:10.1002/btpr.2760.
- Marques, M.P.C., Cabral, J.M.S., Fernandes, P., 2010. Bioprocess scale-up: quest for the parameters to be used as criterion to move from microreactors to lab-scale. J of Chemical Tech & Biotech 85 (9), 1184–1198. doi:10.1002/jctb.2387.
- Martínez-Monge, I., Roman, R., Comas, P., Fontova, A., Lecina, M., Casablancas, A., Cairó, J.J., 2019. New developments in online OUR monitoring and its application to animal cell cultures. Applied microbiology and biotechnology 103 (17), 6903–6917. doi:10.1007/s00253-019-09989-4.
- Maschke, R.W., John, G.T., Eibl, D., 2022a. Monitoring of oxygen, pH, CO2, and biomass in smart single-use shake flasks. Chemie Ingenieur Technik 94 (12), 1995–2001. doi:10.1002/cite.202200094.
- Maschke, R.W., Seidel, S., Bley, T., Eibl, R., Eibl, D., 2022b. Determination of culture design spaces in shaken disposable cultivation systems for CHO suspension cell cultures. Biochemical Engineering Journal 177, 108224. doi:10.1016/j.bej.2021.108224.
- Mazurek, S., 2011. Pyruvate kinase type M2: A key regulator of the metabolic budget system in tumor cells. The International Journal of Biochemistry & Cell Biology 43 (7), 969–980. doi:10.1016/j.biocel.2010.02.005.
- Mazurek, S., Boschek, C.B., Hugo, F., Eigenbrodt, E., 2005. Pyruvate kinase type M2 and its role in tumor growth and spreading. Seminars in Cancer Biology 15 (4), 300–308. doi:10.1016/j.semcancer.2005.04.009.

- Meier, K., Klöckner, W., Bonhage, B., Antonov, E., Regestein, L., Büchs, J., 2016. Correlation for the maximum oxygen transfer capacity in shake flasks for a wide range of operating conditions and for different culture media. Biochemical Engineering Journal 109, 228–235. doi:10.1016/j.bej.2016.01.014.
- Metze, S., Ruhl, S., Greller, G., Grimm, C., Scholz, J., 2020. Monitoring online biomass with a capacitance sensor during scale-up of industrially relevant CHO cell culture fed-batch processes in single-use bioreactors. Bioprocess Biosyst Eng 43 (2), 193–205. doi:10.1007/s00449-019-02216-4.
- Meyer, A., Condon, R.G.G., Keil, G., Jhaveri, N., Liu, Z., Tsao, Y.-S., 2012. Fluorinert, an oxygen carrier, improves cell culture performance in deep square 96-well plates by facilitating oxygen transfer. Biotechnology progress 28 (1), 171–178. doi:10.1002/btpr.712.
- Micheletti, M., Barrett, T., Doig, S.D., Baganz, F., Levy, M.S., Woodley, J.M., Lye, G.J., 2006. Fluid mixing in shaken bioreactors: Implications for scale-up predictions from microlitre-scale microbial and mammalian cell cultures. Chemical Engineering Science 61 (9), 2939–2949. doi:10.1016/j.ces.2005.11.028.
- Möckel, H.-O., Wolleschensky, E., Drewas, S., Rahner, H.-J., 1990. Modelling of the calculation of the power input for aerated single- and multistage impellers with special respect to scale-up. Acta Biotechnologica 10 (3), 215–224. doi:10.1002/abio.370100302.
- Mollet, M., Ma, N., Zhao, Y., Brodkey, R., Taticek, R., Chalmers, J.J., 2004. Bioprocess equipment: characterization of energy dissipation rate and its potential to damage cells. Biotechnology progress 20 (5), 1437–1448. doi:10.1021/bp0498488.
- Montes-Serrano, I., Satzer, P., Jungbauer, A., Dürauer, A., 2022. Characterization of hydrodynamics and volumetric power input in microtiter plates for the scale-up of downstream operations. Biotech & Bioengineering 119 (2), 523–534. doi:10.1002/bit.27983.
- Mora, A., Zhang, S.S., Carson, G., Nabiswa, B., Hossler, P., Yoon, S., 2018. Sustaining an efficient and effective CHO cell line development platform by incorporation of 24-deep well plate screening and multivariate analysis. Biotechnology progress 34 (1), 175–186. doi:10.1002/btpr.2584.

- Mortensen, R.M., Kingston, R.E., 2009. Selection of transfected mammalian cells. Current protocols in molecular biology Chapter 9, Unit9.5. doi:10.1002/0471142727.mb0905s86.
- Moses, S., Manahan, M., Ambrogelly, A., Ling, W.L.W., 2012. Assessment of AMBR[™] as a model for high-throughput cell culture process development strategy. ABB 03 (07), 918–927. doi:10.4236/abb.2012.37113.
- Naddafi, F., Tabarzad, M., Shirazi, F.H., 2019. Dermination of minimum inhibitory concentration (MIC) of hygromycin B in CHO cells. Iranian Journal of Pharmaceutical Science. Accessed 1 February 2022.
- Nagashima, H., Watari, A., Shinoda, Y., Okamoto, H., Takuma, S., 2013. Application of a quality by design approach to the cell culture process of monoclonal antibody production, resulting in the establishment of a design space. Journal of Pharmaceutical Sciences 102 (12), 4274–4283. doi:10.1002/jps.23744.
- Nakashima, Y., Kounoura, M., Malasuk, C., Nakakubo, K., Watanabe, N., Iwata, S., Morita, K., Oki, Y., Kuhara, S., Tashiro, K., Nakanishi, Y., 2019. Continuous cell culture monitoring using a compact microplate reader with a silicone optical technology-based spatial filter. The Review of scientific instruments 90 (3), 35106. doi:10.1063/1.5054824.
- Neunstoecklin, B., Stettler, M., Solacroup, T., Broly, H., Morbidelli, M., Soos, M., 2015.

 Determination of the maximum operating range of hydrodynamic stress in mammalian cell culture. Journal of Biotechnology 194, 100–109. doi:10.1016/j.jbiotec.2014.12.003.
- Neunstoecklin, B., Villiger, T.K., Lucas, E., Stettler, M., Broly, H., Morbidelli, M., Soos, M., 2016. Pilot-scale verification of maximum tolerable hydrodynamic stress for mammalian cell culture. Appl Microbiol Biotechnol 100 (8), 3489–3498. doi:10.1007/s00253-015-7193-x.
- Niehoff, P.-J., Müller, W., Pastoors, J., Miebach, K., Ernst, P., Hemmerich, J., Noack, S., Wierckx, N., Büchs, J., 2023. Development of an itaconic acid production process with Ustilaginaceae on alternative feedstocks. BMC biotechnology 23 (1), 34. doi:10.1186/s12896-023-00802-9.

- Nienow, A.W., 2006. Reactor engineering in large scale animal cell culture. Cytotechnology 50 (1-3), 9–33. doi:10.1007/s10616-006-9005-8.
- Nienow, A.W., 2009. Scale-up considerations based on studies at the bench scale in stirred bioreactors. J. Chem. Eng. Japan / JCEJ 42 (11), 789–796. doi:10.1252/jcej.08we317.
- Nienow, A.W., Scott, W.H., Hewitt, C.J., Thomas, C.R., Lewis, G., Amanullah, A., Kiss, R., Meier, S.J., 2013. Scale-down studies for assessing the impact of different stress parameters on growth and product quality during animal cell culture. Chemical Engineering Research and Design 91 (11), 2265–2274. doi:10.1016/j.cherd.2013.04.002.
- O'Brien, S.A., Hu, W.-S., 2020. Cell culture bioprocessing the road taken and the path forward. Current Opinion in Chemical Engineering 30. doi:10.1016/j.coche.2020.100663.
- Oh, S.K.W., Nienow, A.W., Al-Rubeai, M., Emery, A.N., 1989. The effects of agitation intensity with and without continuous sparging on the growth and antibody production of hybridoma cells. Journal of Biotechnology 12 (1), 45–61. doi:10.1016/0168-1656(89)90128-4.
- Pan, X., 2018. Scale-down of CHO cell fed-batch cultures. Wageningen University.
- Panckow, R.P., Bliatsiou, C., Nolte, L., Böhm, L., Maaß, S., Kraume, M., 2023. Characterisation of particle stress in turbulent impeller flows utilising photo-optical measurements of a flocculation system PART 1. Chemical Engineering Science 267, 118333. doi:10.1016/j.ces.2022.118333.
- Parampalli, A., Eskridge, K., Smith, L., Meagher, M.M., Mowry, M.C., Subramanian, A., 2007. Developement of serum-free media in CHO-DG44 cells using a central composite statistical design. Cytotechnology 54 (1), 57–68. doi:10.1007/s10616-007-9074-3.
- Park, J.U., Han, H.-J., Baik, J.Y., 2022. Energy metabolism in Chinese hamster ovary (CHO) cells: Productivity and beyond. Korean J. Chem. Eng. 39 (5), 1097–1106. doi:10.1007/s11814-022-1062-y.

- Paul, K., Herwig, C., 2020. Scale-down simulators for mammalian cell culture as tools to access the impact of inhomogeneities occurring in large-scale bioreactors. Engineering in Life Sciences 20 (5-6), 197–204. doi:10.1002/elsc.201900162.
- Pereira, S., Kildegaard, H.F., Andersen, M.R., 2018. Impact of CHO Metabolism on Cell Growth and Protein Production: An Overview of Toxic and Inhibiting Metabolites and Nutrients. Biotechnology journal 13 (3), e1700499. doi:10.1002/biot.201700499.
- Pérez-Rodriguez, S., Reynoso-Cereceda, G.I., Valdez-Cruz, N.A., Trujillo-Roldán, M.A., 2022. A comprehensive comparison of mixing and mass transfer in shake flasks and their relationship with MAb productivity of CHO cells. Bioprocess Biosyst Eng 45 (6), 1033–1045. doi:10.1007/s00449-022-02722-y.
- Peter, C.P., Suzuki, Y., Büchs, J., 2006. Hydromechanical stress in shake flasks: correlation for the maximum local energy dissipation rate. Biotech & Bioengineering 93 (6), 1164–1176. doi:10.1002/bit.20827.
- Rameez, S., Mostafa, S.S., Miller, C., Shukla, A.A., 2014. High-throughput miniaturized bioreactors for cell culture process development: reproducibility, scalability, and control. Biotechnology progress 30 (3), 718–727. doi:10.1002/btpr.1874.
- Reinhart, D., Damjanovic, L., Kaisermayer, C., Kunert, R., 2015. Benchmarking of commercially available CHO cell culture media for antibody production. Appl Microbiol Biotechnol 99 (11), 4645–4657. doi:10.1007/s00253-015-6514-4.
- Ritacco, F.V., Wu, Y., Khetan, A., 2018. Cell culture media for recombinant protein expression in Chinese hamster ovary (CHO) cells: History, key components, and optimization strategies. Biotechnology progress 34 (6), 1407–1426. doi:10.1002/btpr.2706.
- Rouiller, Y., Bielser, J.-M., Brühlmann, D., Jordan, M., Broly, H., Stettler, M., 2016. Screening and assessment of performance and molecule quality attributes of industrial cell lines across different fed-batch systems. Biotechnology progress 32 (1), 160–170. doi:10.1002/btpr.2186.

- Routledge, S.J., 2012. Beyond de-foaming: the effects of antifoams on bioprocess productivity. Computational and structural biotechnology journal 3, e201210014. doi:10.5936/csbj.201210014.
- Sani, M.H., 2015. Evaluation of microwell based systems and miniature bioreactors for rapid cell culture bioprocess development and scale-up.
- Schiøtz, B.L., Rosado, E.G., Baekkevold, E.S., Lukacs, M., Mjaaland, S., Sindre, H., Grimholt, U., Gjøen, T., 2011. Enhanced transfection of cell lines from Atlantic salmon through nucoleofection and antibiotic selection. BMC research notes 4, 136. doi:10.1186/1756-0500-4-136.
- Schmidt-Hager, J., Ude, C., Findeis, M., John, G.T., Scheper, T., Beutel, S., 2014. Noninvasive online biomass detector system for cultivation in shake flasks. Engineering in Life Sciences 14 (5), 467–476. doi:10.1002/elsc.201400026.
- Schmitz, J., Hertel, O., Yermakov, B., Noll, T., Grünberger, A., 2021. Growth and eGFP Production of CHO-K1 Suspension Cells Cultivated From Single Cell to Laboratory Scale. Front. Bioeng. Biotechnol. 9, 716343. doi:10.3389/fbioe.2021.716343.
- Sharker, S.M., Rahman, A., 2021. A review on the current methods of Chinese hamster ovary (CHO) cells cultivation for the production of therapeutic protein. Current drug discovery technologies 18 (3), 354–364. doi:10.2174/1570163817666200312102137.
- Sieck, J.B., Budach, W.E., Suemeghy, Z., Leist, C., Villiger, T.K., Morbidelli, M., Soos, M., 2014. Adaptation for survival: phenotype and transcriptome response of CHO cells to elevated stress induced by agitation and sparging. Journal of Biotechnology 189, 94–103. doi:10.1016/j.jbiotec.2014.08.042.
- Sieck, J.B., Cordes, T., Budach, W.E., Rhiel, M.H., Suemeghy, Z., Leist, C., Villiger, T.K., Morbidelli, M., Soos, M., 2013. Development of a Scale-Down Model of hydrodynamic stress to study the performance of an industrial CHO cell line under simulated production scale bioreactor conditions. Journal of Biotechnology 164 (1), 41–49. doi:10.1016/j.jbiotec.2012.11.012.
- Sindelar, R.D., Meibohm, B., Crommelin, D.J.A. (Eds.), 2013. Pharmaceutical Biotechnology: Fundamentals and Applications, 4th ed. Springer, New York, NY.

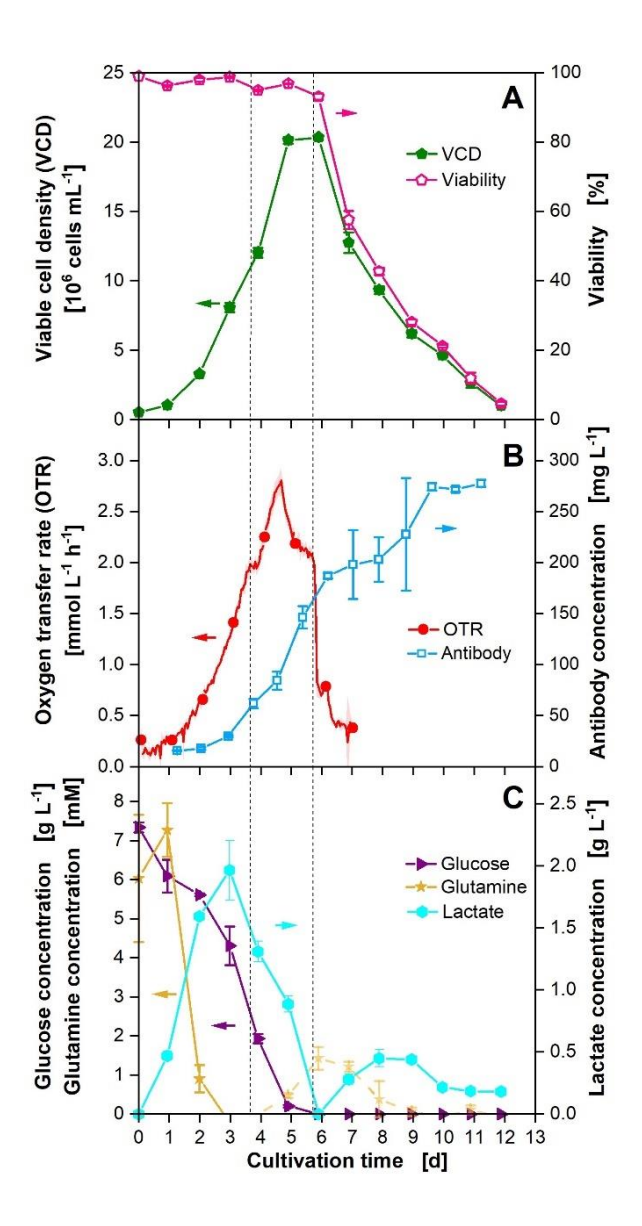
- Sparviero, S., Dicke, M.D., Rosch, T.M., Castillo, T., Salgado-Lugo, H., Galindo, E., Peña, C., Büchs, J., 2023. Yeast extracts from different manufacturers and supplementation of amino acids and micro elements reveal a remarkable impact on alginate production by A. vinelandii ATCC9046. Microb Cell Fact 22 (1), 99. doi:10.1186/s12934-023-02112-3.
- Stöckmann, C., Maier, U., Anderlei, T., Knocke, C., Gellissen, G., Büchs, J., 2003. The oxygen transfer rate as key parameter for the characterization of *Hansenula polymorpha* screening cultures. Journal of industrial microbiology & biotechnology 30 (10), 613–622. doi:10.1007/s10295-003-0090-9.
- Strasser, L., Farrell, A., Ho, J.T.C., Scheffler, K., Cook, K., Pankert, P., Mowlds, P., Viner, R., Karger, B.L., Bones, J., 2021. Proteomic profiling of IgG1 producing CHO cells using LC/LC-SPS-MS3: the effects of bioprocessing conditions on productivity and product quality. Front. Bioeng. Biotechnol. 9, 569045. doi:10.3389/fbioe.2021.569045.
- Tanemura, H., Kitamura, R., Yamada, Y., Hoshino, M., Kakihara, H., Nonaka, K., 2023.
 Comprehensive modeling of cell culture profile using Raman spectroscopy and machine learning. Scientific reports 13 (1), 21805. doi:10.1038/s41598-023-49257-0.
- Tanzeglock, T., Soos, M., Stephanopoulos, G., Morbidelli, M., 2009. Induction of mammalian cell death by simple shear and extensional flows. Biotech & Bioengineering 104 (2), 360–370. doi:10.1002/bit.22405.
- Tharmalingam, T., Goudar, C.T., 2015. Evaluating the impact of high Pluronic® F68 concentrations on antibody producing CHO cell lines. Biotech & Bioengineering 112 (4), 832–837. doi:10.1002/bit.25491.
- Tihanyi, B., Nyitray, L., 2020. Recent advances in CHO cell line development for recombinant protein production. Drug discovery today. Technologies 38, 25–34. doi:10.1016/j.ddtec.2021.02.003.
- Tissot, S., Oberbek, A., Reclari, M., Dreyer, M., Hacker, D.L., Baldi, L., Farhat, M., Wurm, F.M., 2011. Efficient and reproducible mammalian cell bioprocesses without probes and controllers? New biotechnology 28 (4), 382–390. doi:10.1016/j.nbt.2011.02.004.

- TJIO, J.H., Puck, T., 1958. Genetics of somatic mammalian cells. II. Chromosomal constitution of cells in tissue culture. The Journal of experimental medicine 108 (2), 259–268. doi:10.1084/jem.108.2.259.
- Tyupa, D.V., Morozov, A.N., Zakharov, Z.V., Kalenov, S.V., Khamitov, R.A., 2021. Reconstruction of Industrial Processes for Cultivating CHO Cells in a Scale-Down Bioreactor Model. National Research Center Kurchatov Institute, 112 pp.
- Ude, C., Schmidt-Hager, J., Findeis, M., John, G.T., Scheper, T., Beutel, S., 2014. Application of an online-biomass sensor in an optical multisensory platform prototype for growth monitoring of biotechnical relevant microorganism and cell lines in single-use shake flasks. Sensors (Basel, Switzerland) 14 (9), 17390–17405. doi:10.3390/s140917390.
- Velugula-Yellela, S.R., Williams, A., Trunfio, N., Hsu, C.-J., Chavez, B., Yoon, S., Agarabi, C., 2018. Impact of media and antifoam selection on monoclonal antibody production and quality using a high throughput micro-bioreactor system. Biotechnology progress 34 (1), 262–270. doi:10.1002/btpr.2575.
- Villiger, T.K., Morbidelli, M., Soos, M., 2015. Experimental determination of maximum effective hydrodynamic stress in multiphase flow using shear sensitive aggregates. AIChE Journal 61 (5), 1735–1744. doi:10.1002/aic.14753.
- Wahjudi, S.M.W., Petrzik, T., Oudenne, F., Lera Calvo, C., Büchs, J., 2023. Unraveling the potential and constraints associated with corn steep liquor as a nutrient source for industrial fermentations. Biotechnology progress, e3386. doi:10.1002/btpr.3386.
- Walsh, G., Walsh, E., 2022. Biopharmaceutical benchmarks 2022. Nat Biotechnol 40 (12), 1722–1760. doi:10.1038/s41587-022-01582-x.
- Wang, B., Albanetti, T., Miro-Quesada, G., Flack, L., Li, L., Klover, J., Burson, K., Evans, K., Ivory, W., Bowen, M., Schoner, R., Hawley-Nelson, P., 2018. High-throughput screening of antibody-expressing CHO clones using an automated shaken deep-well system. Biotechnology progress 34 (6), 1460–1471. doi:10.1002/btpr.2721.
- Warburg, O., 1956. On the Origin of Cancer Cells. Science 123 (3191), 309–314. doi:10.1126/science.123.3191.309.

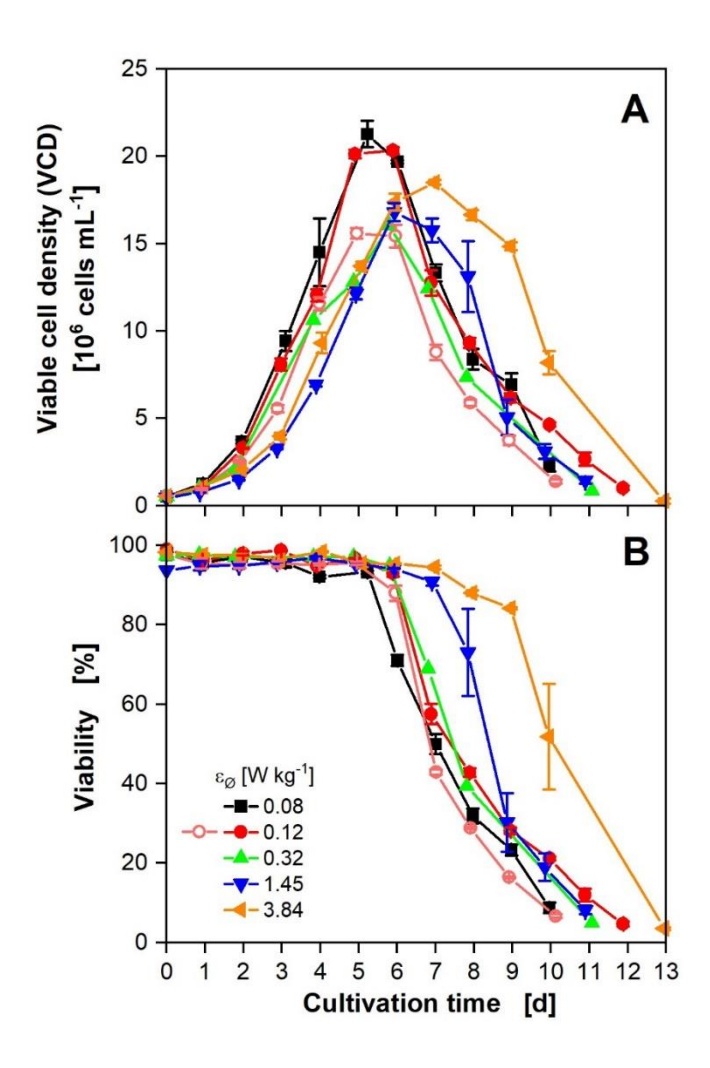
- Wen-Lin Tsai, Jennifer L. Autsen, Julie Ma, Terry Hudson, Jun Luo, 2012. Noninvasive optical sensor technology in shake flasks. BioProcess International (10), 1. Accessed 10 October 2023.
- Wurm, F.M., 2004. Production of recombinant protein therapeutics in cultivated mammalian cells. Nat Biotechnol 22 (11), 1393–1398. doi:10.1038/nbt1026.
- Wutz, J., Steiner, R., Assfalg, K., Wucherpfennig, T., 2018. Establishment of a CFD-based kL a model in microtiter plates to support CHO cell culture scale-up during clone selection. Biotechnology progress 34 (5), 1120–1128. doi:10.1002/btpr.2707.
- Xing, Z., Kenty, B.M., Li, Z.J., Lee, S.S., 2009. Scale-up analysis for a CHO cell culture process in large-scale bioreactors. Biotech & Bioengineering 103 (4), 733–746. doi:10.1002/BIT.22287.
- Xu, S., Hoshan, L., Jiang, R., Gupta, B., Brodean, E., O'Neill, K., Seamans, T.C., Bowers, J., Chen, H., 2017. A practical approach in bioreactor scale-up and process transfer using a combination of constant P/V and vvm as the criterion. Biotechnology progress 33 (4), 1146–1159. doi:10.1002/btpr.2489.
- Yeo, J.H.M., Ho, S.C.L., Mariati, M., Koh, E., Tay, S.J., Woen, S., Zhang, P., Yang, Y., 2017. Optimized selection marker and CHO host cell combinations for generating high monoclonal antibody producing cell lines. Biotechnology journal 12 (12). doi:10.1002/biot.201700175.
- Zhang, J., Pavlova, N.N., Thompson, C.B., 2017. Cancer cell metabolism: the essential role of the nonessential amino acid, glutamine. The EMBO Journal 36 (10), 1302–1315. doi:10.15252/embj.201696151.
- Zhang, J.-H., Shan, L.-L., Liang, F., Du, C.-Y., Li, J.-J., 2022. Strategies and Considerations for Improving Recombinant Antibody Production and Quality in Chinese Hamster Ovary Cells. Frontiers in bioengineering and biotechnology 10, 856049. doi:10.3389/fbioe.2022.856049.
- Zhang, S., Handa-Corrigan, A., Spier, R.E., 1992. Foaming and media surfactant effects on the cultivation of animal cells in stirred and sparged bioreactors. Journal of Biotechnology 25 (3), 289–306. doi:10.1016/0168-1656(92)90162-3.
- Zhang, X., Stettler, M., Sanctis, D. de, Perrone, M., Parolini, N., Discacciati, M., Jesus, M. de, Hacker, D., Quarteroni, A., Wurm, F., 2009. Use of orbital shaken disposable

bioreactors for mammalian cell cultures from the milliliter-scale to the 1,000-liter scale. Advances in biochemical engineering/biotechnology 115, 33–53. doi:10.1007/10_2008_18.

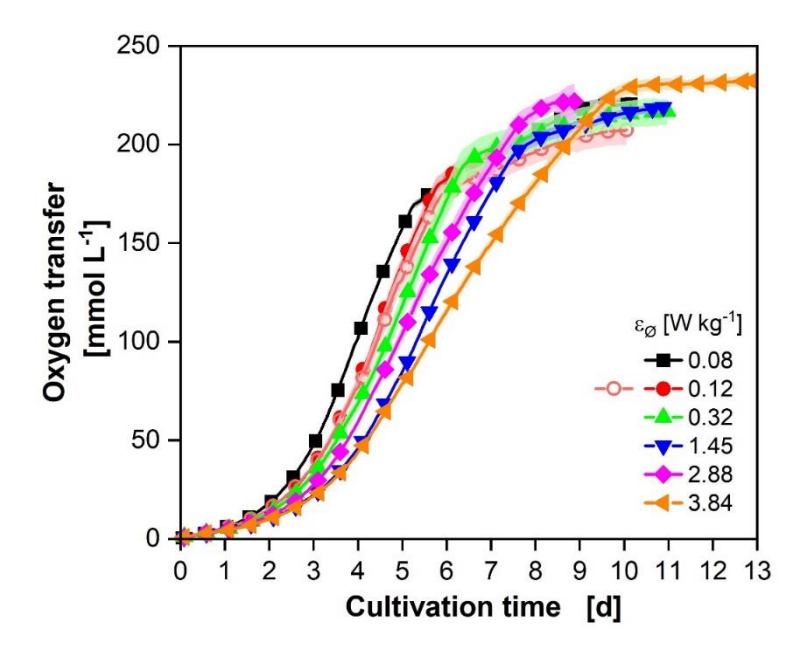
9 Appendix



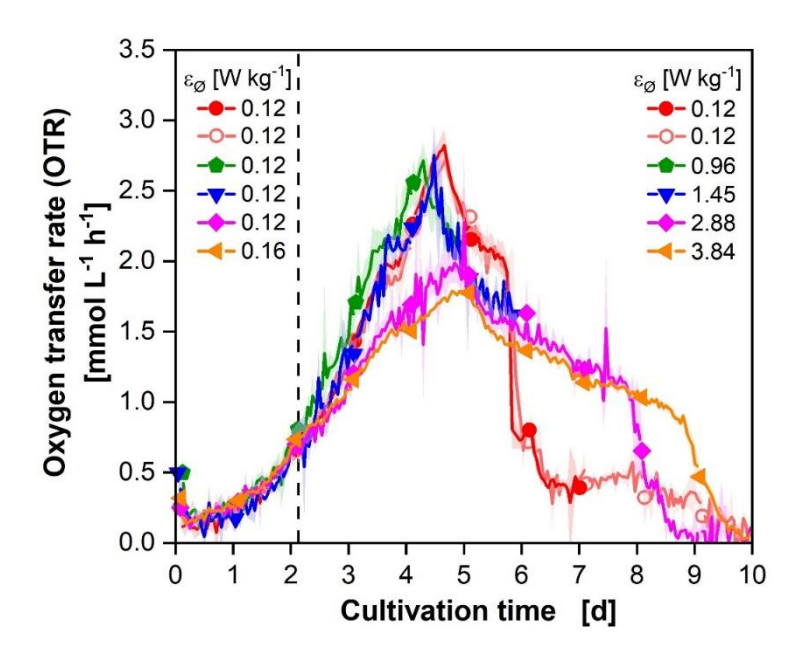
App. Figure 1: Cultivation of CHO DP12 cells in shake flasks under standard conditions (independent repetition of the experiment in Fig 1). The experiments were performed in six replicates. Three replicates were daily sampled for offline analysis and three were used for online monitoring only. All data are shown as mean value of three biological replicates (indicated as error bars or shades). A) Depicted are the viable cell density (VCD) and the viability determined by a CEDEX. B) Shown is the mean oxygen transfer rate (OTR). For clarity, only every twelfth measuring point over time is marked as a symbol. The lines are drawn through all measured values. The outliers in the OTR data due to temperature adaptations after sampling were excluded from the data. In addition, the antibody concentration is shown. C) Corresponding glucose, glutamine, and lactate concentrations are plotted over time. Depletion of glucose and glutamine is marked by dotted vertical lines over all three parts of the figure. Cultivations were performed in a TOM device. Culture conditions: 250 mL TOM glass flasks, temperature (T) = 36.5° C, shaking frequency (n) = 140° rpm, shaking diameter (d₀) = 50° mm, filling volume (V_L) = 50° mL, 5° CO₂, 70° rel. hum., medium: TCX6D + 8° mM glutamine; starting cell density: $5\times10^{\circ}$ cells mL⁻¹.



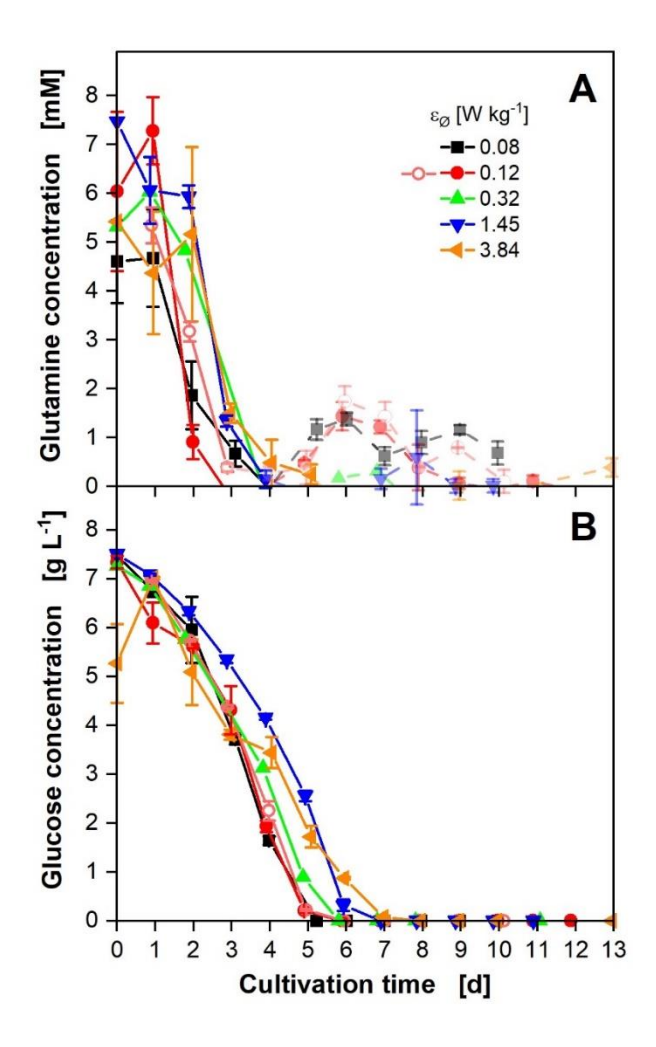
App. Figure 2: Viable cell density and viability of CHO DP12 cells in shake flasks with varying average energy dissipation rates ($\varepsilon_{\varnothing}$). All data are shown as the mean value of three biological replicates. A) Depicted is the viable cell density (VCD) and B) the viability, both determined by a CEDEX. Culture conditions: flask size, shaking frequency, shaking diameter, and filling volume see Table 1, temperature (T) = 36.5° C, 5° CO₂, 70° C rel. hum., medium: TCX6D + 8 mM glutamine; starting cell density: 5×10^{5} cells mL⁻¹.



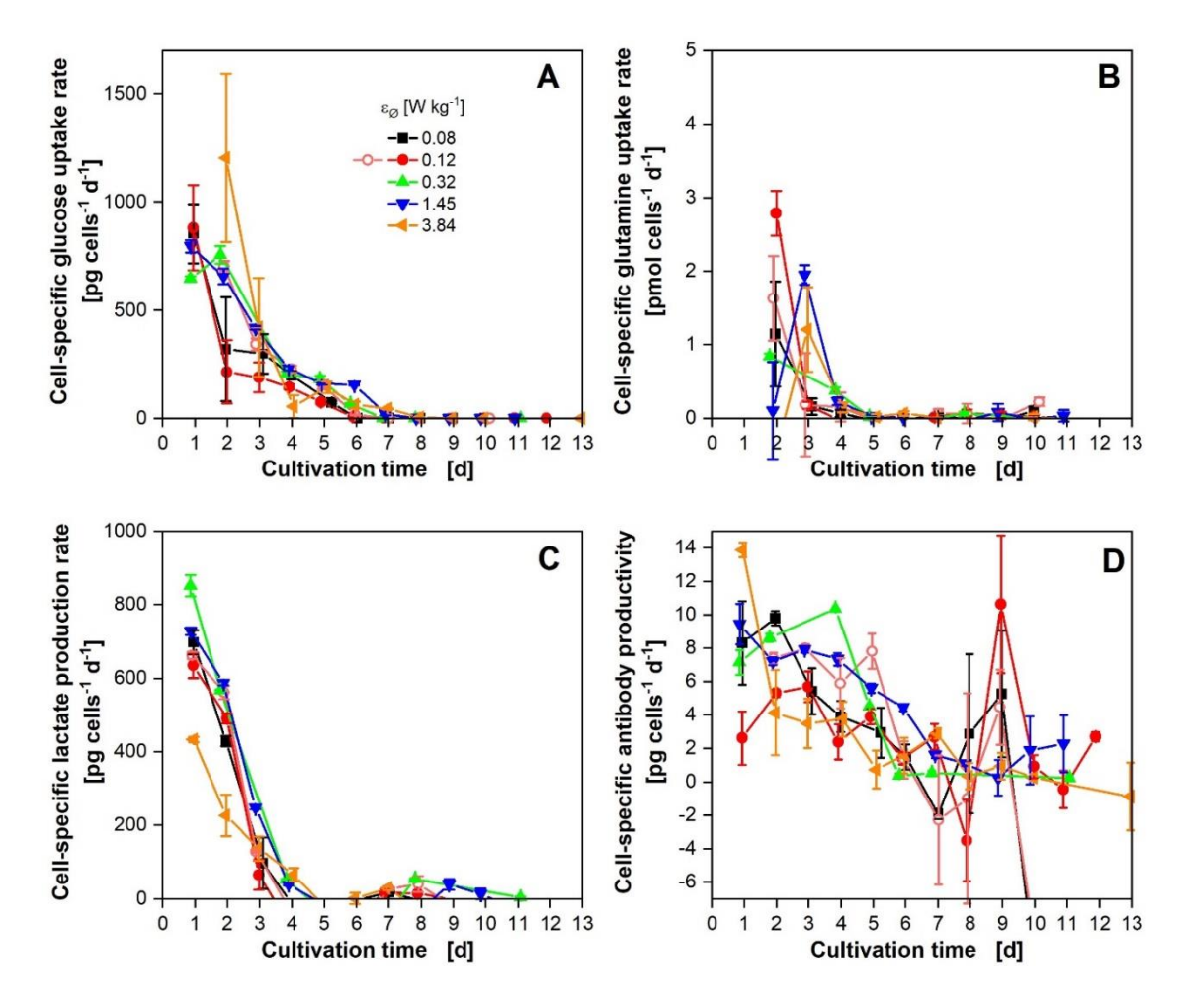
App. Figure 3: Mean oxygen transfer rate of CHO DP12 cells in shake flasks with varying average energy dissipation rates ($\varepsilon_{\varnothing}$). The mean oxygen transfer (integral of the oxygen transfer rate) of the 3 replicates from Figure 5 is shown with standard deviations illustrated as shaded areas. For clarity, only every twelfth measuring point over time is marked as a symbol. The lines are drawn through all measured data points. Culture conditions: flask size, shaking frequency, shaking diameter, and filling volume see Table 1, temperature (T) = 36.5°C, 5 % CO_2 , 70 % rel. hum., medium: TCX6D + 8 mM glutamine; starting cell density: $5x10^5$ cells mL⁻¹.



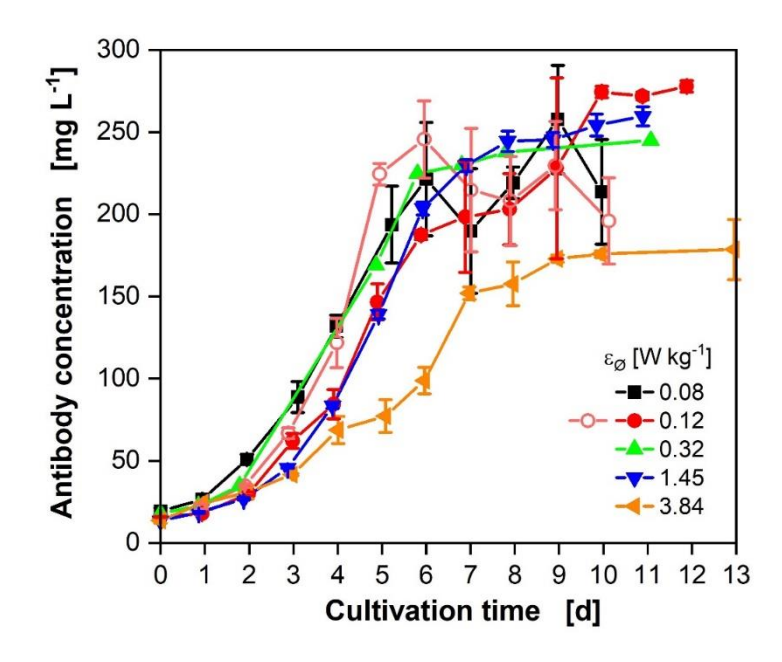
App. Figure 4: Cultivation of CHO DP12 cells in shake flasks with variation of shaking frequencies. The experiments started with an average energy dissipation rate ($\varepsilon_{\varnothing}$) of 0.12 W kg⁻¹ or 0.16 W kg⁻¹. After roughly two days (see vertical dotted line), ε was increased to different levels. The mean oxygen transfer rate (OTR) is shown with standard deviations illustrated as shaded areas. For clarity, only every 24th measuring point over time is marked as a symbol. The lines are drawn through all measured data points. The outliers in the OTR data due to temperature adaptations after opening the incubation hood were excluded from the data. Culture conditions: flask size, shaking frequency, shaking diameter, and filling volume see Table 1, temperature (T) = 36.5°C, 5 % CO₂, 70 % rel. hum., medium: TCX6D + 8 mM glutamine; starting cell density: 5×10^5 cells mL⁻¹.



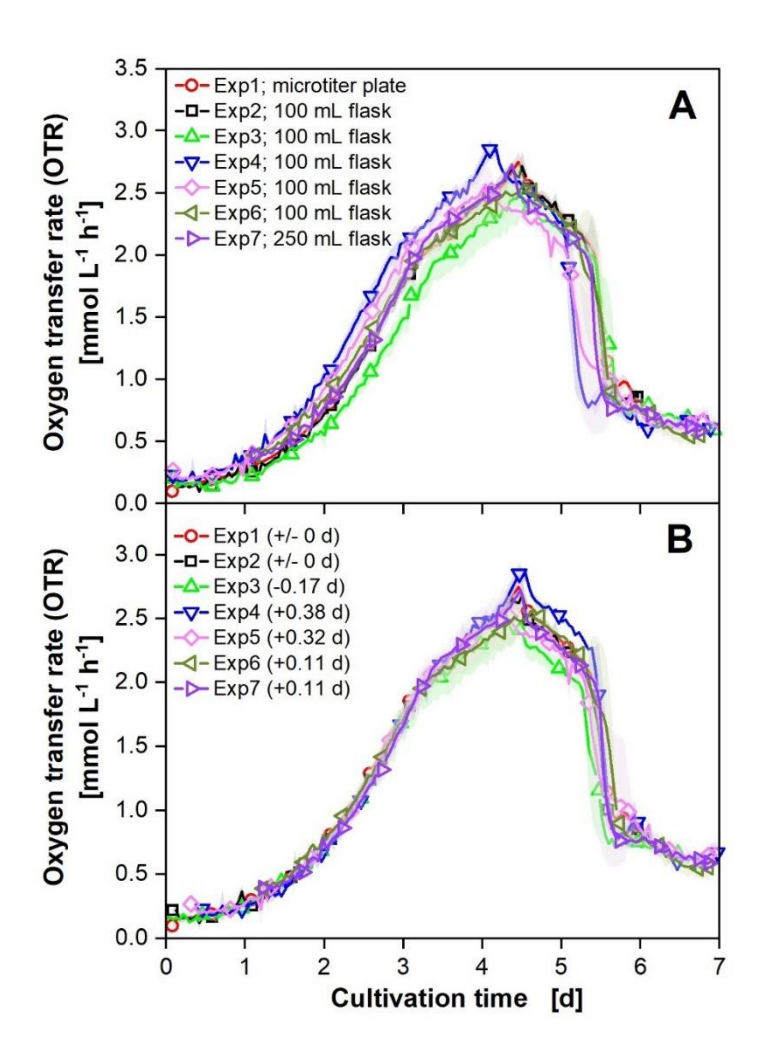
App. Figure 5: Glutamine and glucose concentrations of CHO DP12 cell cultivations in shake flasks with varying average energy dissipation rates ($\varepsilon_{\varnothing}$). Mean value of A) glutamine concentrations and B) glucose concentrations of three replicates (cultivations depicted in Figure 5). Culture conditions: flask size, shaking frequency, shaking diameter, and filling volume see Table 1, temperature (T) = 36.5°C, 5 % CO₂, 70 % rel. hum., medium: TCX6D + 8 mM glutamine; starting cell density: 5×10^5 cells mL⁻¹.



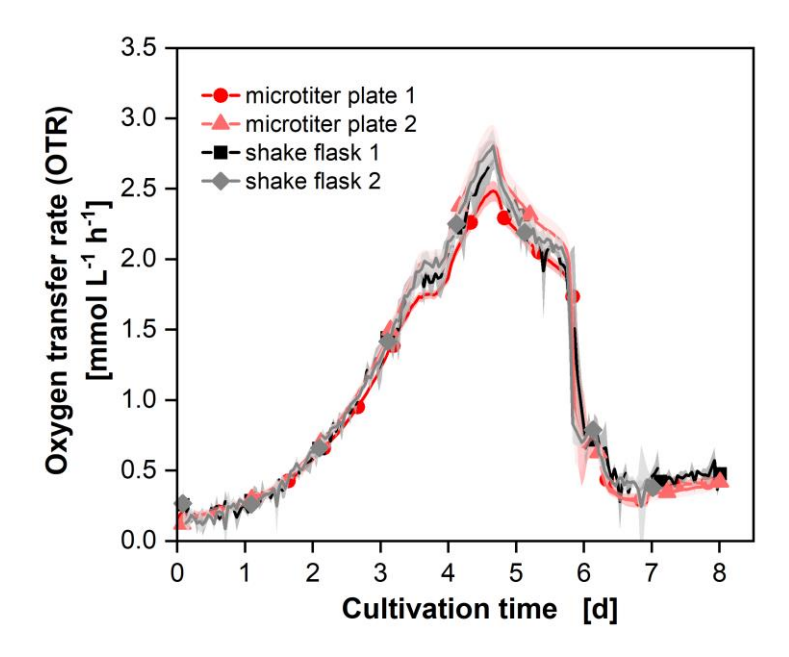
App. Figure 6: Cell-specific production and uptake rates of CHO DP12 cell cultivations in shake flasks with varying average energy dissipation rates ($\varepsilon_{\varnothing}$): A) cell-specific glucose uptake rate, B) cell-specific glutamine uptake rate, C) cell-specific lactate production rate and D) cell-specific antibody productivity. Culture conditions: flask size, shaking frequency, shaking diameter, and filling volume see Table 1, temperature (T) = 36.5°C, 5 % CO₂, 70 % rel. hum., medium: TCX6D + 8 mM glutamine; starting cell density: $5x10^5$ cells mL⁻¹.



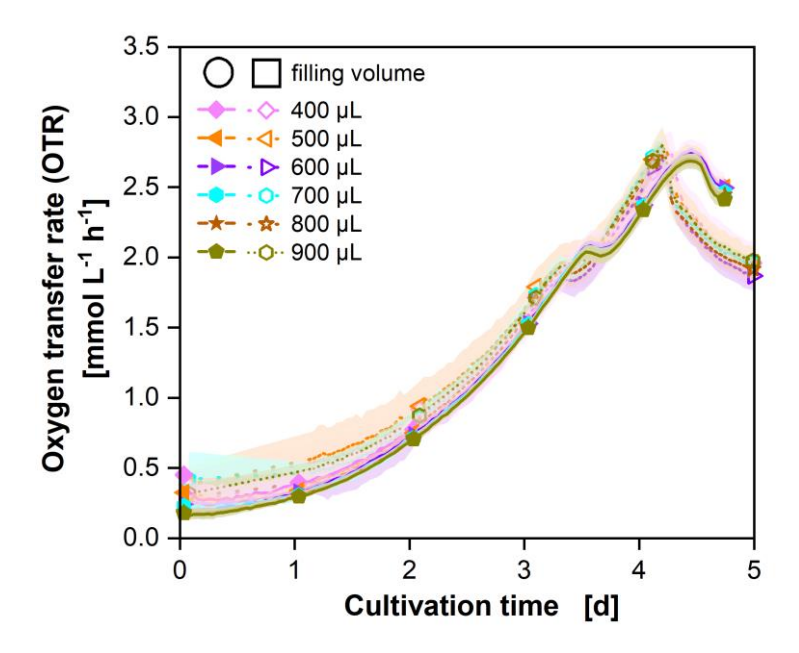
App. Figure 7: Antibody concentrations of CHO DP12 cell cultivations in shake flasks with varying average energy dissipation rates ($\varepsilon_{\varnothing}$). The mean value of three replicates is depicted (cultivations shown in Figure 5). Culture conditions: flask size, shaking frequency, shaking diameter, and filling volume see Table 1, temperature (T) = 36.5°C, 5 % CO₂, 70 % rel. hum., medium: TCX6D + 8 mM glutamine; starting cell density: 5×10^5 cells mL⁻¹.



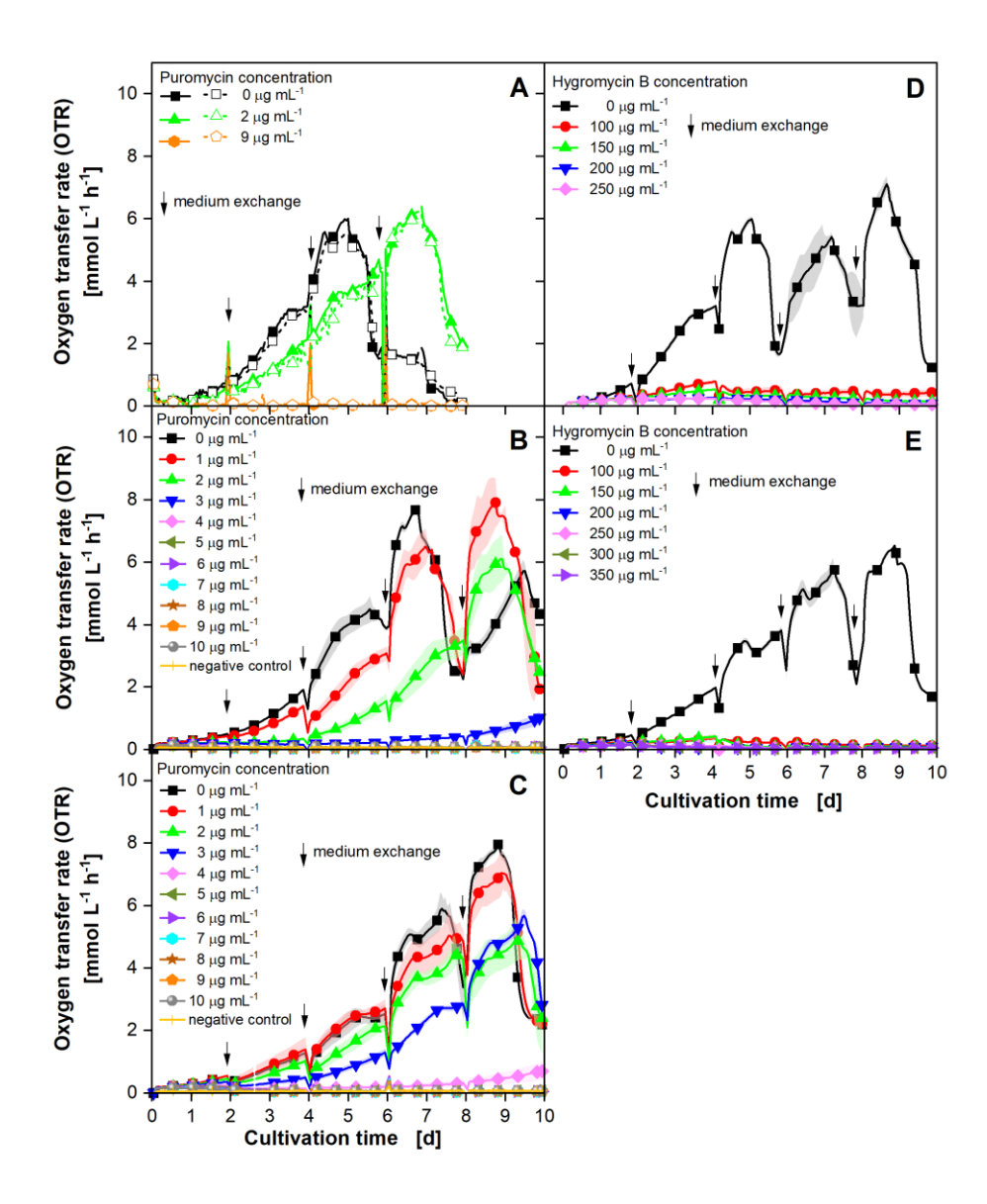
App. Figure 8: Reproducibility of oxygen transfer rate (OTR) determination of CHO-K1 cell cultures. The OTR was determined by the μ TOM device in a 96-deep-well microtiter plate (Exp 1) and by a Kuhner TOM device in shake flasks (Exp2 – Exp7). Experiment one (red line and open circles) and two (black line and open squares) are the same experiments as in Figure 9. The low standard deviations are shown as shaded areas and indicate good reproducibility. For clarity, only every twelfth measuring point over time is marked as a symbol. (A) Original OTR-data. (B) Data corrected for differences in the lag phase by shifting the OTR curves along the x-axis. Culture conditions TOM device: 100 mL / 250 mL glass flasks, temperature (T) = 36.5°C, shaking frequency (n) = 140 rpm, shaking diameter (d₀) = 50 mm, filling volume (V_L) = 20 / 50 mL, 5 % CO₂, 70 % rel. hum., medium: TCX6D + 8 mM glutamine; starting cell density: $5x10^5$ cells mL⁻¹. Culture conditions μ TOM device: 96-deep-well microtiter plate, temperature (T) = 36.5°C, shaking frequency (n) = 850 rpm, shaking diameter (d₀) = 3 mm, filling volume (V_L) = 1 mL, 5 % CO₂, humidified, medium: TCX6D + 8 mM glutamine; starting cell density: $5x10^5$ cells mL⁻¹.



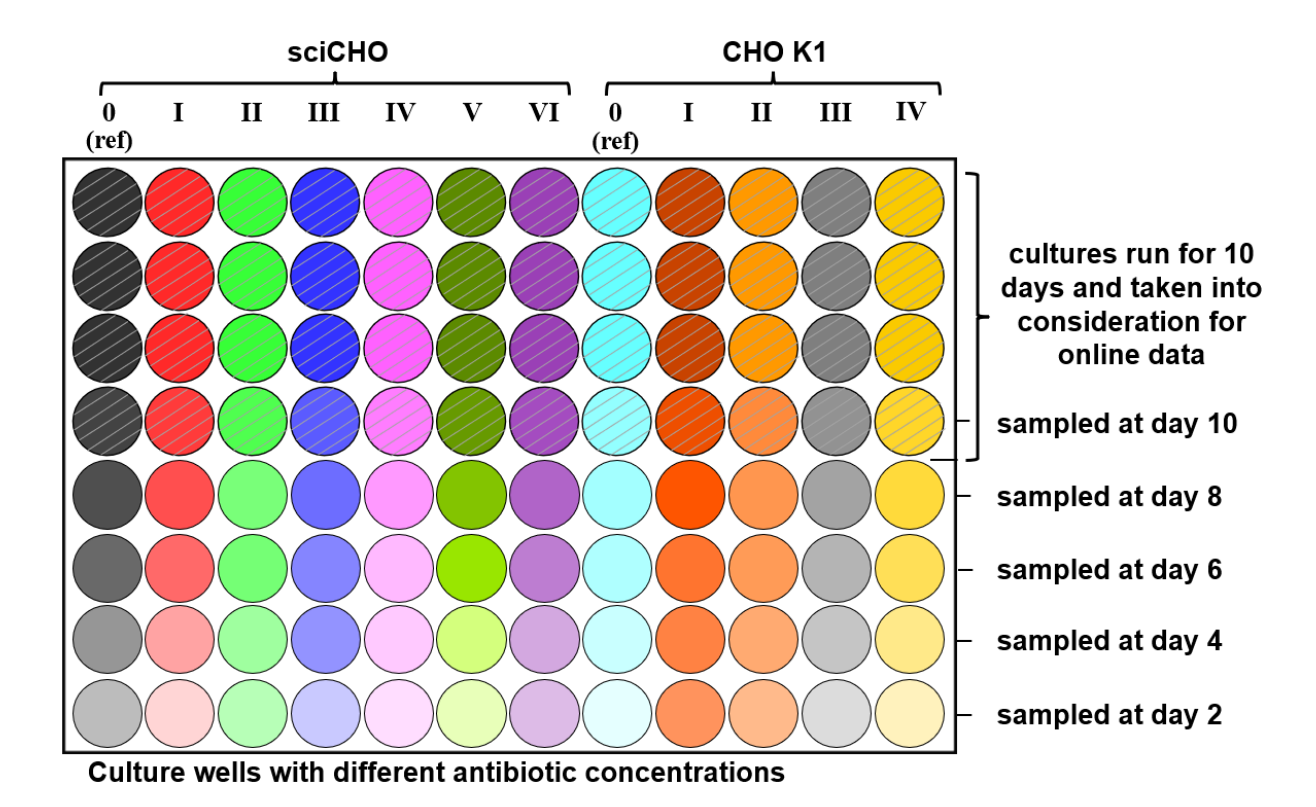
App. Figure 9: Oxygen transfer rate (OTR) of CHO DP12 cell cultures. Figure 10 with the corresponding standard deviations indicated as shaded areas. Two independent experiments (1 and 2) were performed. For both experiments, a round 96-deep-well microtiter plate and 250 mL shake flasks were inoculated. The µTOM device was used for online monitoring of the microtiter plates (dark red line and circles; light red line and triangles) and the TOM device for the shake flasks (black line and squares; grey line and diamonds). For clarity, only every 24th measuring point over time is marked as a symbol. The microtiter plate experiments were performed in 72 (Exp 1) and 66 (Exp 2) replicates and the shake flask experiments in 3 replicates each. Culture conditions TOM device: 250 mL glass temperature (T) = 36.5°C, shaking frequency (n) = 140 rpm, shaking diameter (d₀) = 50 mm, filling volume (V_L) = 50 mL, 5 % CO₂, 70 % rel. hum., medium: TCX6D + 8 mM glutamine; starting cell density: 5x10⁵ cells mL⁻¹. Culture conditions µTOM device: round 96-deep-well microtiter plate, temperature (T) = 36.5°C, shaking frequency (n) = 850 rpm, shaking diameter $(d_0) = 3 \text{ mm}$, filling volume $(V_L) = 1 \text{ mL}$, $5 \% \text{ CO}_2$, humidified, medium: TCX6D + 8 mM glutamine; starting cell density: 5x10⁵ cells mL⁻¹.



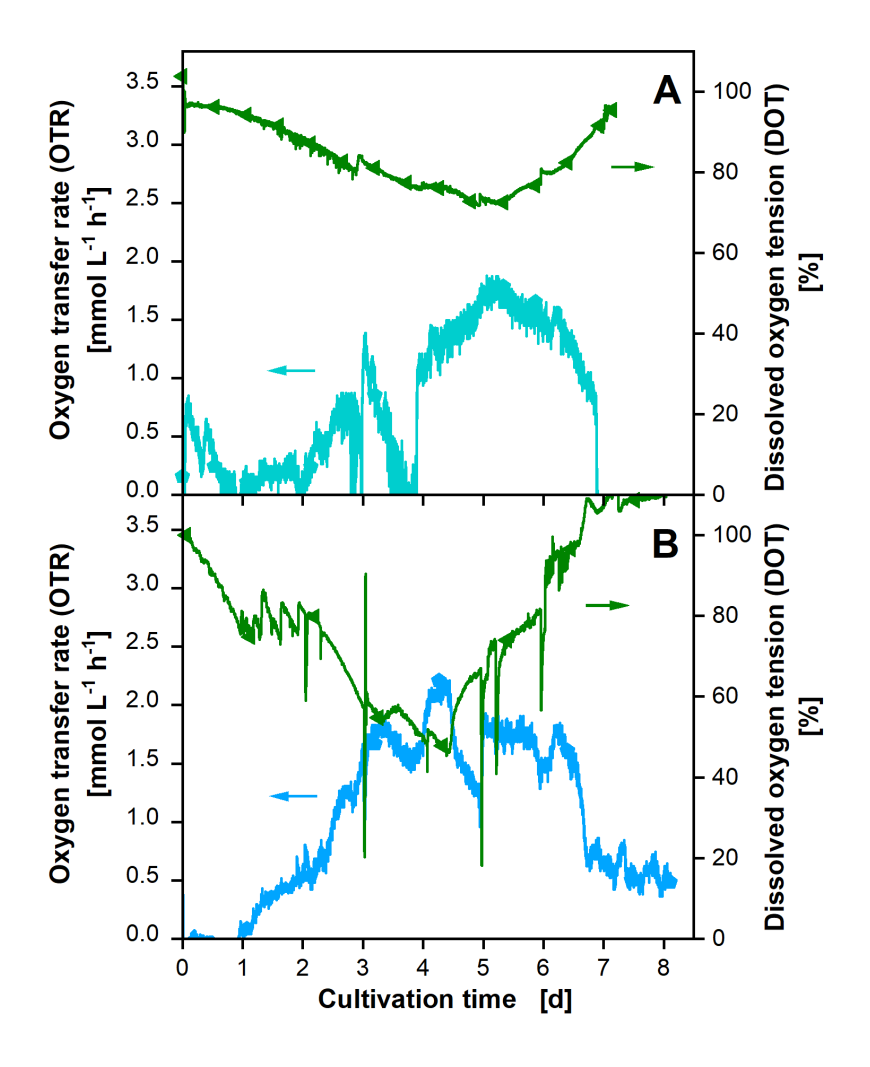
App. Figure 10: Oxygen transfer rate (OTR) of CHO DP12 cell cultures monitored by the μ TOM device with different filling volumes. OTR curves of cultivations in a round 96-deep-well microtiter plate (N = 8 for each filling volume) are depicted in solid lines. OTR curves of cultivations in a square 96-deep-well plate (N = 3 or 6 for each filling volume) are depicted as dotted lines. For clarity, only one measuring point per day over time is marked as a symbol. The standard deviations are shown as shaded areas. Culture conditions: temperature (T) = 36.5°C, shaking frequency (n) = 850 rpm, shaking diameter (d₀) = 3 mm, varying filling volume (V_L), 5 % CO₂, humidified, medium: TCX6D + 8 mM glutamine; starting cell density: 5×10^5 cells mL⁻¹.



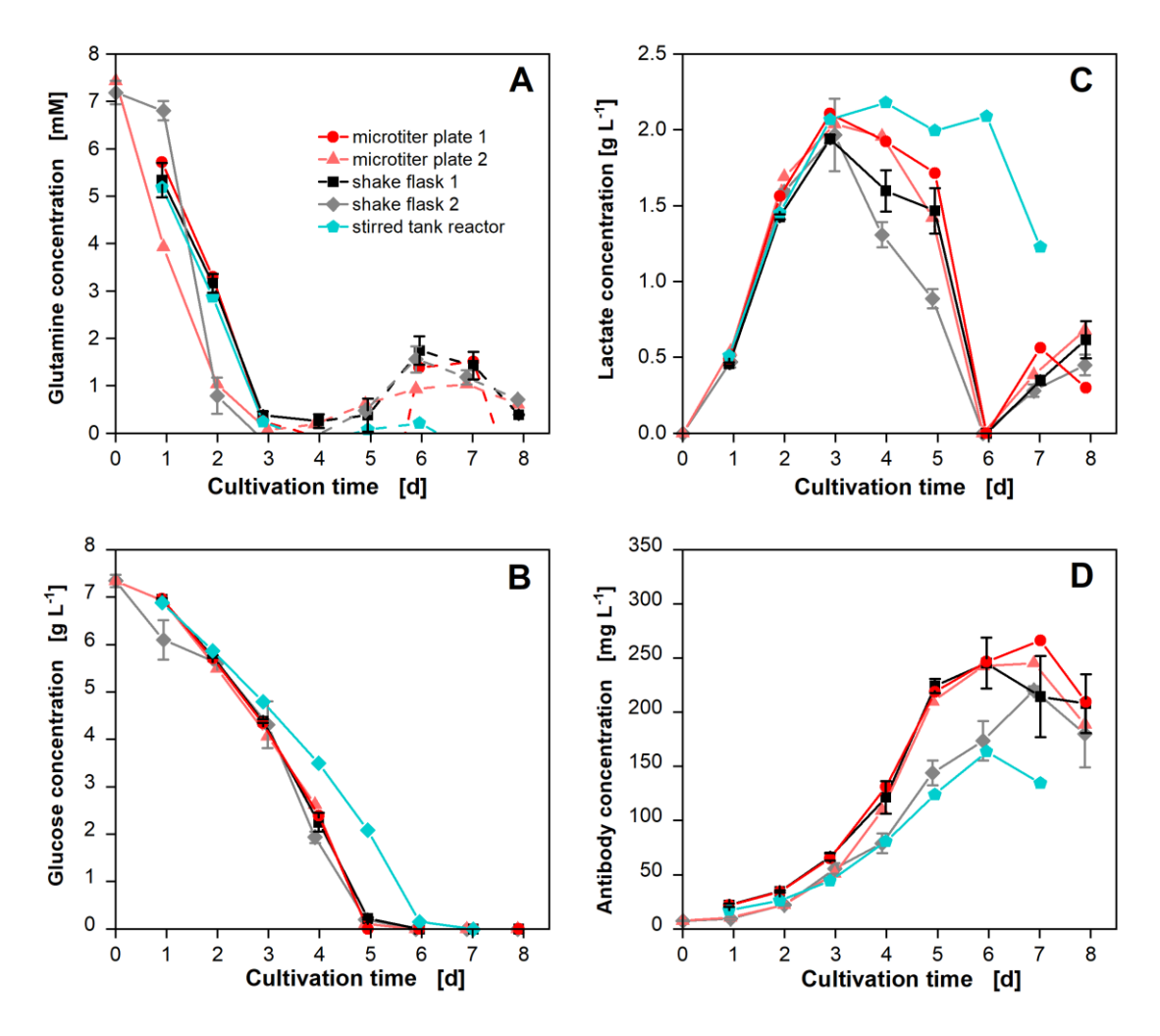
App. Figure 11: Original oxygen transfer rate (OTR) data of kill curves including the outliers due to temperature adaptations after medium exchange. Kill curves (A) for CHO-K1 cells in 100 mL glass shake flasks with the antibiotic puromycin, (B) for CHO-K1 cells in 96-deep-well microtiter plates with puromycin, (C) for sciCHO cells in 96-deep-well microtiter plates with hygromycin B and (E) for sciCHO cells in 96-deep-well microtiter plates with hygromycin B. The standard deviations are shown as shaded areas. For clarity, only every twelfth measuring point over time is marked as a symbol. Culture conditions TOM device: 100 mL glass flasks, temperature (T) = 36.5°C, shaking frequency (n) = 140 rpm, shaking diameter (d_0) = 50 mm, filling volume (d_0) = 20 mL, 5 % d_0 CO2, 70 % rel. hum., medium: TCX6D + 8 mM glutamine + varying concentrations of puromycin; starting cell density: d_0 CO2, shaking frequency (n) = 850 rpm, shaking diameter (d_0) = 3 mm, filling volume (d_0) = 1 mL, 5 % d_0 CO2, humidified, medium: TCX6D + 8 mM glutamine + varying antibiotic concentrations; starting cell density: d_0 CO3 cells mL-1.



App. Figure 12: Experimental strategy used with the antibiotic hygromycin B. Seven different antibiotic concentrations were used with sciCHO cells and five different concentrations with CHO-K1 cells in eight replicates each. Every two days one well per antibiotic concentration was sampled for offline analysis. Afterward, the medium was exchanged for the remaining wells. A total of four wells per concentration (diagonal-hatched) ran over the entire cultivation time of 10 days. Those four wells were taken into consideration for the online monitored oxygen transfer rate (OTR) in the μ TOM device.



App. Figure 13: Original OTR and DOT data from stirred tank reactor cultivations. CHO DP12 cell cultivations in a stirred tank reactor with a stirring speed of A) n = 360 rpm (refer to Figure 18) and B) n = 100-250 rpm (refer to Figure 19). Depicted is the oxygen transfer rate (OTR) with all measuring points (blue line and pentagons) and the dissolved oxygen tension (DOT) (green line and sideward triangle). For clarity, only one measuring point per day is plotted. Culture conditions: $1.5 \, L$ reactor, temperature (T) = $36.5^{\circ}C$, stirrer speed (n_{ST}) = $360 \, rpm$ or $100-250 \, rpm$ (Rushton turbine), filling volume (V_L) = $600 \, mL$, $5 \, \% \, CO_2$, aeration = $0.2 \, vvm$ (sparged), medium: $TCX6D + 8 \, mM$ glutamine; starting cell density: $5x10^5 \, cells \, mL^{-1}$.



App. Figure 14: Offline measured metabolite and product concentrations of the cultivations shown in Figure 18. CHO DP12 cell cultivations were performed in round 96-deep-well plates (dark and light red lines / circles and upward triangle), shake flasks (black and gray lines / squares and diamonds) and a stirred tank reactor (blue line and pentagon). Depicted are A) glutamine concentrations B) glucose concentrations C) lactate concentrations and D) IgG antibody titer.

App. Table 1: OTR $_{max}$ values for different filling volumes in round 96-deep-well microtiter plates according to Dinger et al. (2022).

filling volume [µL]	OTR _{max} [mmol L ⁻¹ h ⁻¹]
200	52.8
300	35.2
400	26.4
500	21.1
600	17.6
700	15.1
800	13.2
900	11.7
1000	10.5

App. Table 2: Variables for calculation of the scale-up parameters.

variable	value
L _{O2}	0.00118 mol L ⁻¹ bar ⁻¹
pR	1 bar
y O2,in	0.21 mol mol ⁻¹
V _m	22.414 L mol ⁻¹
q	0.2 L L ⁻¹ min ⁻¹
С	0.32
α	0.74
β	0.42
VL	600 mL
р	1 bar
dR	105 mm
d	45 mm
ρ	1000 kg m ⁻³